SYNTHESIS OF PYRROLIDINYL PEPTIDE NUCLEIC ACID CARRYING NOVEL HYDROPHILIC β-AMINO ACID SPACER

HARUTHAI PANSUWAN

A Thesis Submitted to the Graduate School of Naresuan University
in Partial Fulfillment of the Requirements
for the Master of Science Degree in Chemistry
May 2017

Copyright 2017 by Naresuan University

Thesis entitled "Synthesis of pyrrolidinyl peptide nucleic acid carrying novel hydrophilic β amino acid spacer"

By Miss Haruthai Pansuwan

has been approved by the Graduate School as partial fulfillment of the requirements for the Master of Science in Chemistry of Naresuan University

Oral Defense Committee

..... Chair

(Chanitsara Sriwattanawarunyoo, Ph.D.)

Chaturong Suparpprom ..... Advisor

(Assistant Professor Chaturong Suparpprom, Ph.D.)

Boonjira Rut ..... Co – Advisor

(Assistant Professor Boonjira Rutnakornpituk, Ph.D.)

Tirayut Vilai ..... Co – Advisor

(Professor Tirayut Vilaivan, Ph.D.)

Thanesuan Nuanyai ..... External Examiner

(Thanesuan Nuanyai, Ph.D.)

Approved

.....

(Panu Putthawong, Ph.D.)

Associate Dean for Administration and Planning

for Dean of the Graduate School

19 MAY 2017

ACKNOWLEDGEMENT

I wish like to express heartfelt thanks to my advisor: Assistant Professor Chaturong Suparpprom for suggestion for research, counsel, compassion and encouragement for research and experimentation. I would like to thank the all thesis committee: Professor Tirayut Vilaivan, Assistant Professor Boonjira Rutnakornpituk, Dr.Chanitsara Sriwattana-warunyoo and Dr.Thanesuan Nuanyai for great comments that are useful for research. Furthermore, dignitaries that made this research is successful, I also grateful Professor Tirayut vilaivan, Mrs.Chotima Vilaivan and members of TV group from Department of Chemistry, Faculty of Science, Chulalongkorn University for great skill for research, counseling and assistance in the use of tools and equipment. Thanks, all instructors from Department of Chemistry, Faculty of Science, Naresuan University for guidance and knowledge. I also express thank CS group and my friends for encourage and precious helps. Finally, appreciate my parents who give love, warmth and financial support throughout my life.

Haruthai Pansuwan

Title	SYNTHESIS OF PYRROLIDINYL PEPTIDE NUCLEIC ACID CARRYING NOVEL HYDROPHILICβ-AMINO ACID SPACER
Author	Haruthai Pansuwan
Advisor	Assistant Professor Chaturong Suparpprom, Ph.D.
Co - Advisor	Professor Tirayut Vilaivan, D.Phil. Assistant Professor Boonjira Rutnakornpituk, Ph.D.
Academic Paper	Thesis M.Sc in Chemistry, Naresuan University, 2016
Keywords	PNA, hydrophilic side chain, water solubility

ABSTRACT

Peptide Nucleic Acid (PNA) is a DNA analogue in which achiral *N*-(2-aminoethyl glycine) replaced the deoxyribose-phosphate core structure of DNA. PNA has natural backbone without negative charge of phosphate group which contributes to high stability of PNA·DNA duplex compared to DNA·DNA duplex because of the absence of electrostatic repulsion. Presently, various PNA systems have widely developed and used for various applications. Pyrrolidinyl PNA with D-prolyl-2-amino-1-cyclopentanecarboxylic acid backbone or *acpc*PNA is the one of PNA system that has interesting DNA binding properties. ACPC spacer could be modified by replacing a methylene carbon in the five-membered ring with nitrogen to afford APC spacer. The nitrogen atom of APC spacer can be further modified by various means such as reductive alkylation. In this work, the water solubility of *acpc*PNA was improved by the addition of hydrophilic side chain *via* APC spacer. Hydroxybutyl (C4OH), aminobutyl ($C4NH_2$) and guanidinobutyl (C4Gua) side chains were attached to APC spacer *via* reductive alkylation. The modified acpcPNA still retained high affinity with complementary DNA. The singly-modified homothymine PNA (Ac-TTTTTTTTT-LysNH_2) showed T_m value (with DNA) at 67.1, 71.9 and 72.9 °C for C4OH, $C4NH_2$ and C4Gua, respectively compared to 72.5 °C of unmodified PNA. For mix base sequence, singly-modified PNA (Ac-GTAGATCACT-LysNH_2) showed T_m value (with DNA) at 53.3, 58.3 and 58.3 °C for C4OH, $C4NH_2$ and C4Gua, respectively. Triply-modified PNA sequence (Ac-GTAGATCACT-LysNH_2) showed

T_m values at 54.4, 65.1 and 66.8 °C for C4OH, $C4NH_2$ and C4Gua, respectively compared to 58.0 °C of mix base unmodified PNA. The aminobutyl and guanidinobutyl side chain can increase thermal stability of the PNA·DNA duplexes better than the hydroxybutyl, which is consistent with their positively charged nature.

In addition, water solubility of the modified PNA was studied by adding the minimum volume of water to obtain a saturated aqueous solution of PNA. All modified PNA showed significantly improved water solubility from 3.25 mM (unmodified) to 31.82, 12.04 and 13.32 mM for C4OH, $C4NH_2$ and C4Gua, respectively. The results showed that the side chain modification can improve water solubility without compromising the DNA binding properties of *acpc*PNA.

LIST OF CONTENTS

LIST OF TABLES

LIST OF FIGURES

LIST OF FIGURES (CONT.)

LIST OF FIGURES (CONT.)

LIST OF FIGURES (CONT.)

LIST OF FIGURES (CONT.)

LIST OF FIGURES (CONT.)

LIST OF FIGURES (CONT.)

LIST OF FIGURES (CONT.)

ABBREVIATIONS

aeg	=	aminoethylglycine
aep	=	aminoethylprolyl
*acpc*PNA	=	D-prolyl-2-aminocyclopen-tanecarboxylic acid
*apc*PNA	=	3-aminopyrrolidine-4-carboxylic acid
*apc/acpc*PNA	=	The 1 or 3 unit of *apc*PNA was inserted in PNA sequence of *acpc*PNA.
AcOH	=	acetic acid
A	=	adenine
A^{Bz}	=	N^6-benzoyladenine
Ac	=	acetyl
Ac_2O	=	acetic anhydride
aq	=	aqueous
Bz	=	benzoyl
Boc	=	*tert*-butoxycarbonyl
Boc_2O	=	di-*tert*-butyl dicarbonate
C	=	cytosine
C^{Bz}	=	N^4-benzoylcytosine
CCA	=	α-cyano-4-hydroxy cinnamic acid
$CDCl_3$	=	deuterated chloroform
CH_2Cl_2	=	dichloromethane
DNA	=	deoxyribonucleic acid
DMSO-d_6	=	deuterated dimethylsulfoxide
D_2O	=	deuterium oxide
DMF	=	*N,N'*-dimethylformamide
DIEA	=	*N,N*-Diisopropylethylamine
DIAD	=	diisopropylazodicarboxylate
DBU	=	1,8-diazabicycloundec-7-ene
EtOAc	=	ethyl acetate
Fmoc	=	9-fluorenylmethoxycarbonyl

ABBREVIATIONS (CONT.)

Fmoc-OSu	=	9-fluorenylmethyl *N*-succinimidyl carbonate, *N*-(9-Fluorenylmethoxycarbonyloxy)succinimide
FRET	=	förster resonance energy transfer
g	=	gram
G	=	guanine
G^{Ibu}	=	N^2-isobutyrylguanine
h	=	hour
HOAT	=	1-hydroxy-7-azabenzotriazole
HPLC	=	high performance liquid chromatography
Hz	=	hertz
IR	=	Infrared
IBX	=	2-iodoxybenzoic acid
Ibu	=	isobutyryl
K_2CO_3	=	Potassium carbonate
Lys	=	lysine
mg	=	milligram
mL	=	milliliter
mmol	=	millimol
MeOH	=	methanol
min	=	minute
m/z	=	mass to charge ratio
MALDI-TOF	=	matrix-assisted laser desorption/ionization-time of flight
nm	=	nanometer
NMR	=	nuclear magnetic resonance
NaCl	=	Sodium chloride
PNA	=	polyamide nucleic acid or peptide nucleic acid
PfpOTfa	=	pentafluorophenyl trifluoroacetate
Pfp	=	pentafluorophenyl
ppm	=	part per million

ABBREVIATIONS (CONT.)

RNA	=	ribonucleic acid
R_f	=	retention factor
RT	=	room temperature
SPR	=	surface plasmon resonance
s	=	singlet
ss	=	single strand
T^{Bz}	=	N^3-benzoylthymine
TrCl	=	trityl chloride
TLC	=	thin layer chromatography
T	=	thymine
T_m	=	melting temperature
t_R	=	retention time
TFA	=	trifluoroacetic acid
UV	=	ultraviolet
µL	=	microliter
µmol	=	micromole
J	=	coupling constant
δ	=	chemical shift
γ	=	gamma
α	=	alpha
°C	=	degree celsius
s	=	singlet
t	=	triplet
m	=	multiplet

CHAPTER I

INTRODUCTION

Peptide nucleic acid (PNA) is a synthetic DNA mimic in which firstly presented by Peter E. Nielsen in 1991 (**Figure 1**). [1] The core structure of DNA, sugar-phosphate backbone, is replaced by achiral *N*-(2-aminoethylglycine) unit (known as *aeg* unit). The *aeg*PNA's uncharged structure shows high binding affinity with complementary DNA and RNA strand by occurrence of hydrogen bonding between nucleobase of DNA or RNA and nucleobase on PNA backbone according to Watson-Crick base pairing rule. The occurred PNA·DNA duplex showed higher stability than DNA·DNA duplex because PNA had no negative charge and no electrostatic repulsion with phosphate group (**Figure 2**). Moreover, the unnatural PNA had enzymatic resistant to protease and nuclease degradation. So, PNA has been applied to chemical biology and biotechnology as hybridization probe, molecular diagnostic and gene therapy agent. [2]

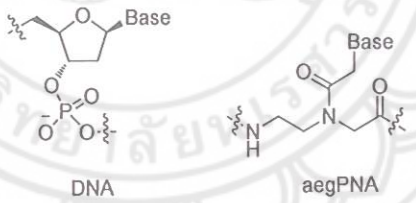

Figure 1 The structure of DNA and *aeg*PNA

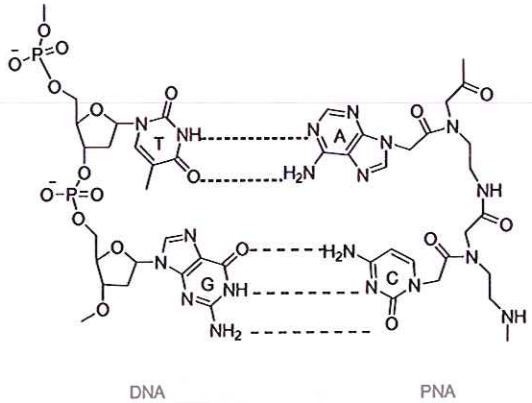

Figure 2 The hydrogen bonding of nucleobase between DNA and PNA *via* Watson-Crick base pairing rule

Later, core structure of PNA was continuously modified by many research groups to increase rigidity, vary size of membered ring and carbon side chain, introduce chiral center or hetero atom for improve various properties of PNA. For example, α-PNA was a PNA containing L-α-amino acid which was synthesized from *N*-Boc-L-serine. [3] Amino-ethylprolyl PNAs (*aep*PNA) is replaced core structure with prolyl unit (proline ring) and directly attached to nucleobase leading to chiral and cationic structure. [4] The properties of *aep*PNA provided high stability for hybridization and improvement of solubility due to positive charge at protonated nitrogen atom. The other example, aromatic peptide nucleic acids (APNA) consisted of aromatic moiety which could be preorganized to form duplex or triplex. [5] APNA and complementary DNA duplex was hybridized by dipole-quadrupole or π-π staking interactions. Next, pyrrolidinone PNA (*pyr*PNA) was connected aminoethylglycine backbone with methylenecarbonyl linker to form pyrrolidinone ring structure. [6] The (3*S*,5*R*)-stereoisomer of *pyr*PNA can specifically bind with RNA. The UV-titration curve showed 2:1 ratio of PNA·RNA as triplex structure which could bind through Hoogsteen hydrogen bonding. The structures of α-PNA, *aep*PNA, APNA and *pyr*PNA were shown in **Figure 3**.

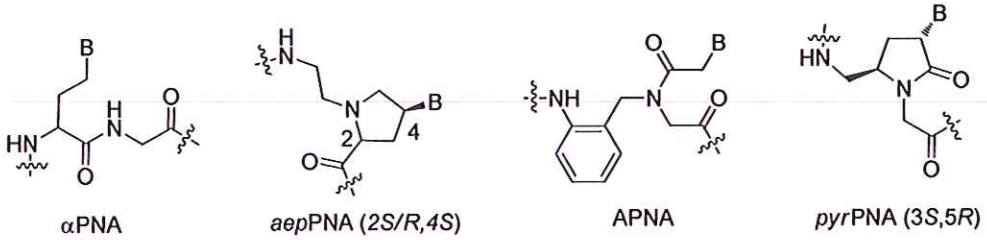

Figure 3 Examples of PNA analogues

To be used in biological system, PNA can be enhanced water solubility and cellular delivery by increasing cationic charge or hydrophilic group in various positions. For example, peptide nucleic acid/peptide amphiphile conjugate (PNA-PA) (**Figure 4**), the alkyl segment and lysine were attached in terminus of PNA for increasing water solubility. [7] The PNA-PA could form nanofibers network upon pH 7 and soluble in water at pH 4. The PNA-PA showed the character of supramolercular which was confirmed by TEM micrograph and β-sheet pattern was determined by circular dichroism. The heptamer thymine of PNA-PA has high stability for binding with oligonucleotide (ΔT_m 16 °C). In addition, there is some report about polyethylene glycol or PEG derived PNA for water solubility. A novel block copolymer probe that composed of an allele-specific PNA and PEG so called PEG-*b*-PNA was reported. [8] PEG-*b*-PNA could form complex with hairpin-structured DNA and determined by affinity capillary electrophoresis (ACE). PEG segment has affected to decreasing electrophoretic mobility by exerting a large amount of hydrodynamic friction.

Furthermore, some amino acids are alternative option for increasing solubility such as lysine or serine. The octa (L-lysine) was designed to produce positively charged on PNA. [9] The result exhibited improvement of water solubility under physiological condition. The hexamer and heptamer PNA are consisted of cationic nucleobase and tetralysine. [10] These modified PNA demonstrated the selectivity in triple helical binding with *ds*RNA due to its positively charge character. The cationic PNA and lysine-PNA have important role for cellular uptake. The modification of PNA or hydrophilic group can help to enhance stability, rigidity and water solubility for application in cellular uptake.

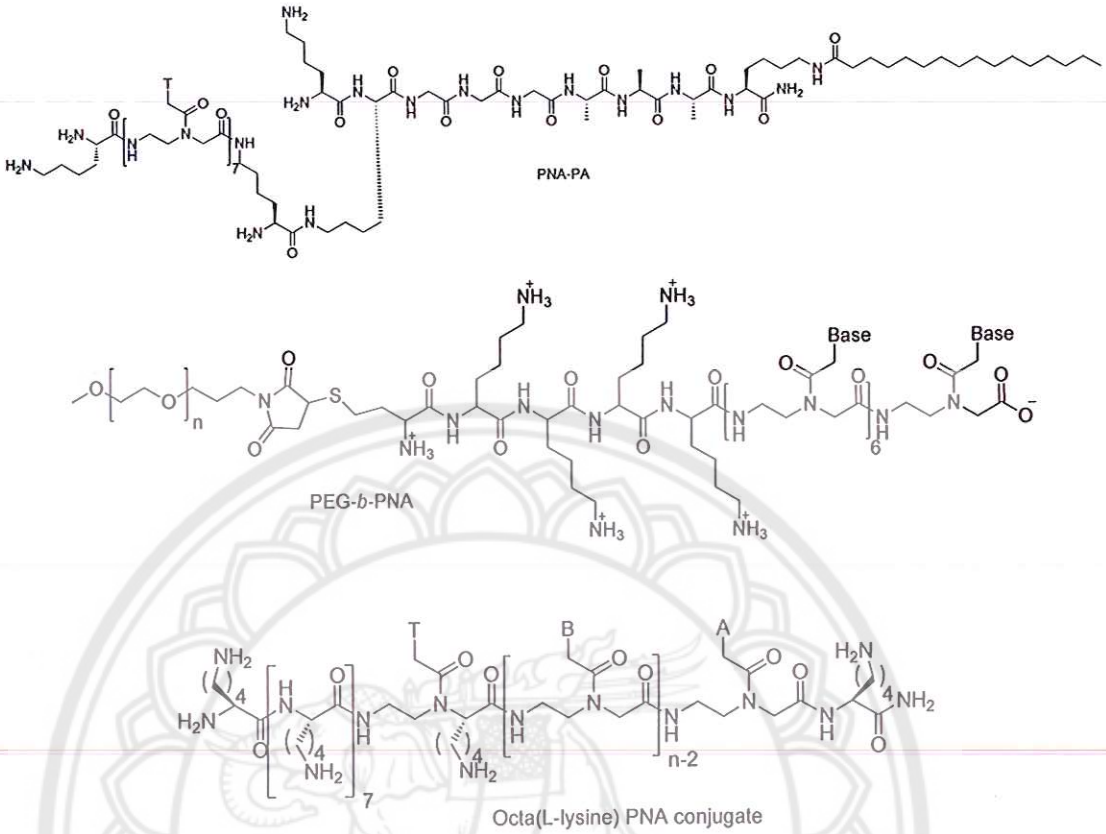

Figure 4 Examples of hydrophilic modification of PNA

In 2005, Vilaivan and colleagues proposed D-prolyl-2-aminocyclopentane carboxylic acid backbone (ACPC spacer) (**Figure 5**). [11] The ACPC spacer was developed from previous study of D-amino-pyrrolidine carboxylic acid (DAPC spacer). The result showed that (1*S*, 2*S*)-*acpc*PNA can bind with complementary DNA in 1:1 ratio. Furthermore, the DNA, *aeg*PNA and *acpc*PNA were compared the binding properties by surface plasmon resonance technique (SPR). [12] The SPR sensorgram of *acpc*PNA exhibited higher sequence specificity manner than the others. Among three PNA systems, the conformationally rigid structure of *acpc*PNA displayed the arrangement fit with target DNA.

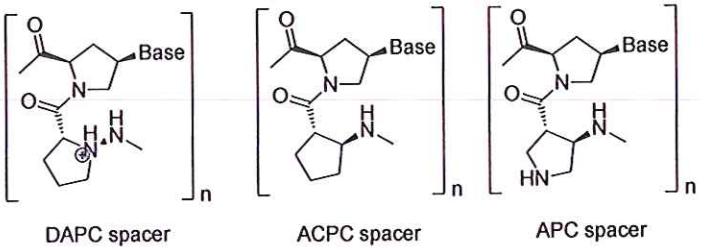

Figure 5 The structure of *dapc*PNA, *acpc*PNA and *apc*PNA

*acpc*PNA has been continuously developed by adding heteroatom as nitrogen in cyclopentane ring. In 2011, Reenubthue and co-worker successfully synthesized 3-aminopyrrolidine-4-carboxylic acid or APC spacer **(Figure 5)**. [13] The hybridization with DNA have been recognized by thermal melting temperature value (T_m) and showed slightly change from original *acpc*PNA. The modified *apc*PNA can be added functional group at nitrogen atom position with amide formation at any position in original *acpc*PNA sequence. Next, Ditmangklo and co-worker reported the fluorescence thiazole orange-labled on *apc/acpc*PNA. [14] The aldehyde function of thiazole orange reacted with nitrogen atom of APC spacer *via* reductive alkylation under mild condition click chemistry. The fluorescent probe on *apc/acpc*PNA and complementary DNA could form hybrid and exhibited strong signal and specificity.

However, *acpc*PNA system does not yet report about the development of water solubility and non-specificity binding prevention. In this work, *acpc*PNA system will be developed by labeling hydrophilic side chain to increase solubility, stability and reduce non-specific interaction. The hydrophilic side chains are used to hydrophilic labeled *apc/acpc*PNA such as 4-hydroxybutyl, 4-aminobutyl and 4-guanidinobutyl group by react with PNA by reductive alkylation in various positions of homothymine and mix base sequence. Then, the hydrophilic labeled *apc/acpc*PNA will be studied the bio-physical properties with DNA including water solubility.

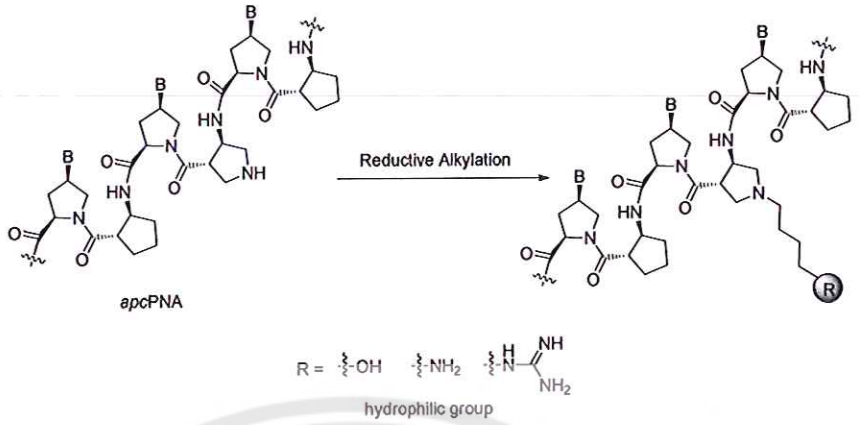

Figure 6 Synthetic plan of linker-modified hydrophilic *acpc*PNAs

Objectives of this research

1. Synthesis of aldehyde function of 3 hydrophilic side chain (4-trityloxy-1-butanal, 4-phthalimido-1-butanal and 4-guanidino-1-butanal)

2. Synthesis of hydrophilic labeled *apc/acpc*PNA by post synthetic reductive alkylation

3. Study the hybridization of hydrophilic labeled *apc/acpc*PNA with DNA and compared with unmodified *acpc*PNAs by thermal melting temperature (T_m) technique

4. Study the solubility properties of hydrophilic labeled *apc/acpc*PNA compared with unmodified *acpc*PNAs by UV spectroscopy

CHAPTER II

LITERATURE REVIEWS

The modification of *aeg*PNA for increase solubility

In 1999, Kuwahara, et al. reported new version of PNA; *oxy*PNA or OPNA (**Figure 7**). To addition the polarity into the molecule, the ether linkage was replaced in core structure of *aeg*PNA to improve hydrophilicity and water solubility. [15, 16] OPNA (A_{12}) hybrided with DNA (T_{12}) in 1:1 molar ratio while *aegPNA* (A_{12}) was binding DNA (T_{12}) in 1:2 ratio. The exhibiting of *aeg*PNA:DNA (1:2) was suggested turning point due to it has some unknown structure that coexists with the double-stranded form (**Figure 8A**). The researcher further studied chain-length and influence of nucleobase type on OPNA. The various length of o(A_n)-d(T_n) (n = 6, 9, 12 and 15) hybrids were measured in **Figure 8B**. The melting curve of n=12, the melting curves on heating were essentially the same as the association curves on cooling for all chain lengths examined. The sharp melting curves of the OPNA-DNA hybrids are advantageous in detecting mismatches in base sequences. showed very transitions that it has advantageous to detecting mismatch sequence. For influence of nucleobase type on OPNA, the melting temperature of purine rich on OPNA have more stable than pyridine rich on OPNA as shown in **Figure 8C**. Purine sequence of *aeg*PNA had limitation in application use due to its aggregation so that purine sequence of OPNA can be applied instead of *aeg*PNA. In addition, OPNA also showed stable hybridization in parallel direction and all or none type hybridization.

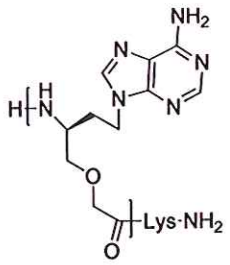

Oxy-PNA

Figure 7 The structure of *oxy*PNA

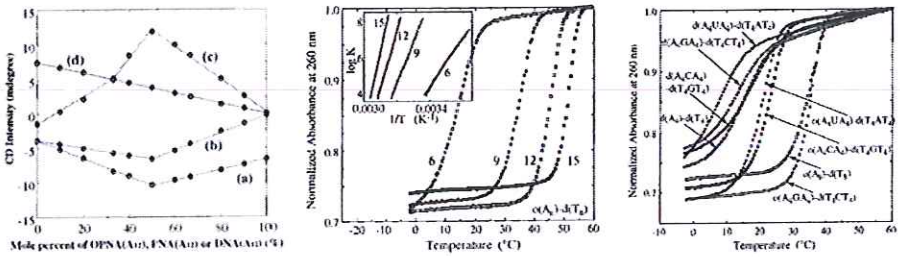

Figure 8 A) Job plots for CD intensities (a) DNA(A_{12})·DNA(T_{12}) (b) OPNA(A_{12}) DNA(T_{12}) (c) PNA(A_{12})·DNA(T_{12}) (d) OPNA(A_{12})·DNA(C_{12}) B) Temperature dependence of absorption intensity at 260 nm for equimolar mixtures of o(A_n)-d(T_n) with n= 6, 9, 12 and 15 and C) Melting curves of complementary hybrids of O(A_4NA_4)·d($T_4N'T_4$) pairs and d(A_4NA_4) d($T_4N'T_4$) pairs while N,N' = A, G, U(T) and C

In 2006, Dragulescu-Andrasi, et al. had developed the *aeg*PNA by adding amino acid at gamma position. [17] L-serine was selected because L-configuration is less disruptive than D-configuration. The hydroxyl group of serine can form hydrogen bond with water molecule to increase water solubility (**Figure 9**). The CD spectrum of synthesized PNA was shown in **Figure 10**. P1 does not exciton coupling pattern in nucleobase absorption regions (220-300 nm) when P2-P5 showed right handed helical characterization. When the number of lysine increased, the spectra at 210 nm showed clearly amplitude because of amide transition (n→π*). The stabilities of ^{L}S-γPNA (P2-P5) were investigated by melting transitions (T_m) experiment and compared with *aeg*PNA (P1). ^{L}S-γPNA·DNA duplex has more stable than *aeg*PNA·DNA duplex. The increasing T_m has ~2°C for DNA and ~3°C for RNA. For 3 units' modification, T_m values of P3 and P4 are not affecting significantly (**Table 1**). In addition, sequence specificity can observe by compare between *aeg*PNA (P1) and ^{L}S-γPNA (P5). ^{L}S-γPNA can form duplex with DNA and RNA (complementary and single-mismatch sequence) in **Figure 11**. The ΔT_m of P5 has more different than P1 and the ΔT_m of single-base mismatch hybridization of P5 was in the range of 16-19°C for DNA and 12-18°C for RNA. So that the addition of L-serine at gamma position on *aeg*PNA can hybridize and discriminate between complementary and single mismatch sequence.

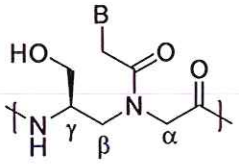

^{L}S-γPNA

Figure 9 The structure of L-serine derived γPNA

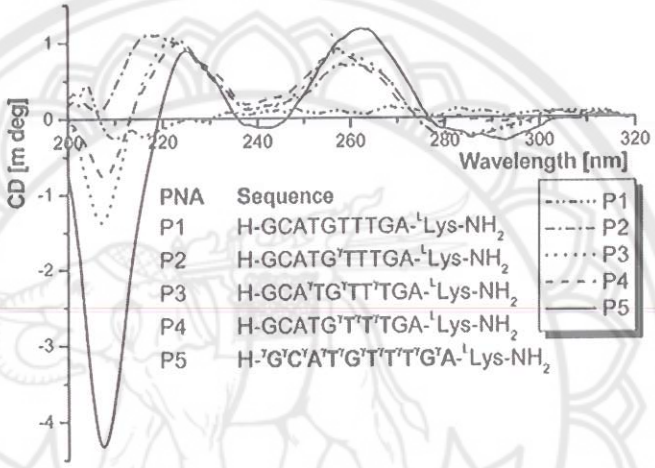

Figure 10 CD spectra of *aeg*PNA (P1) and modified ^{L}S-γPNA (P2-P5)

Table 1 T_m of hybridization between ^{L}S-γPNA-RNA with DNA and RNA

PNA	T_m of DNA	T_m of RNA	ΔT_m of DNA	ΔT_m of RNA
P1	44	54	-	-
P2	48	57	+4	+3
P3	53	60	+9	+6
P4	53	59	+9	+5
P5	63	64	+19	+10

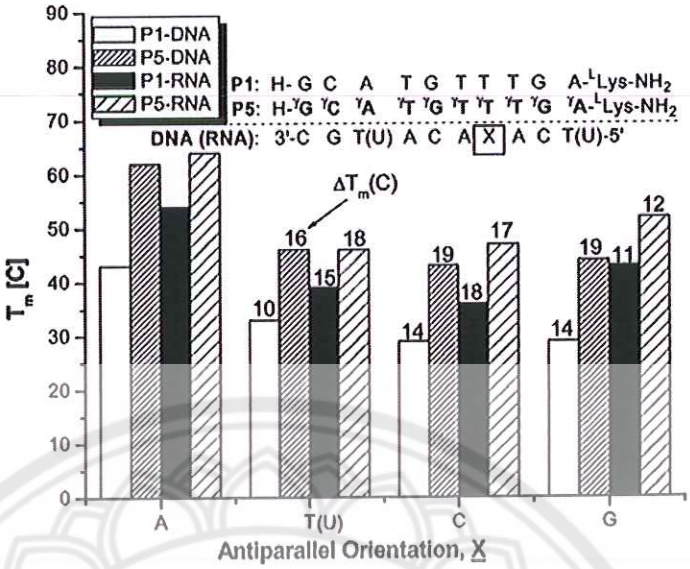

Figure 11 T_m's of *aeg*PNA(P1)-DNA, ^{L}S-γPNA(P5)-DNA, *aeg*PNA(P1)-RNA and ^{L}S-γPNA(P5)-RNA hybridization in the case complementary (X = A) and single mismatch sequence (X = T(U), C and G)

In 2005, Englund, E.A., et al. [18] had successfully developed novel stemless molecular beacon probe. The *γ*-position on *aeg*PNA was substituted by lysine (*S* configuration) and ethylene glycol for side chain to link with fluorophore **(Figure 12)**. The researcher selected *γ* position that able to tolerate a large fluorophore and no affected to duplex stability. Fluorene is a type of fluorophore which it can be quenched by thymine nucleobase *via* compaction or hydrophobic interaction in single strand. The fluroene is able to emit fluorescence signal in duplex due to decreasing the interaction with thymine residue **(Figure 13)**.

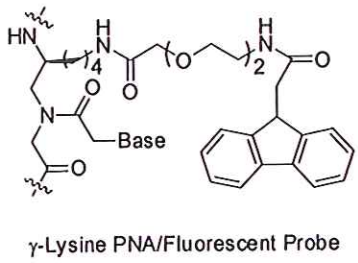

Figure 12 The structure of *γ*-Lysine PNA with fluorescent probe

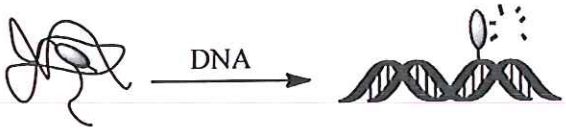

A

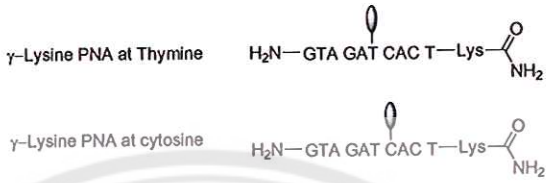

B

Figure 13 A) Stemless Molecular Beacon B) Sequence of *γ*-lysine PNA at thymine and *γ*-lysine PNA at cytosine

The results of thermal melting temperature (T_m) in **Table 2** showed the effect of *γ*-lysine PNA at thymine and cytosine position. The both PNA have slightly T_m higher than original *aeg*PNA. For fluorescent investigation, *γ*-lysine PNA at thymine position (PNA1) can bind with complementary DNA (~4 fold higher than single strand) and TT mismatch DNA (~2.5 fold higher than single strand) as shown in **Figure 14A** and site specific determination by added *γ*-lysine PNA at cytosine (PNA6) exhibited a similar increase as PNA1. The fluorene can quenched even if not directly incorporated on a thymine PNA residue (**Figure 14B).**

Table 2 Thermal melting temperature data (T_m) of hybridization between the modified PNA with complementary DNA (DNA2) and mismatch antiparallel DNA (DNA3-5) *in parentheses is ΔT_m between complementary duplex and single mismatch duplex

PNA	T_m(°C)			
	DNA2	DNA3	DNA4	DNA5
*aeg*PNA	48.9	36.0 (12.9)	34.0 (14.9)	32.0 (16.9)
γ-Lysine PNA at thymine	50.5	30.0 (20.5)	29.9 (20.6)	34.9 (15.6)
γ-Lysine PNA at cytosine	50.3		-	

* DNA2; 5'AGTGATCTA3', DNA3; 5'AGTGTTCTA3', DNA4; 5'AGTGGTCTA3' and DNA3; 5'AGTGCTCTA3'

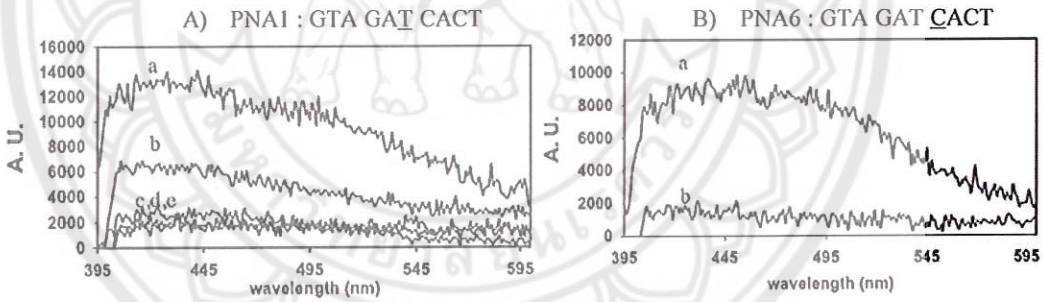

Figure 14 Fluorescence signal of hybridization A) PNA1 was hybrided with complementary DNA (a), mismatch DNA (b,c and d) and single stand PNA1 (e) B) PNA6 was hybrided with complementary DNA (a) and single stand PNA6 (b)

In 2003, Danith, H. Ly, et al. [19] had studied a novel PNA for anti-gene and anti-sense drug development. It is known that the original *aeg*PNA has some limitation about water solubility and aggregation. In this report, the researcher introduced guanidinium functional and ethylene glycol group into the PNA backbone to overcome the drawback of *aeg*PNA. (**Figure15**). It was found that the positive charge

at terminus of GPNA $(T_g)_{10}$ could improve water solubility and decrease aggregation in aqueous solution when compared with unmodified PNA. Furthermore, GPNA was attached fluorophore at *N* terminus and delivered into HCT116 cell. The fluorescent signal of GPNA was compared with the standard cell penetrating peptide (TAT). The results of GPNA exhibited remarkable cellular uptake properties while maintaining Watson-Crick recognition with complementary DNA strands (**Figure 16**).

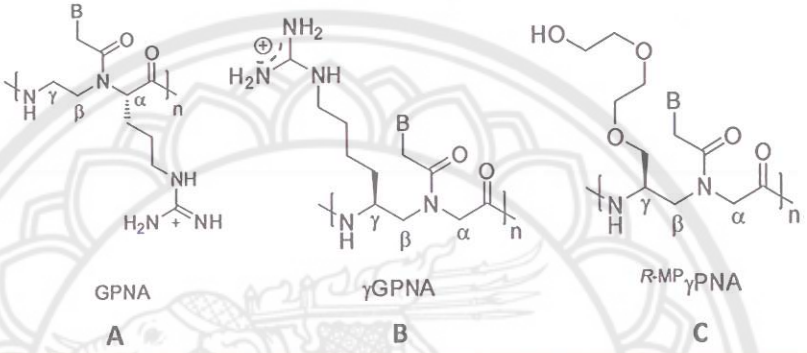

Figure 15 The structure of A) GPNA, B) *γ*GPNA and C) $^{R\text{-}MP}\gamma$PNA

Figure 16 Fluorescence microscope of HCT116 cells when TAT = Flu-Tyr-Gly-Arg-Lys-Lys-Arg-Arg-Gln-Arg-Arg-Arg

Later, Sahu, B., et al. [20] had further developed GPNA by attach the lysine moiety in gamma position. The terminal lysine was modified to guanidinium group in gamma position such as *γ*GPNA (**Figure 15B**). *γ*GPNA oligomers can hybridize with complementary DNA and RNA. The T_m data increased around 2°C when the number of gamma modification increased (**Figure 17**). Remarkably, the *S* configuration of guanidinium group can more improve than *R* configuration in binding properties with

DNA and RNA. The results in **Table 3** compared between γGPNA and unmodified PNA and showed that γGPNA is more stable and specific than unmodified PNA.

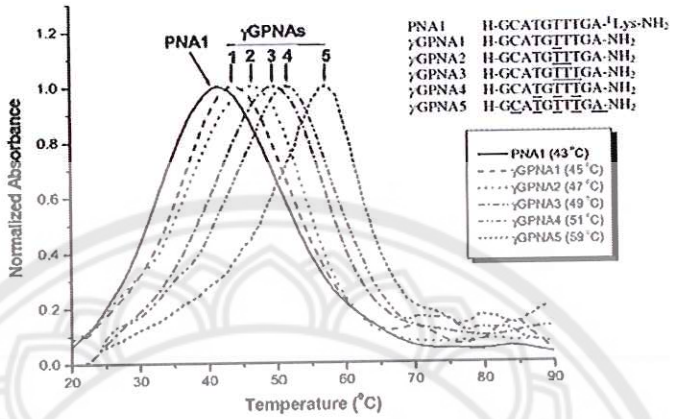

Figure 17 First derivative plot of thermal melting curve of PNA-DNA duplex and γGPNA-DNA duplex by vary the position (1, 2, 3, 4 and 5 positions)

Table 3 T_m of PNA and γGPNA with complementary DNA and single mismatch DNA

PNA : H-GCATGTTTGA-^{L}Lys-NH_2			DNAX : 3'-CGTACXAACT-5'		
γGPNA5 : H-GCATGTTTGA-^{L}Lys-NH_2			RNAX : 3'-CGUACXAACU-5'		
	PNA-DNAX	γGPNA-DNAX		PNA-RNAX	γGPNA-RNAX
X= A	43°C	59°C	X= A	50°C	60°C
X= C	25°C (-18)	39°C (-20)	X= C	33°C (-17)	40°C (-20)
X= G	25°C (-18)	40°C (-19)	X= G	40°C (-10)	48°C (-12)
X= T	32°C (-11)	40°C (-19)	X= T	39°C (-11)	49°C (-11)

*Parenthesis is ΔT_m between complementary duplex and single mismatch duplex.

TAMRA tags were also attached in *N* terminus of γGPNA for cellular uptake experiment as shown in **Figure 18**. γGPNA can penetrate into endoplasmic reticulum (ER) of HeLa cell because of electrostatic interaction between γGPNA and RNA molecule. The fluorescent signal was compared with the cell penetrating peptide (TAT) and concluded that γGPNA have utility for application to antisense, diagnostic and pharmaceutical science.

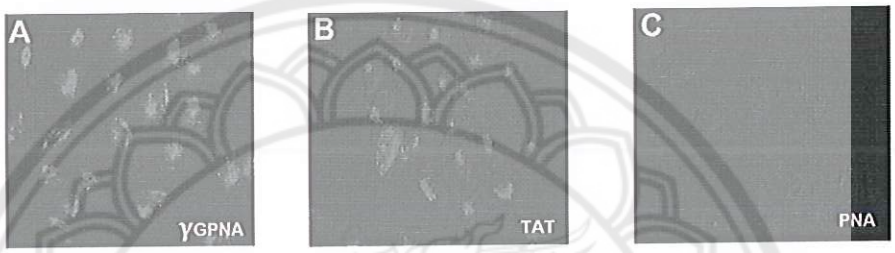

Figure 18 The fluorescent images of HeLa cells incubated with 1 μM of γGPNA6, TAT and PNA, respectively

The other study on γPNA was operated by the same group; the water solubility of γGPNA was evaluated by adding hydrophilic group as (*R*)-diethylene glycol at gamma position of PNA backbone (**Figure 15C**). The reason for using (*R*)-diethylene glycol (R-MP) is its small size, hydrophilic and nontoxicity to cell. [21] $^{R\text{-}MP}$γPNA1 (H-GCATGTTTGA-NH_2) was modified by introducing R-MP group for 10 units. Thermal melting temperature (T_m) showed at 68°C for $^{R\text{-}MP}$γPNA1 and 45°C for unmodified *aeg*PNA when it hybridized with DNA target. From these results, it can be concluded that the addition of diethylene glycol can enhance the binding properties 2.3°C per R-MP unit.

Furthermore, water solubility characterization and self-aggregation were investigated. The unmodified *aeg*PNA (H-ACGGGTAGAATAACAT-NH_2) can be aggregated at the saturated concentration 39 mM. $^{R\text{-}MP}$γPNA2 (H-ACGGGTAGAA TAACAT-NH_2) was modified R-MP group in 8 position which affected to aggregation at the saturated concentration over 500 mM. $^{R\text{-}MP}$γPNA2 was also evaluated self-aggregation by Forster resonance energy transfer (FRET) technique.

The FRET experiment consisted of fluorophore donor (FITC) and fluorophore acceptor (TAMRA). The FITC probe was attached at *N* terminus of *aeg*PNA-X and $^{R\text{-}MP}\gamma$PNA-X. The TAMRA probe was attached at C terminus of *aeg*PNA-Y and $^{R\text{-}MP}\gamma$PNA-Y. *aeg*PNA-X sequence was aggregated together with *aeg*PNA-Y sequence owning to energy transfer of FITC to TAMRA *via* FRET phenomenon. Thus, TAMRA look emitting at wavelength 583 nm whereas $^{R\text{-}MP}\gamma$PNA-X and $^{R\text{-}MP}\gamma$PNA-Y do not showed the signal of TAMRA emission. This result presented effectively solubility and reduced aggregation of $^{R\text{-}MP}\gamma$PNA (**Figure 19**).

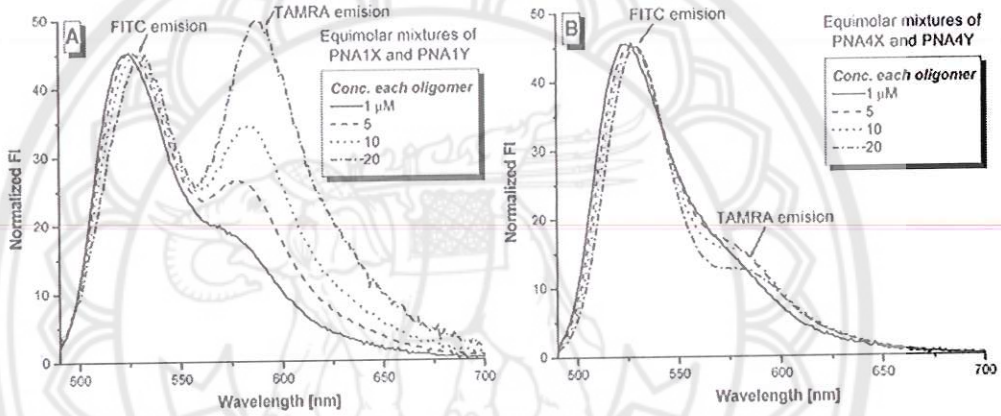

Figure 19 A) Fluorescent spectra of *aeg*PNA-X·*aeg*PNA-Y B) Fluorescent spectra of $^{R\text{-}MP}\gamma$PNA-X·$^{R\text{-}MP}\gamma$PNA-Y

In part of non-specific interaction study, *aeg*PNA, $^{R\text{-}MP}\gamma$PNA2 and non-complementary DNA were investigated by gel-shift assay as shown in **Figure 20**. The concentration of 10 μM *aeg*PNA on gel electrolysis (PNA:DNA ratio; 25:1) displayed slightly color band of DNA when the increasing concentration of *aeg*PNA. It does not seem to any band of DNA to precipitate *aeg*PNA·DNA in solution and non-specific interaction with plastic. In contrast, $^{R\text{-}MP}\gamma$PNA2 is very clearly to DNA band because the modified PNA can reduce non-specific interaction.

*aeg*PNA : H-ACGGGTAGAATAACAT-NH_2

$^{R\text{-}MP}\gamma$PNA2 : H-ACGGGTAGAATAACAT-NH_2

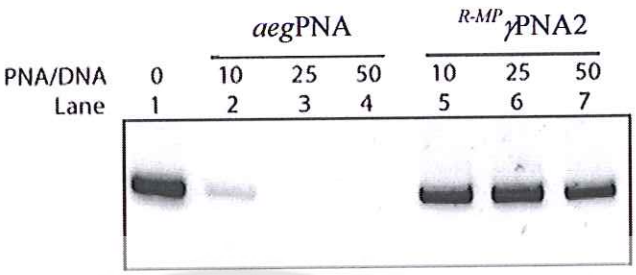

Figure 20 The results of gel-shift assay at various concentration of PNA

All results confirmed that the addition of hydrophilic (*R*)-diethylene glycol at gamma position can improve solubility, nontoxicity, reduce nonspecific binding and aggregation by solvation of MP side chain.

In 2013, Goldman, J.M., et al. [22] designed novel γ-Peptide Nucleic Acid Amphiphile (γPNAA). The polyethylene glycol and long chain hydrocarbon group was added on *aeg*PNA in order to produce hydrophilic and hydrophobic properties in the same molecule (**Figure 21**). DNA probe, γPNAA probe and target DNA were produced in the form of sandwich hybridization. Capillary electrophoresis (CE) is a type of molecular separation techniques which can consider the different sizes of interest molecule. For synthesis of γPNAA, polyethylene glycol was attached in gamma position and long chain hydrocarbon was attached at the terminus of *aeg*PNA. The functional groups are able to enhance solubility and help to isolate in CE. The electropherogram showed non hybrid and hybrid sandwich in different time due to unequal size of molecule (**Figure 22**). The perfect match and mismatch sequence of DNA can isolate at high temperature (40 °C). Moreover, this work can efficiently apply to miRNA detection. And this work can confirmed that the diethylene glycol or polyethylene glycol group can improve solubility in PNA molecule.

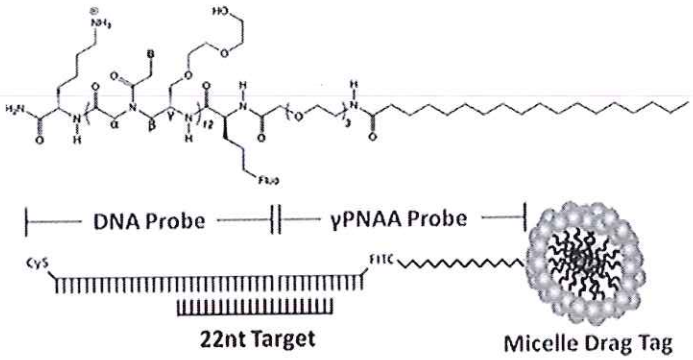

Figure 21 The structure of γPNA Amphiphile (C to N) and sandwich hybridization of short nucleic acids and interaction with micelle drag tags

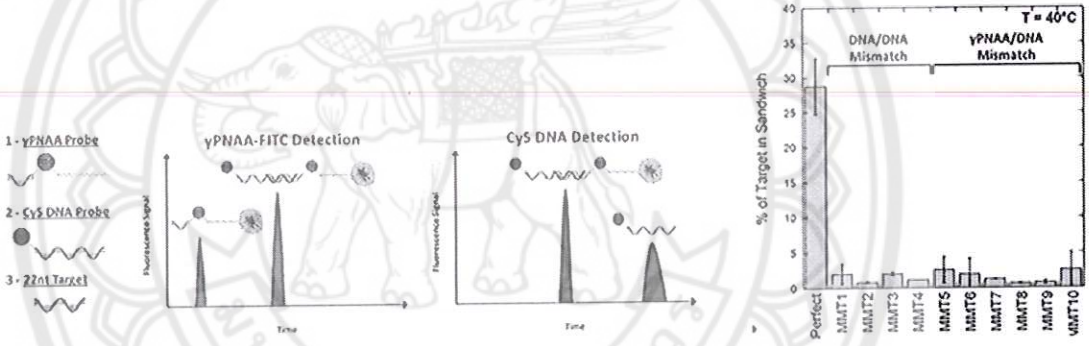

Figure 22 Detection of sandwich hybridization by electropherogramand graph between %target of sandwich and single base mismatch at 40°C

In 2014, Jain, D. R., et al. [23] modified the other version of PNA system by focusing on improvement in aqueous solubility properties. In this article, gamma position of PNA was modified by adding ethylamino (*eam*) and ethyleneguanidino (*egd*) as shown in **Figure 23**. The number of *γ*-(*S*-*eam*) and *γ*-(*S*-*egd*)-*aeg*PNA were designed by replacing *eam* and *egd* in *N*-/*C*-terminus and center position of PNA oligomers as shown in **Table 4**. P2-P10 (1 to 3 units) can significantly enhance the stability of PNA·DNA duplex compared with unmodified PNA (P1). The efficacy of *eam* and *egd* groups was depend on the nature of cationic group, position and numbers of modifications. The *eam* and *egd* at C-terminus were stabilized in PNA·DNA

duplexes better than center and *N*-terminus as shown in **Figure 24**. Besides, ΔT_m's of *eam* and *egd* PNAs have a range of -10 to -18.5°C when compared with unmodified PNA (6°C) which depending on the number of modifications.

In summary, the all modified PNAs have high stability, sequence specificity and high binding affinity. The guanidino-modified PNAs have more stability than amino-modified PNAs because of charge-charge interaction between permanent positive charged guanidino group and negatively charge of DNA.

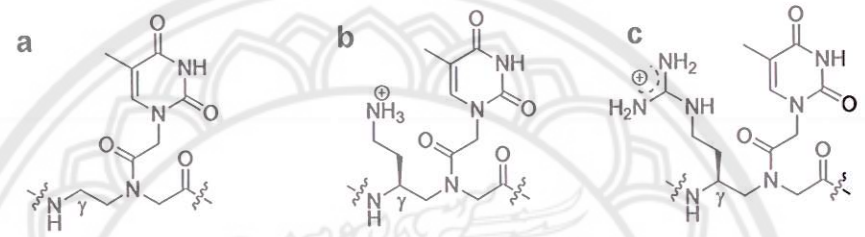

Figure 23 The structures of a. *aeg*PNA b. *γ*-(*S-eam*)-*aeg*PNA and c. *γ*-(*S-egd*)-*aeg*PNA

Table 4 PNA oligomers and UV-T_m (°C) values of PNA·DNA and PNA: RNA Duplexes

Entry	Oligomers	Sequences	DNA1	DNA2	RNA1
P1	*aeg*-PNA	H-T T A C C T C A G T-LysNH$_2$ 1 2 3 4 5 6 7 8 9 10	43.4	37.4	36.3
P2	eam-t$_{2a}$-PNA	H-T t$_a$ A C C T C A G T-LysNH$_2$	47.3	36.7	58.2
P3	eam-t$_{6a}$-PNA	H-T T A C Ct$_a$ C A G T-LysNH$_2$	47.1	35.0	57.2
P4	eam-t$_{10a}$-PNA	H-T T A C C T C A G t$_a$-LysNH$_2$	49.2	36.2	59.6
P5	eam-t$_{2a,6a}$-PNA	H-T t$_a$ A C Ct$_a$ C A G T-LysNH$_2$	49.7	37.2	59.3
P6	egd-t$_{2\gamma}$-PNA	H-T t$_\gamma$ A C C T C A G T-LysNH$_2$	45.9	35.4	55.3
P7	egd-t$_{6\gamma}$-PNA	H-T T A C Ct$_\gamma$ C A G T-LysNH$_2$	48.8	36.3	55.3
P8	egd-t$_{10\gamma}$-PNA	H-T T A C C T C A G t$_\gamma$-LysNH$_2$	52.0	37.0	61.2
P9	egd-t$_{2\gamma,6\gamma}$-PNA	H-T t$_\gamma$ A C Ct$_\gamma$ C A G T-LysNH$_2$	51.9	38.4	62.0
P10	egd-t$_{2\gamma,6\gamma,10\gamma}$-PNA	H-T t$_\gamma$ A C Ct$_\gamma$ C A G t$_\gamma$-LysNH$_2$	57.4	38.9	63.0

** t_a = ethyleneamino (*eam*) modified PNA-T unit and t_γ = ethyleneguanidino (*egd*) modified PNA-T unit. DNA1 (ap; antiparallel) = 5′ACTGAGGTAA 3′; DNA2 (mm;mismatch) = 5′ACTGCGGTAA 3′; RNA1 (ap; antiparallel) = 5′ACUGAGGUAA 3′. All samples were prepared in 10 mMsodiumphosphate buffer containing 10 mM NaCl and 0.1 mM EDTA at 2 μM strand concentration each. The T_m's are accurate up to ±0.5 °C.

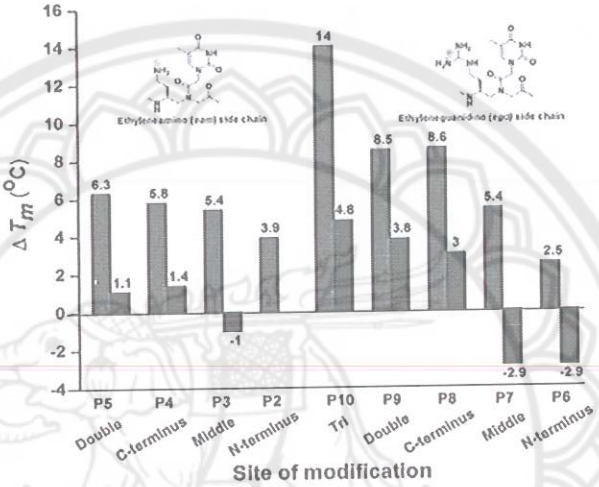

Figure 24 Comparative ΔT_m values for PNA·DNA and PNA·RNA duplexes

For cellular uptake study, PNA oligomers were attached with 5(6)-carboxyfluorescein at *N*-terminus (**Table 5**) and treated in NIH 3T3 and MCF-7 cell. Laser confocal microscopy was used for monitoring PNA oligomers in the cell. The fluorescent signal displayed bright cytoplasm around nuclear membrane as shown in **Figure 25** that insist efficiently cell permeability of modified PNAs.

Table 5 The fluorescein at N-terminus of modified PNA oligomers

Entry	Oligomers	Sequences
*cf*P1	*aeg*-PNA-*cf*	*cf*-T T A C C T C A G T-LysNH$_2$
*cf*P2	eam-t_{2a}-PNA-*cf*	*cf*-T t_a A C C T C A G T-LysNH$_2$
*cf*P5	eam-$t_{2a,6a}$-PNA-*cf*	*cf*-T t_a A C Ct_a C A G T-LysNH$_2$

Table 5 (cont.)

Entry	Oligomers	Sequences
*cf*P6	egd-$t_{2\gamma}$-PNA-*cf*	*cf*-T t_γ A C C T C A G T-LysNH_2
*cf*P9	egd-$t_{2\gamma,6\gamma}$-PNA-*cf*	*cf*-T t_γ A C Ct_γ C A G T-LysNH_2
*cf*P10	egd-$t_{2\gamma,6\gamma,10\gamma}$-PNA-*cf*	*cf*-T t_γ A C Ct_γ C A G t_γ-LysNH_2

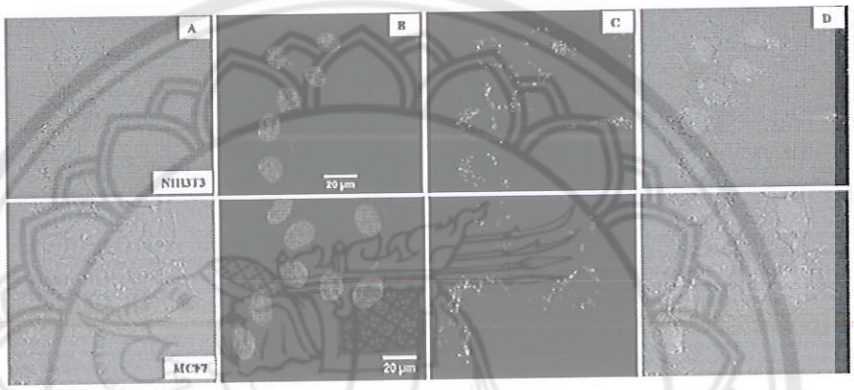

Bright-field image | Hoechst 33342 stained image | Green fluorescent image | Superimposed image of A, B, and C

Figure 25 Distribution of three guanidino-modified PNA (*cf*P10) inside NIH 3T3 and MCF-7 cells

Pyrrolidine PNA system

Conformationally constrained pyrrolidinyl PNA system was previously reviewed by Kumar. V. A. and coworker. [24] They studied pyrrolidine ring structure base on *aeg*PNA system. The modified structure-PNA system, the methylene or carbonyl bridge was used for connecting carbon position ($\alpha, \beta, \alpha', \beta'$ or α'') in some PNA unit. The hybridization of most PNA with DNA target presents stable affinity and base specificity. In some cases, conformationally constrained cyclic structure can increase rigidity to structure and it can either increase or reduce stable hybridization **(Figure 26)**.

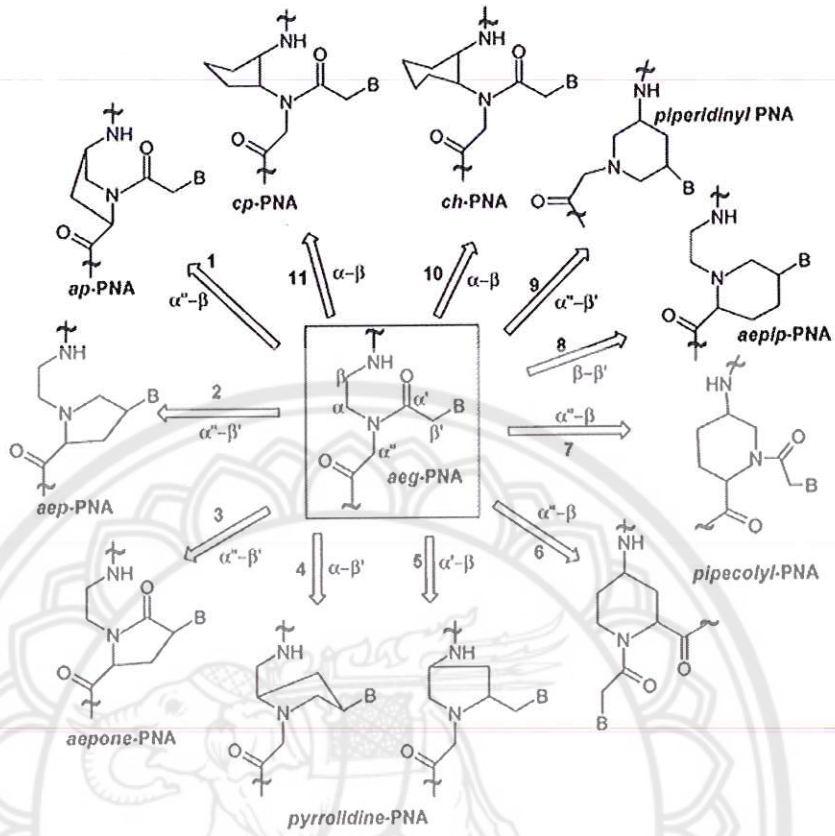

Figure 26 The structure of PNA base on pyrrolidine ring modification

One of interesting conformationally constrained pyrrolidinyl PNA system is pyrrolidinyl PNA (D-prolyl-2-aminocyclopentane carboxylic acid backbone) so called *acpc*PNAs that reported by Vilaivan and coworker. [11] ACPC system consisted of 2 components as pyrrolidine cyclic (2'*R*,4'*R*-hydroxyproline) and *β*-amino acid containing five-membered ring (**Figure 27**). ACPC structure has possible four configurational isomer such as 1*S*,2*S*-ACPC, 1*R*,2*R*-ACPC, 1*S*,2*R*-ACPC and 1*R*,2*S*-ACPC and make its a high rigid molecule. Their structures were studied the hybridization with complementary DNA as shown in **Figure 28**. The only *trans*-(1*S*, 2*S*)-2-aminocyclopentanecarboxylic acid, *SS*-ACPC can from stable hybrid to DNA in 1:1 ratio and discriminated between single mismatch and complementary sequence (ΔT_m 18-25°C). Their properties can applied in diagnosing genetic diseases or the investigation of base sequence on DNA.

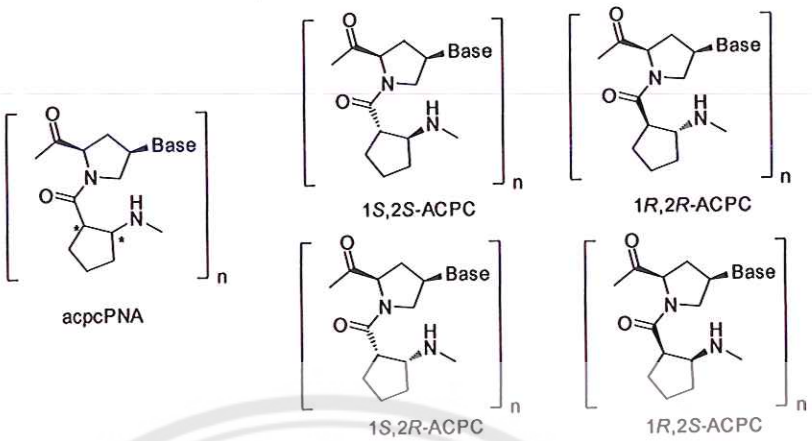

Figure 27 The structure of *acpc*PNA

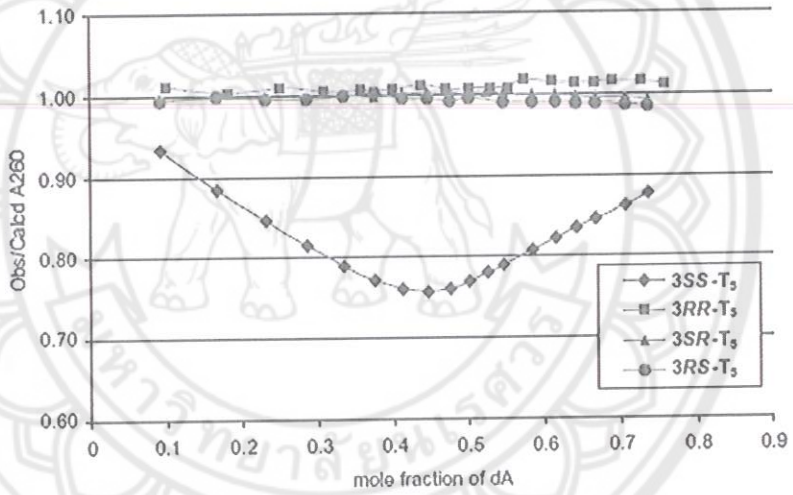

Figure 28 UV titration plot of poly(dA) and all four isomers of PNA

In 2006, Srisuwannaket, et al. [25] studied the influence of base sequence of *SS*-ACPC to DNA binding properties. The *acpc*PNA can usually hybrid with DNA in accordance to Watson-Crick base pairing rule (A·T, C·G). Base specificity were determined by sequence TTTTXTTTT (X= T, A, G and C) and DNA sequence AAAAYAAAA (Y= A, T, C and G). T_m data showed that *acpc*PNA can bind with complementary DNA more apparently stable than mismatch DNA as shown in **Figure 29**.

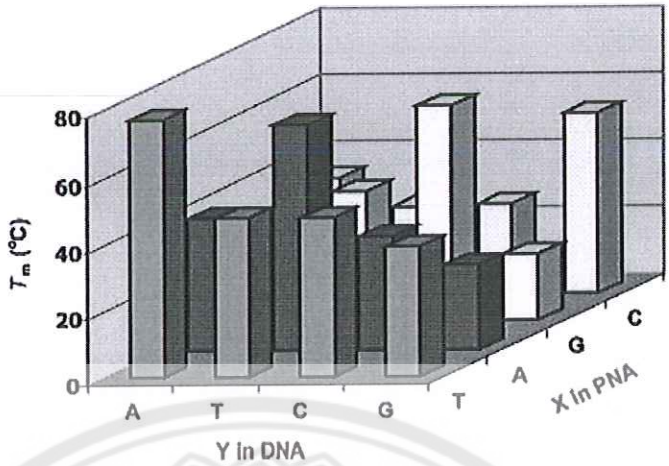

Figure 29 The melting temperature of hybridization between PNA·DNA (pT_4XT_4 with dA_4YA_4 ; X,Y= A, T, C and G)

In addition, the direction of unsymmetrical mix base sequence was studied and indicated that *acpc*PNA can bind in antiparallel. The T_m data in **Table 6** showed the thermal melting temperature between *acpc*PNA and complementary or mismatch DNA. The decreasing T_m value of single mismatch DNA was considered from reducing in a range of 23.8-28.7 °C for *acpc*M10 and 12.6-16.5 °C for *acpc*M15. The discrimination of T_m can explain the difference between complementary and single mismatch DNA binding of this PNA system which can be considered as DNA sensor probe in biotechnology work.

Table 6 The results of thermal melting temperature of *acpc* M10 and *acpc* M15 with DNA

Direction and DNA	*acpc*PNA M10 : GTA GAT CAC T		*acpc*PNA M15 : TGT ACG TCA CAA CTA	
	DNA (5'-3')	**T_m(°C)[b]**	**DNA (5'-3')**	**T_m(°C)[c]**
Parallel	CATCTAGTGA	<20	ACATGCAGTGTTGAT	<20 (56)
Antiparallel	AGTGATCTAC	57.6	TAGTTGTGACGTACA	78.6, 73.7 (69)

Table 6 (cont.)

Direction and DNA	*acpc*PNA M10 : GTA GAT CAC T		*acpc*PNA M15 : TGT ACG TCA CAA CTA	
	DNA (5'-3')	T_m(°C)[b]	**DNA (5'-3')**	T_m(°C)[c]
Single-mismatch antiparallel	AGTGTTCTAC	33.8	TAGTTGTTACGTACA	63.1, 59.1 (51)
	AGTGCTCTAC	31	TAGTTGTAACGTACA	65.0, 61.0 (49)
	AGTGGTCTAC	28.9	TAGTTGTCACGTACA	65.2, 61.1 (50)

[b] Measured at [NaCl] = 0 mM.

[c] Measured at [NaCl] = 0, 100 mM; values in parentheses are the corresponding T_m of PNA 1 at [NaCl] = 100 mM taken from ref 26.

In 2010, Ananthanawat, et al. [12] reported the face-to-face comparison of *acpc*PNA and *aeg*PNA in case of DNA hybridization. Surface plasmon resonance technique (SPR) was used in this study. Hybridization efficiency (%HE) was determined the binding properties in aqueous condition. For starting up, *acpc*PNA·DNA and *aeg*PNA·DNA duplex have 19 and 30%HE respectively and enhance the hybridization by increasing ionic strength concentration. However, if the NaCl concentration has over 250 mM, the hybridization of *aeg*PNA·DNA was decrease stability from 60% to 50% due to polyelectrolyte while the %HE of *acpc*PNA·DNA have slightly change. (**Figure 30**). In addition, sensorgram graph (**Figure 31**) displayed binding signal between *acpc*PNA and complementary DNA while no binding signal between *acpc*PNA and mismatch DNA so that *acpc*PNA has selectivity and discriminate between mismatch and complementary DNA.

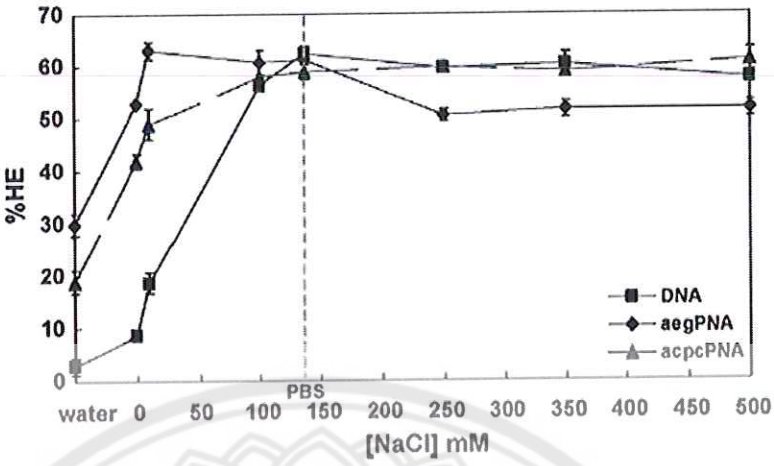

Figure 30 %Hybridization efficiency of DNA, *acpc*PNA and *aeg*PNA was immobilized on surface with biotin and complementary DNA in NaCl concentration condition since 0-500 mM

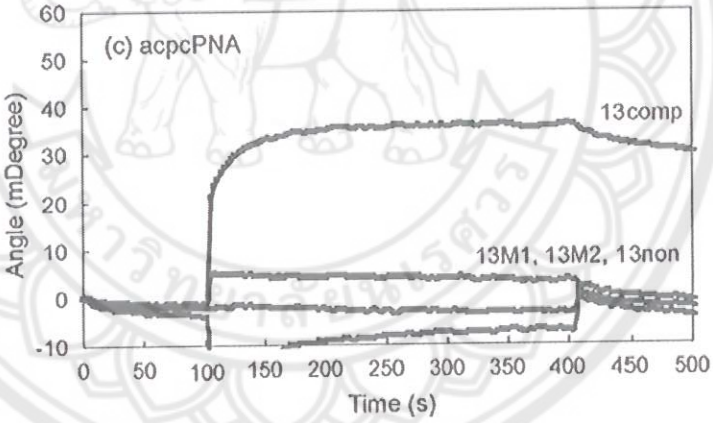

Figure 31 SPR sensorgram between *acpc*PNA and DNA. Sequence of *acpc*PNA5'(N)-biotin-linker-TTCCCCTTCCCAA-3'(C) DNA 13comp (TTGGGAAGGGGAA) 13M1 (TTGGGAGGGGGAA) 13M2 (TTGGGCACGGGAA) and 13non (TAGTTGTTACGTACA)

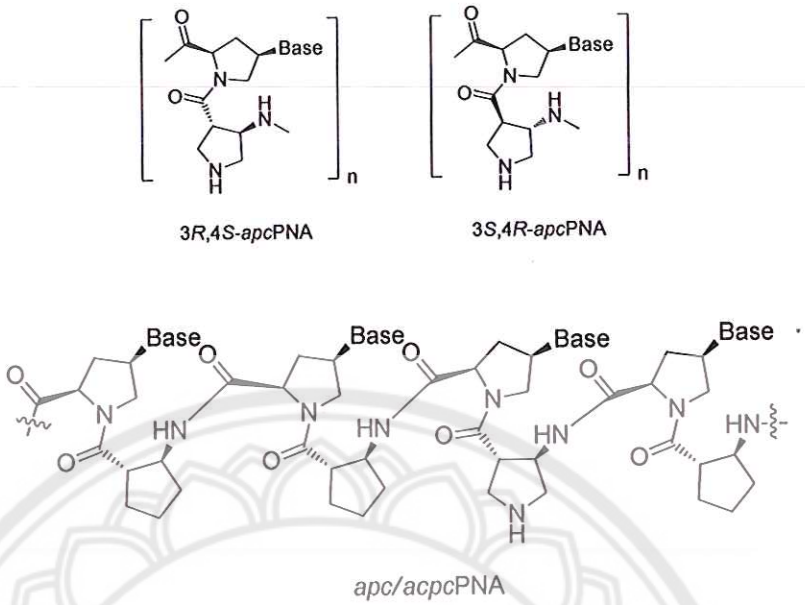

Figure 32 The structure of *apc*PNA and *apc/acpc*PNA

In 2011, Reenabthue, et al. [13] further developed *acpc*PNA system. The nitrogen atom was replaced into a part of aminocyclopentanecarboxylic acid (ACPC). 3-aminopyrrolidine-4-carboxylic acid (APC) is consisting of (3*R*,4*S*)-APC and (3*S*,4*R*)-APC as shown in **Figure 32** and verify hybridization properties by thermal melting temperature. The fully and internal modified (3*R*,4*S*)-APC-T9 can form stable hybrid with complementary DNA. On the other hand, (3*S*,4*R*)-APC showed unstable hybridization because of T_m value down to 20°C. The T_m value in **Table 7** indicate that 3*R*,4*S* stereoisomer have effectively binding affinity. Outstandingly, PNA3 has T_m value at 71.1°C which slightly decreased compared with unmodified *acpc*PNA (ΔT_m - 1.4°C). The binding of 3*R*,4*S*-APC confirmed by UV titration experiment. PNA1 and PNA3 could form hybrid with DNA as shown in **Figure 33.** The advantage of APC system is that it can add other functional group at nitrogen atom of cyclopentane ring such as fluorescence tag, hydrophilic group. This can open up the plenty modification on *acpc*PNA.

Table 7 Thermal melting temperature data of *acpc/acp*PNA

PNA	Sequence (N→C)	T_m (°C)
PNA1	Bz-TTTTTTTTT-LysNH$_2$	55.5
PNA2	Bz-TTTTTTTTT-LysNH$_2$	<20
PNA3	Bz-TTTTTTTTT-LysNH$_2$	71.1
PNA4	Bz-TTTTTTTTT-LysNH$_2$	28.3
PNA5	Bz-GTAGATCACT-LysNH$_2$	50.8
PNA6	Ac-TTTT(^{Py})TTTTT-LysNH$_2$	62.2
PNA7	Ac-GTAGA(^{Py})TCACT-LysNH$_2$	44.3

T = *ss*ACPC-T; T = (3*R*,4*S*)-APC-T, T = (3*S*,4*R*)-APC-T; (Py) = pyrene-1-carbonyl binding with complementary DNA (dA9 for PNA1–PNA4 and PNA6, dAGTGATCTAC for PNA5, PNA7 and PNA8). Values refer to the T_m decrease relative to that of unmodified acpcPNA under identical conditions (T_m of hybrids with complementary DNA Ac-TTTTTTTTT-LysNH$_2$: 72.5 °C; Ac-GTAGATCACT-LysNH$_2$: 52.2 °C).

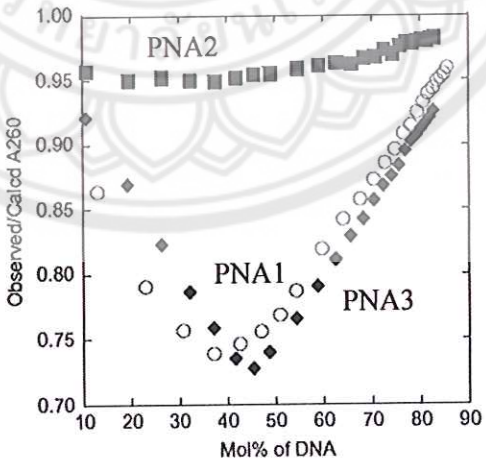

Figure 33 UV titration of *apc/acpc*PNA and their complementary DNA (dA9)

CHAPTER III

RESEARCH METHODOLOGY

General Procedure

1. Instrument

All reaction was performed in oven-dried glassware. The weights of all chemicals were determined by the Metler Toledo electrical balance and Sartorious electronic analytical balance. The solvent evaporation was carried out on diaphragm pump, a Refco Vacubrand pump and Büchi Rotavapor R-200 with a water aspirator model B-490. The reaction process was used the magnetic stirred and heater of Heidolph and HARMONY. ^{1}H and ^{13}C spectra were recorded on Bruker Avance 400 NMR spectrometer operating at 400 MHz for ^{1}H and 100 MHz for ^{13}C and Varian Mercury-400 plus. FT-TR spectrum was recorded on Perkin Elmer spectrum GX FT-IR spectrometer. Reverse phase high performance column chromatography (reverse phase HPLC) was performed on Water Delta 600 controller system equipped with a gradient pump and a Water 2996 photodiode array detector, column for separation: ACE 5 A71197, C18-AR, 150 x 4.6 mm, 5 μm particle size and analysis: UPS, 50 x 4.6 mm, 3 μm particle size. The fraction compounds after HPLC were freezed and lyophilized on a Freeze dryer (Labconco). MALDI-TOF mass spectra were obtained on a Microflex MALDI-TOF mass spectrometry (Bruker Daltonik GmbH, Bremen, Germany). UV absorption and Thermal melting temperature (T_m) cures were measured on 260 nm with a CARY 100 Bio UV-Visible spectrophotometer (Varian). Circular dichroism (CD) spectra were performed a JASCO J-815 CD spectrometer. Optical density (OD) was determined by Nanodrop 2000. High resolution mass spectrometry (HRMS) was performed on a MicroTOF (Bruker) spectrometer (Department of Chemistry, Faculty of Science, Mahidol University).

2. Materials

The all chemicals were purchased from Merck, Fluka, Acros Organics or Aldrich Chemical Co., Ltd. These chemicals were used without purification.Solvent for reaction and crystallization was reagent grade. Commercial grade solvents received

from UCI Labscan and silica gel 70-230 mesh for column chromatography. Thin layer chromatography (TLC) from MERK D.C. silica gel 60 F_{254}0.2 MM and visualized using UV light 254 nm was monitored reaction. Methanol for HPLC experiment was HPLC grade and MilliQ water from Ultrapure water system with Millpak® 40 filter unit 0.22 μM, Millipore (USA) was filtered through membrane filter (13mmΦ, 0.45 μM, Nylon). The solid phase peptide synthesis consisted of Tenta gel S RAM resin and Trifluoroacetic acid 98% from Fluka. Fmoc-Lys(Mtt)-OH and Fmoc-L-Lys(Boc)-OPfp was obtained from Calbiochem Novabiochem Co. Ltd. *N,N'*-dimethylformamide for coupling reaction was obtained from RCILabscan. Acetic anhydride was obtained from IDB, Laboratory Reagent and JTBaker.Nitrogen gas was obtained from Thai Industrial Gas (TIG) purity 99.5%. 5(6)-Carboxyfluorescein*N*-hydroxysuccinimide ester was obtained from Sigma-Aldrich. The oligonucleotides were purchased from Pacific Science (Bangkok, Thailand) or BioDesign Co., Ltd. (Bangkok, Thailand). The PNA monomers (A, T, C, and G), ACPC spacer was supported by Vilaivan research group at Chulalongkorn university. APC spacer was synthesized according to previous report. [25]

Experiment Procedure

1. **Synthesis of aldehyde modifier**

1.1 Synthesis of 4-trityloxy-1-butanol [27]

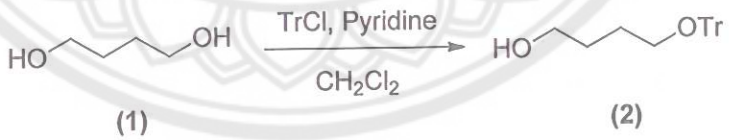

1,4-Butanediol 13.65 mL (150 mmol) and pyridine 2.42 g (30 mmol) was dissolved in 20 mL of CH_2Cl_2. Triphenylmethylchloride (TrCl) 5.14 g (15 mmol) was add to the reaction over 5 min. The solution was stirred at room temperature for 3 h to reaction completely (R_f 0.38 used Hexane:EtOAc ratio 3:1). After that, 30 mL of brine was added to the solution and extracted with CH_2Cl_2 (50 mLx3). The organic layer was dried over anhydrous $MgSO_4$ and the solvent was removed. The purification of product by column chromatography with EtOAc:Hexane as an eluent (1:2) to obtain

a white solid in 4.53g (92.4%yield). This product was confirmed by ^{1}H NMR spectroscopy and compared with a reference. [27]

^{1}H NMR (400 MHz, $CDCl_3$) :δ_H 1.69 [4H, *m*, C<u>H</u>$_2$C<u>H</u>$_2$], 3.13 [2H, *t*, *J*=6 Hz, C<u>H</u>$_2$OTr], 3.63 [2H, *t*, *J*=6 Hz, C<u>H</u>$_2$OH], 7.22-7.34 [9H, m, C<u>H</u>-Benzene], 7.44-7.46 [6H, m, C<u>H</u>-Benzene] ^{13}C NMR (400 MHz, $CDCl_3$) : δ_C 26.7, 30.1, 63.0, 63.6, 127.1, 127.9, 128.8, 129.8, 144.4.

1.2 Synthesis of 4-trityloxy-1-butanal

4-Trityloxy-1-butanol 2.30 g (7.12 mmol) was dissolved in DMSO 5 mL. Iodobenzoic acid (IBX) 2.10 g (7.5 mmol) was added and stirred at room temperature until reaction was completed (R_f 0.69 used Hexane:EtOAc ratio 2:1). EtOAc (20 mL) was added to solution and solid was filtrated out. The solution was extracted with brine (10 mL) and EtOAc (20mLx3). The organic layer was separated and the solvent removed and then purified by column chromatography with Hexane:EtOAc ratio (2:1) to obtain produce as a colorless oil 1.91 g (81.3%yield).

^{1}H NMR (400 MHz, $CDCl_3$): δ_H 1.96 [2H, *m*, C<u>H</u>$_2$], 2.56 [2H, *t*, *J* = 8.0 Hz, C<u>H</u>$_2$CHO], 3.16 [2H, *t*, *J* = 8.0 Hz, C<u>H</u>$_2$OC(C_6H_5)$_3$], 7.24-7.34 [6H, *m*, C<u>H</u>-Benzene], 7.44-7.45 [9H, *m*, C<u>H</u>-Benzene], 9.81 [1H, *s*, C<u>H</u>O] ^{13}C NMR (100 MHz, $CDCl_3$): δ_C 23.0, 41.2, 62.7, 127.1, 127.9, 128.8, 144.3, 202.5 HRMS (ESI+): m/z calcd for $C_{23}H_{22}O_2$: 353.1512 $[M+Na]^+$ found : 353.1508

1.3 Synthesis of 4-guanidino-butanol [28]

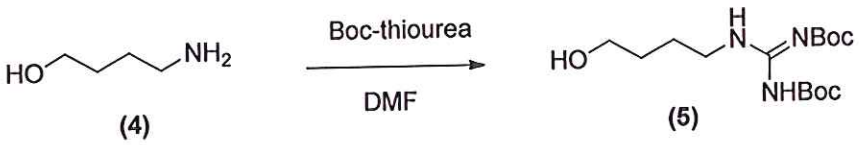

4-Amino-1-butanol 0.90 mL (10 mmol) was dissolved with 5 mL of DMF and added Boc-thiourea 2.82 g (10.2 mmol). Sulfur dioxide was occurred in the reaction and monitored to product by thin layer chromatography. The solution was extracted with EtOAc (20mLx3) and then washed with brine (20 mLx3). The organic layer was evaporated solvent under reduced pressure and purified by column chromatography with hexane:EtOAc (1:1) to obtain the product as a white solid 1.07 g (32.6%yield). The identity of product was confirmed by ^{1}H NMR spectroscopy.

^{1}H NMR (400 MHz, $CDCl_3$): δ_H 1.52 [18H, *s*, (6x$C\underline{H}_3$Boc)] 1.62-1.73 [4H, *m*, $C\underline{H}_2C\underline{H}_2$] 2.89 [1H, *br*, O$\underline{H}$] 3.45-3.50 [2H, *m*, NH$C\underline{H}_2$] 3.67 [2H, *t*, *J* = 8 Hz, $C\underline{H}_2$OH] 8.50 [1H, *s*, N$\underline{H}$] 11.51 [1H, *s*, N$\underline{H}$Boc] ^{13}C NMR (400 MHz, $CDCl_3$) : δ_C 25.8, 28.2, 29.6, 40.9, 62.1, 80.1, 83.6, 153.3, 156.1, 162.7

1.4 Synthesis of 4-guanidino-1-butanal [29]

4-Guanidino-butanol (1.00 g, 3.25 mmol) was oxidized by IBX (0.98 g, 3.5 mmol) in DMSO 5 mL at room temparature. The solution must be homogeneous until get complete reaction within 3 h and white solid occurred as byproduct. (R_f 0.65 using Hexane:EtOAc ratio 1:1). The reaction was extracted with EtOAc and brine to obtain 4-guadinine-1-butanal as a colorless oil 0.51 g. (47.9%yield)

^{1}H NMR (400 MHz, $CDCl_3$): δ_H 1.43 [18H, *s*, 6x$C\underline{H}_3$Boc] 1.84 [2H, *m*, $CH_2C\underline{H}_2CH_2$] 2.47 [2H, *t*, *J* = 4 Hz, $C\underline{H}_2$CHO] 3.40 [2H, *dd*, *J* = 20, 8 Hz, $C\underline{H}_2$NH] 9.71 [1H, *s*, C$\underline{H}$O] ^{13}C NMR (100 MHz, $CDCl_3$): δ_c 21.8, 28.1, 28.3, 40.1, 41.1, 79.4, 83.3, 153.3, 156.3, 163.5, 201.1.

1.5 Synthesis of 4-phthalidino-butanol [30]

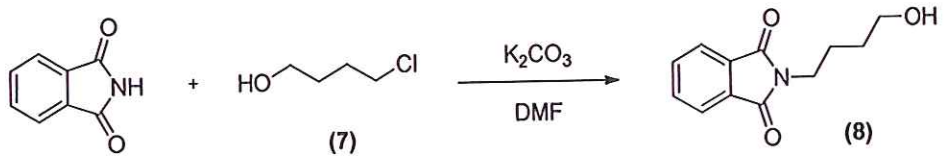

Dry K_2CO_3 6.94 g (50.2 mmol) and phthalimide 7.36 g (50 mmol) were dissolved in 10 mL of dry DMF. 4-chloro-1-butanol 5.43 mL (50 mmol) was added in solution and reaction was refluxed for 12 h. After that, the K_2CO_3 was filtrated out. The residue solution was evaporated and extracted with DCM (20 mLx3). The organic layer was evaporated the solvent out and then the crude was purified by column chromatography with EtOAc:hexane (1:2) to give 1.32 g of colorless liquid (75.4%yield).

^{1}H NMR (400 MHz, $CDCl_3$): δ_H 1.61 [2H, *m*, C$\underline{H}_2$OH] 1.78 [2H, *m*, C$\underline{H}_2$ phthalimide] 2.60 [1H, *br*, O$\underline{H}$] 3.69-3.74 [4H, *m*, C$\underline{H}_2$C$\underline{H}_2$] 7.71-7.83 [4H, *m*, C$\underline{H}$-phenyl] ^{13}C NMR (100 MHz, $CDCl_3$): δ_c25.1, 29.8, 37.8, 62.2, 123.2, 134.0, 168.54.

1.6 Synthesis of 4-phthalimido-butanal

The hydroxyl group of 4-phthalimide-1-butanol 1.57 g (6.8 mmol) was oxidized by 2.00 g of IBX (7.1 mmol) in DMSO 5 mL at room temperature. The reaction was monitored by TLC with 2:1 ratio of hexane:EtOAc. After reaction was completed, 10 mL of $NaHCO_3$ was added to the solution and extracted with EtOAc (20 mLx3). The organic layer was evaporated the solvent out and the crude product was purified by column chromatography. The 4-phthalimido-1-butanal was obtained as colorless oil 0.92g. (64.8%yield)

^{1}H NMR (400 MHz, $CDCl_3$): δ_H 2.00 [2H, *m*, C$\underline{H}_2$] 2.53 [2H, *dt*, *J* = 7.2 Hz, C$\underline{H}_2$NH] 3.73 [2H, *t*, *J* = 6.8 Hz, C$\underline{H}_2$CHO] 7.73-7.86 [4H, *m*, C$\underline{H}$-phthalimide], 9.76 [1H, *s*, C$\underline{H}$O] ^{13}C NMR (100 MHz, $CDCl_3$): δ_C 21.2, 37.2, 41.1, 123.3, 132.0, 133.8, 168.4, 200.7.

2. PNA monomer

*apc*PNA, *acpc*PNA spacer and pyrrolidinyl PNA monomers (Fmoc-A^{Bz}-OPfp, Fmoc-T-OPfp, Fmoc-C^{Bz}-OPfp and Fmoc-G^{Ibu}-OH) were supported by Prof. Tirayut Vilaivan's laboratory and synthesized according to previous report. [25]

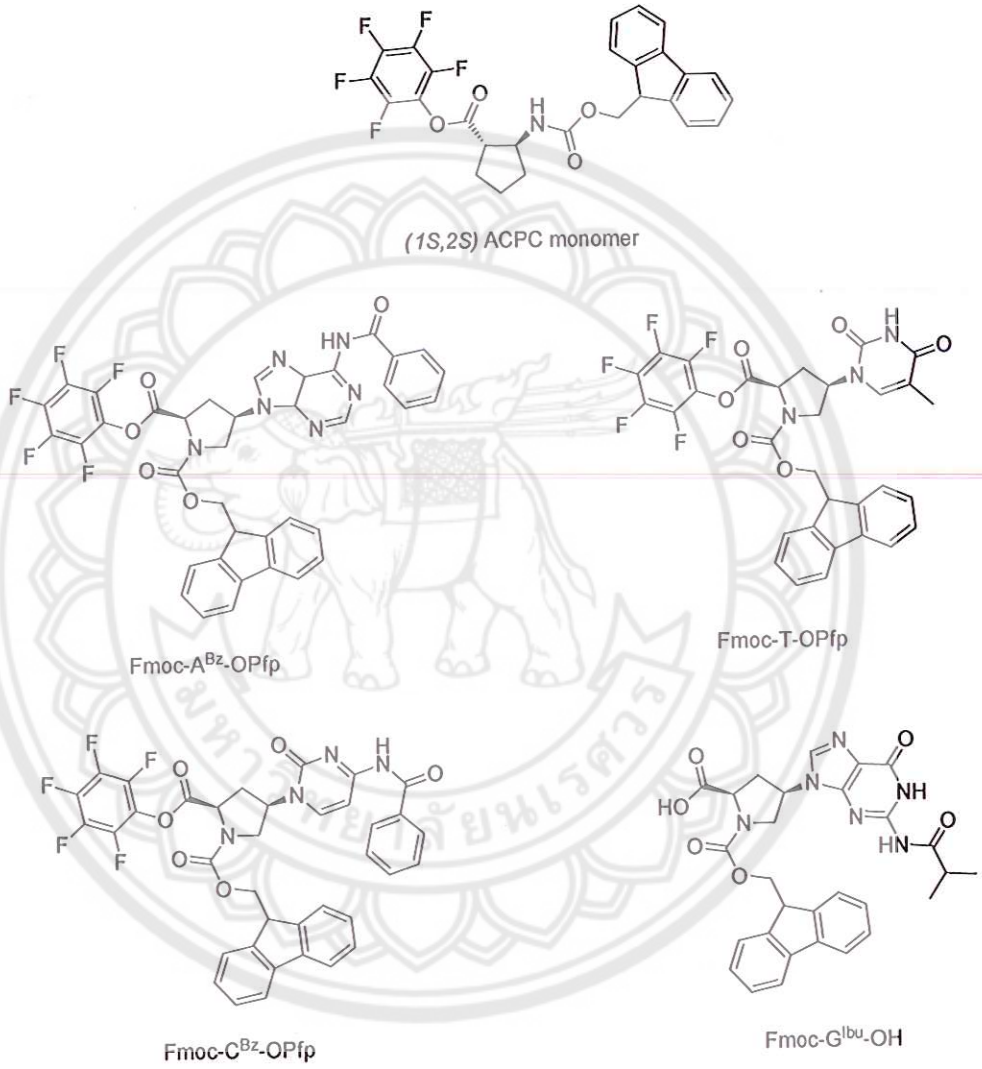

Figure 34 The structure of (1*S*,2*S*) ACPC monomer, Fmoc-A^{Bz}-OPfp, Fmoc-T-OPfp, Fmoc-C^{Bz}-OPfp and Fmoc-G^{Ibu}-OH

3. Synthesis of *apc/acpc*PNA on solid support

The synthesis of PNA sequences consists of 3 major steps as deprotection, coupling and capping and stock solution for each step was prepared as following

Stock solution preparations

1. Stock#1 was prepared by mixing 200 μL of piperidine, 20 μL of DBU and 780 μL of anhydrous DMF.

2. Stock#2 was prepared by mixing 70 μL of DIEA and 930 μL of anhydrous DMF.

3. Stock#3 was prepared by mixing 9.9 mg of HOAt and 180 μL of anhydrous DMF.

Solid phase peptide synthesis of PNA

The 7.1 mg of TantaGel S RAM Fmoc resin was prepared by swelled in DMF for 30 min and then washing with DMF. The resin was dried by apply pressure from rubber teat (**Figure 34**).

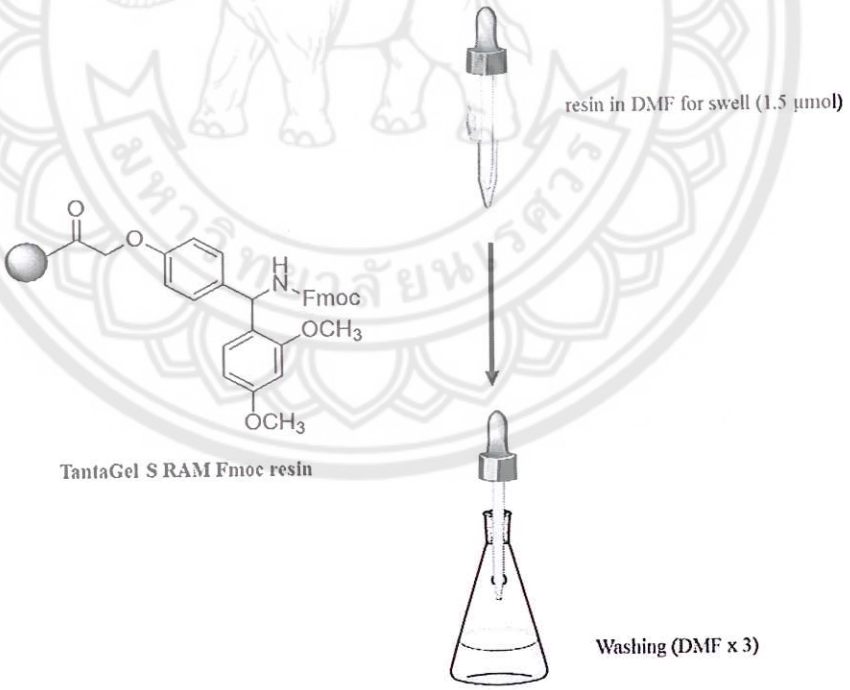

Figure 35 The structure of resin and diagram of solid phase peptide synthesis

PNA oligomerization consist of three major step as following

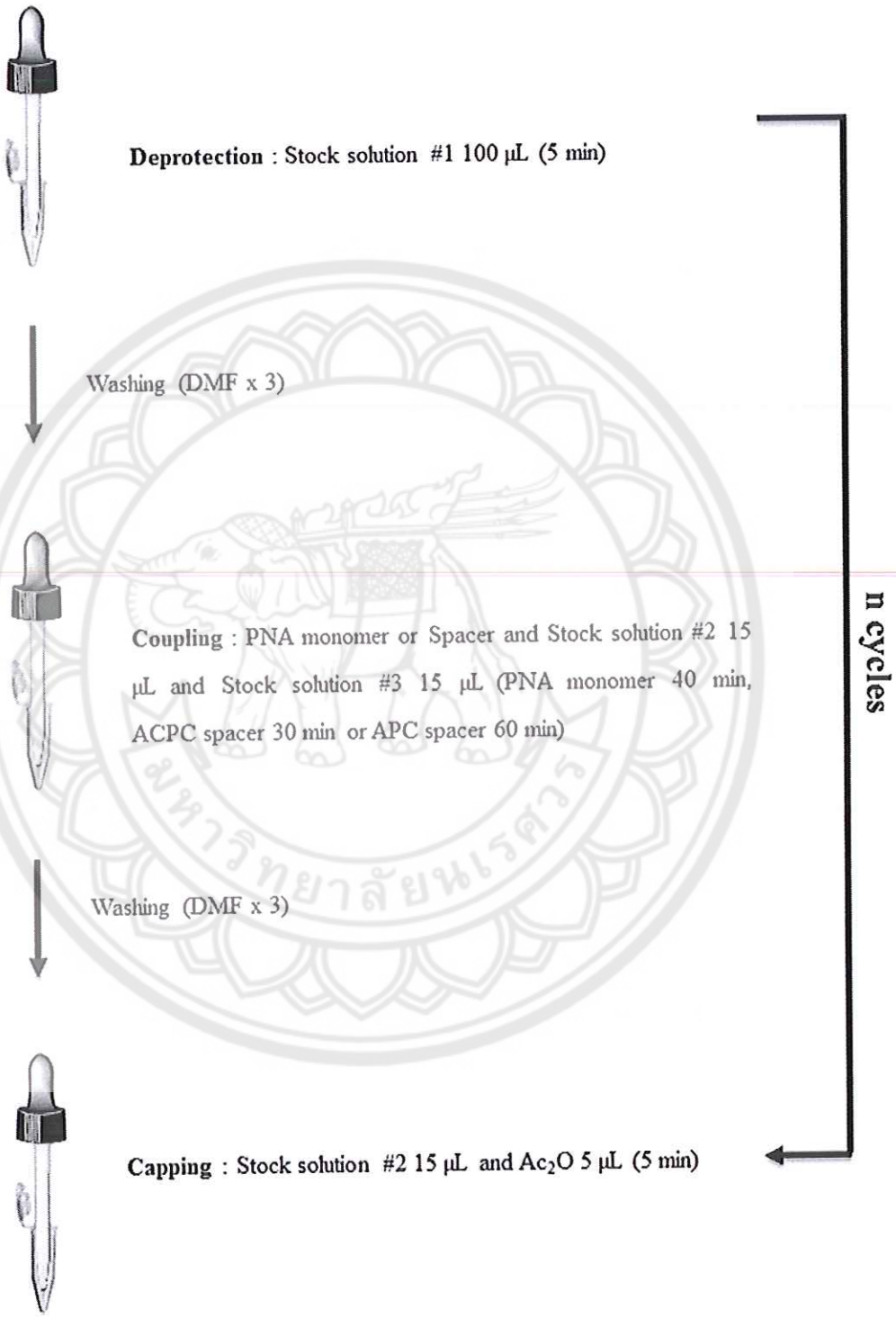

Figure 36 Diagram of deprotection, coupling and capping step

1. Deprotection: for removal of Fmoc protecting group at *N* terminus of PNA monomer or spacer.

2. Coupling: the active PNA monomer or spacer was attached at *N* terminus of PNA chain.

3. Capping: the unreacted amino group of the growing PNA chain was reacted with Ac_2O to prevent further reactions.

PNA Sequence in this study (sequence from N to C)

T_4XT_4 : Ac-TTTTTTTTT-LysNH$_2$

$M_{10}X1$: Ac-GTAGATCACT-LysNH$_2$

$M_{10}X3$: Ac-GTAGATCACT-LysNH$_2$

Synthesis of PNA oligomers, starting from TantaGel S RAM Fmoc resin 7.1 mg (1.5 μmol) was pipetted in custom-made dropper and swelled in DMF. Fmoc protecting group of solid support was treated with 100 μL of deprotection reagent (stock#1) for 5 min and washed with DMF (10 mLx3). Amino acid (Fmoc-Lys-(Boc)-OPfp) 4.8 mg (7.5 μmol) was coupling to sequence with 15 μL of stock#2 and 15 μL of stock#3 in coupling step for 40 min. The end capping, the unreacted sequence was treated with 5 μL of Ac_2O and 15μL of stock#2 for 5 min. Then the cycles were repeated from deprotecting step again. For onwards coupling step, one of pyrrolidinyl monomers was used to start the peptide chain; 4.4 mg of Fmoc-A^{Bz}-OPfp, 3.7 mg of Fmoc-T-OPfp, 4.3 mg of Fmoc-C^{Bz}-OPfp or 3.5 mg of Fmoc-G^{Ibu}-OH for each cycle. Then the cycles were repeated and changed the coupling step with 3.8 g of APC spacer or 3.1 mg of ACPC. Overall cycles were repeated until get the desired PNA sequence.

4. Reductive alkylation of *apc/acpc*PNA on solid supports

Nucleobase protecting group of *apc/acpc*PNA was deprotected with NH_3/dioxane (1:1) at 60 °C overnight. After deprotection, *apc/acpc*PNA (0.5 μmol) was treated with hydrophilic aldehyde (15 μmol) (C_4OH; 4-trityloxy-1-butanal, C_4NH_2; 4-phthalimido-1-butanal and C_4Gua; 4-guanidino-1-butanal), $NaBH_3CN$ (30 μmol) and acetic acid (30 μmol) in 100 μL of methanol at room temperature for 4 hour. For C_4OH and C_4Gua, the trityl- and Boc-protecting group were deprotected with TFA in cleavage step from solid support. For C_4NH_2, the phthalimide-protecting group was subsequently deprotected by 40% aqueous methylamine solution at room temperature for 3 h. The identities of the hydrophilic-modified acpcPNAs were

confirmed by MALDI-TOF mass spectrophotometry with α-cyano-4-hydroxy cinnamic acid as a matrix. The m/z of PNA showed mass increase of 73, 114, 72 unit for singly modified *acpc*PNAs and 219, 342, 216 unit for triply modified *acpc*PNAs.

5. The cleavage of hydrophilic-modified*acpc*PNAs

The hydrophilic-modified *acpc*PNAs were cleaved from the solid support by TFA (500 μL×3) for 2 h and the TFA was removed under a stream of nitrogen in fume hood. The crude PNA was precipitated by diethyl ether and centrifuged to obtain hydrophilic-modified *acpc*PNAs as a white solid.

6. The purification and characterization of hydrophilic-modified *acpc* PNAs

The crude of hydrophilic-modified *acpc*PNAs was added 120 μL of MilliQ water for purification by reverse phase HPLC with column: ACE 5 A71197, C18-AR, 150x4.6 mm. The gradient system consists of 0.1% trifluoroacetic acid in MilliQ water (solvent A) and 0.1% trifluoroacetic acid in MeOH (solvent B). The flow rate of solvent at 0.5 mL/min for 5 min by starting from 90:10 of A:B ratio until 10:90 of A:B ratio and then the system will reverse back to 90:10 of A:B ratio. The hydrophilic-modified *acpc*PNAs was monitored by UV absorbance at 260 and 300 nm. The fractions containing the hydrophilic modified *acpc*PNAs were confirmed by MALDI-TOF mass spectrophotometer. These were combined and freeze dried to give the desired PNA.

The characterization of PNA

1. Thermal melting temperature (T_m)experiment

A 1 μM solution of hydropilic-modified acpcPNA and 1.2 μM of DNA were prepared in 10 mM phosphate buffer pH 7.0 and 100 mM sodium chloride. Thermal melting temperature (T_m) was carried out by CARY 100 Bio UV-Vis spectrophotometer at 260 nm by temperature heating from 20-90°C (block temperature). The temperature was increased 1 °C/min. The temperature was recorded as the block temperature and was corrected by a linear equation obtained from a built-in temperature probe. The melting temperature was evaluated from the maximum of the first derivative after smoothing using KaliedaGraph 4.0 (Synergy Software) and analysis of the data was performed on a PC compatible computer using Microsoft

Excel (Microsoft Corporation). T_m values obtained from independent experiments were accurate to with ±0.5 °C.

Correct temperature and normalized absorbance are defined as follows.

Correct Temp. = $(0.9696 \times T_{block}) - 0.8396$

Normalized Abs. = $Abs_{observed}/Abs_{initial}$

2. Circular dichroism spectroscopy (CD)

In cuvette of path length 1 cm, 10 mM phosphate buffered pH 7.0 was added and then 2.5 μM of hydrophilic-modified acpcPNA was subsequently added. The mixture solution was measured circular dichroism from 400 to 200 nm at the rate of 100 nm/min. Then, 2 μM of complementary DNA was titrated by adding each 3.5 μL to the solution. All spectra were processed and carried out by average of 4 scans and recorded with Microsoft Excel and OriginPro7G (OriginLab Corporation). The baselines were subtracted to get the processed CD spectrum.

3. Solubility experiment

After hydrophilic-modified acpcPNAs was dried by freeze dryer (Labconco), each PNA fractions in eppendorf was dissolved in a minimum amount of MilliQ water and centrifuged at 14000 rpm for 10 min. The concentration of the supernatant was determined by measuring the UV absorption at 260 nm using a Nanodrop 2000 spectrophotometer. The ε value of T_4XT_4 and both mix base 10mers ($M_{10}X1$ and $M_{10}X3$) were 79.2 and 96.6, respectively.

CHAPTER IV

RESULTS AND DISCUSSION

In this work, three hydrophilic modifiers as 4-hydroxybutyl (C_4OH), 4-aminobutyl (C_4NH_2) and 4-guanidinobutyl (C4Gua) were attached into *apc/acpc*PNA for enhance water solubility of *acpc*PNA by comparing with unmodified *acpc*PNA. The 4-carbon length (C4) of hydrocarbon chain was chosen in this study because it can appropriately extend from PNA·DNA duplex. The hydrophilicmodifier's terminus was hydroxyl, amino and guanidino group as hydrogen bond forming donor and acceptor with water or polar molecule. The preparation of hydrophilic modifier as 4-trityloxy-1-butanal **(Figure 37A)** 4-guanidino-1-butanal **(Figure 37B)** and 4-phthadino-1-butanal **(Figure 37C)** and attachment to PNA sequence including biophysical binding properties and water solubility properties will be discussed in this chapter.

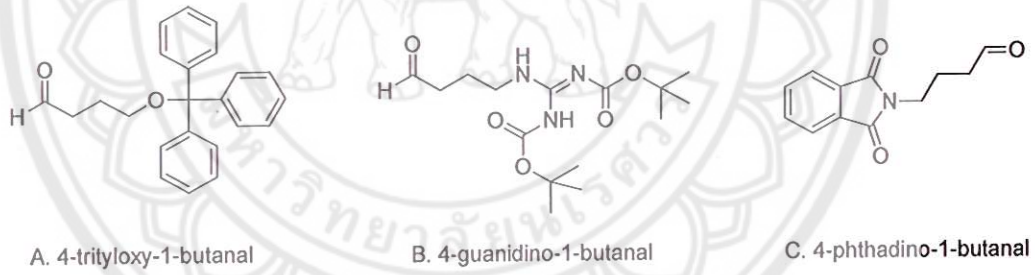

Figure 37 The structure of hydrophilic modifier

Synthesis of aldehyde modifier

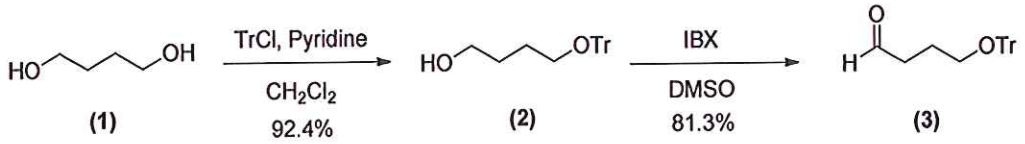

Figure 38 Synthesis of 4-trityloxy-1-butanal (3)

Commercial available 1,4-butanediol (**1**) was used as starting material. One of the hydroxyl group of 1,4-butanediol was stoichiometically protected with triphenylmethyl chloride (TrCl) in the presence of pyridine. 4-Trityloxy-1-butanol (compound 2) was obtained in 92.4% yield and the mechanism was shown in **Figure 39**. After that, the remaining hydroxyl group was further oxidized to aldehyde group with 2-iodoxybenzoic acid (IBX) to give 4-trityloxy-1-butanal (**3**) in 81.3% yield. The mechanism of this reaction was illustrated in **Figure 40**. [31] After oxidation, the characterization of the obtained product by ^{1}H NMR spectroscopy showed the appearance of proton of phenyl group in range of 7.2-7.5 ppm and sharp peak of hydrogen adjacent to carbonyl group asthe proton of aldehyde appeared at 9.8. (**Figure 41**)

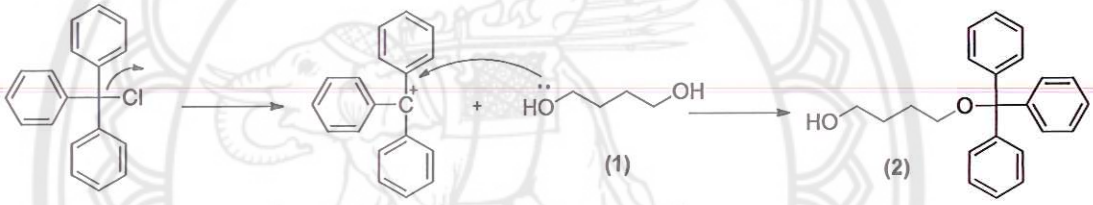

Figure 39 The mechanism of 4-trityloxy-1-butanol (2)

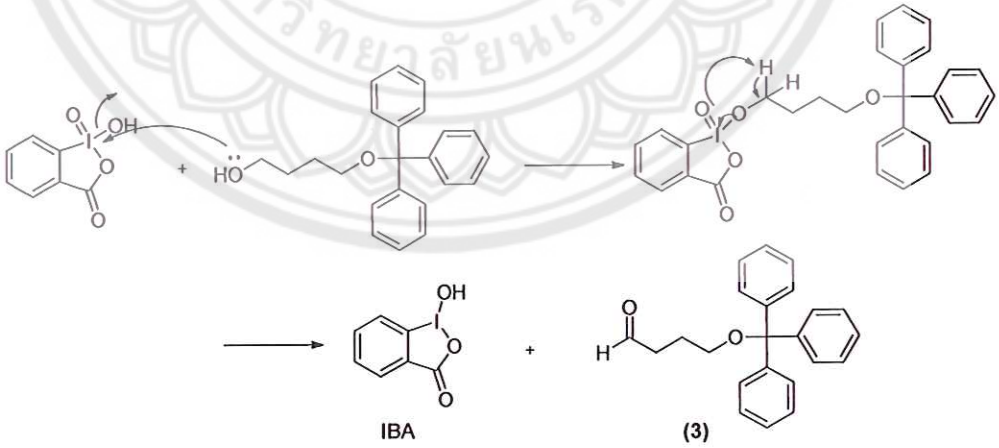

Figure 40 The mechanism of synthesis of 4-trityloxy-1-butanal (3)

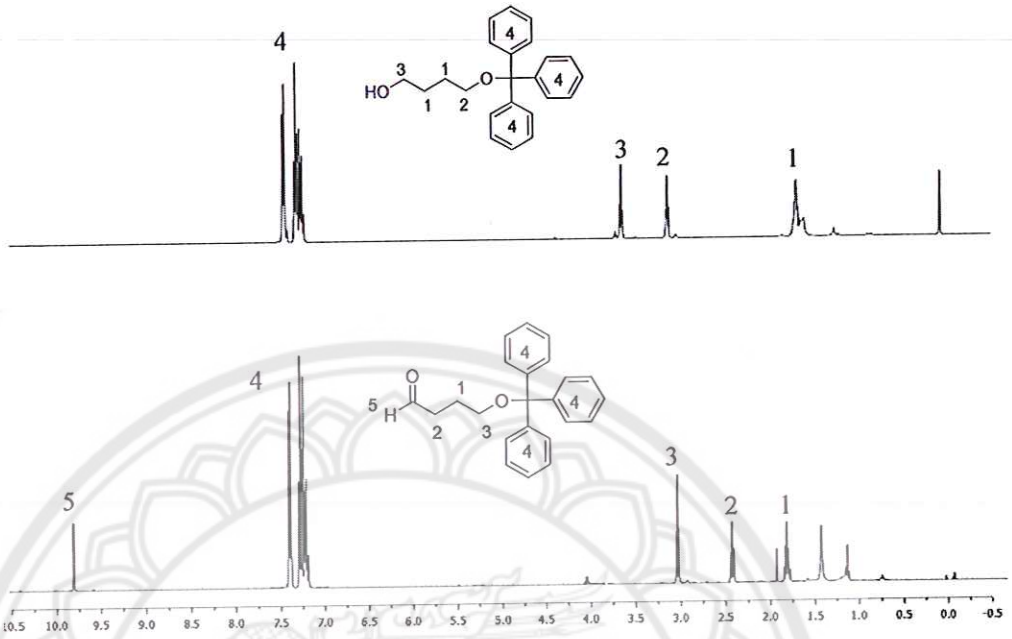

Figure 41 ^{1}H NMR spectrum of 4-trityloxy-1-butanol (2) and 4-trityloxy-1-butanal (3)

4-Guanidino-1-butanal (**6**) was synthesized starting from commercially available 4-amino-1-butanol (**4**) and *bis*-Boc-thiourea that was prepared from the reaction of thiourea with di-*tert*-butyl dicarbonate (Boc_2O) (**Figure 42**). Boc protecting group was chosen in this aldehyde modifier bacause it can be easily removed by TFA between the cleavage step in peptide synthesis. In this reaction, *N,N'*-Di-(*tert*-butoxycarbonyl)-thiourea (*bis*-Boc-thiourea) was changed to carbodiimide intermediate (**Figure 43**) and then reacted with primary amino group of 4-amino-1-butanol (**4**) to obtain 4-guanidino-1-butanol (**5**) in 32.6% yield (**Figure 44**).

Oxidation from compound **5** to 4-guanidino-1-butanal (**6**) was prepared with IBX as same as above described. The identity of this product was monitored by ^{1}H NMR spectroscopy. Peak at 1.5 ppm confirm Boc group character and peak at 9.7 ppm confirmed aldehyde functional group as shown in (**Figure 45**).

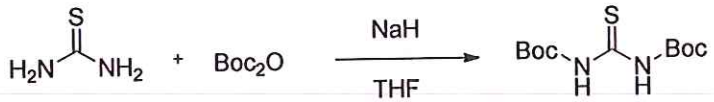

Figure 42 Synthesis of *bis*-Boc-thiourea

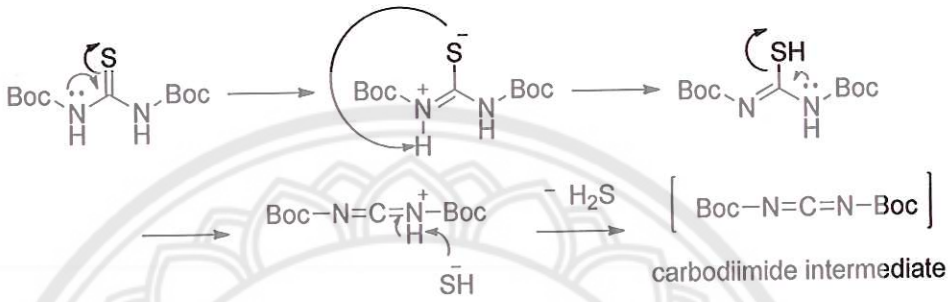

Figure 43 The mechanism of carbodiimide intermediate

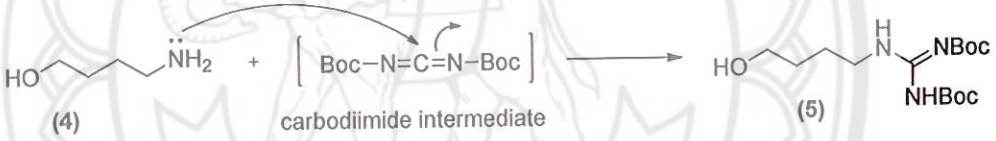

Figure 44 The synthesis of 4-guanidino-1-butanol (5)

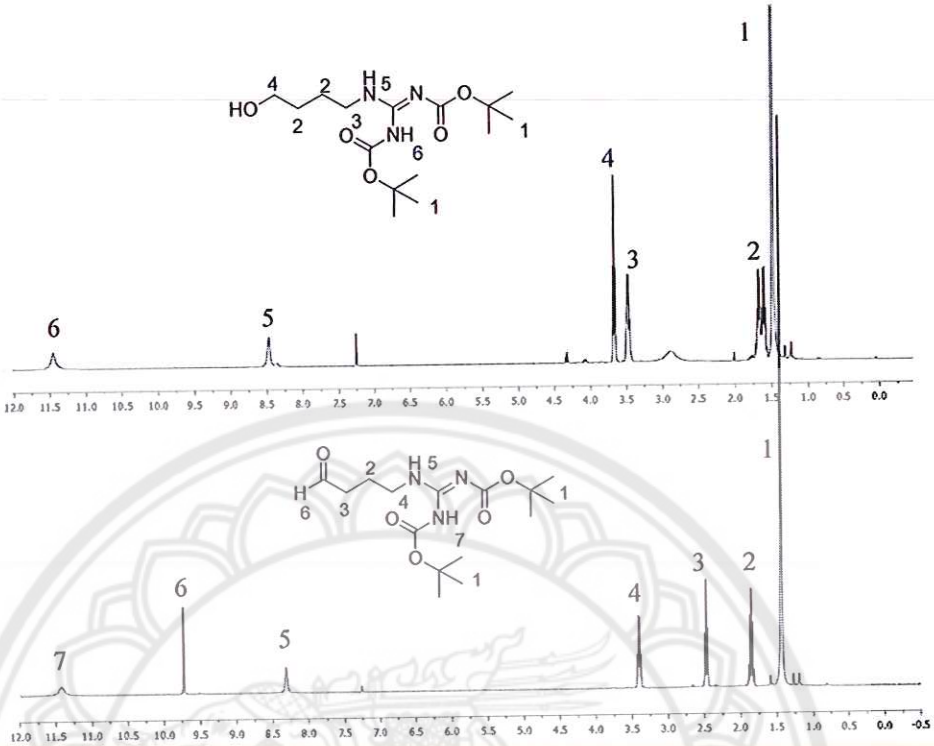

Figure 45 ^{1}H NMR spectrum of 4-guanidino-1-butanol (5) and 4-guanidino-1-butanal (6)

For 4-amino-1-butanal modifier, the primary amine of 4-amino-1-butanol **(1)** was firstly protected with Boc protecting group and the hydroxyl group was oxidized. However, no peak of aldehyhe was observed in 9.5-10.5 ppm range (**Figure 46**), which suggest the cyclization of the *N*-Boc 4-aminobutanal (7). Changing the protecting group to Fmoc group did not also prevent the cyclization following this oxidation. Next, the phthalimido group was attempted as a new protecting group for this situation. 4-Chloro-1-butanol **(8)** was reacted with phthalimide (9) and then oxidized to aldehyde (**Figure 47**). In addition, the phthalimide group can be removed by hydrazinolysis or aminolysis in the last step of peptide synthesis.

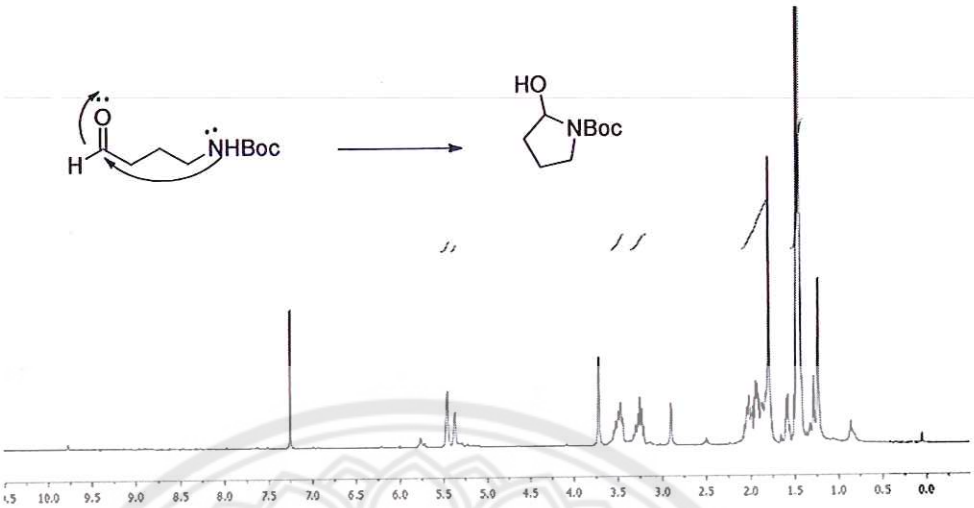

Figure 46 The mechanism and ^{1}H NMR spectrum of cyclization of *N*-Boc-4-aminobutanal (7)

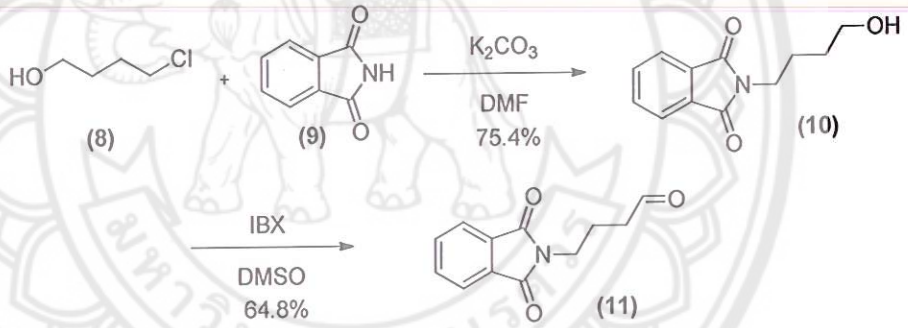

Figure 47 Synthesis of 4-phthalimido-1-butanal (11)

The mechanism of preparation of compound 9 was shown in **Figure 47**. Phthalimide was deprotonated by K_2CO_3 and reacted at the electrophilic carbon of compound 10 under reflux condition (75.4%). The other hydroxyl group was oxidized by IBX to give 4-phthalimido-1-butanal (**11**) in 64.8% yield. The identity of phathalimide group can be confirmed by ^{1}H NMR spectrum in a range of 7.5-8.0 ppm and aldehyde peak at 9.75 ppm as shown in **Figure 49**.

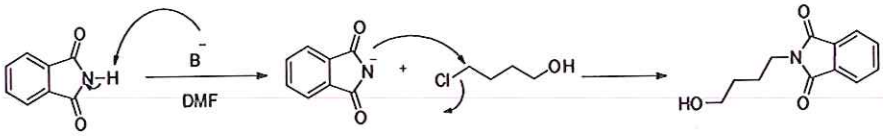

Figure 48 The mechanism of synthesis of 4-phthalidino-butanol (10)

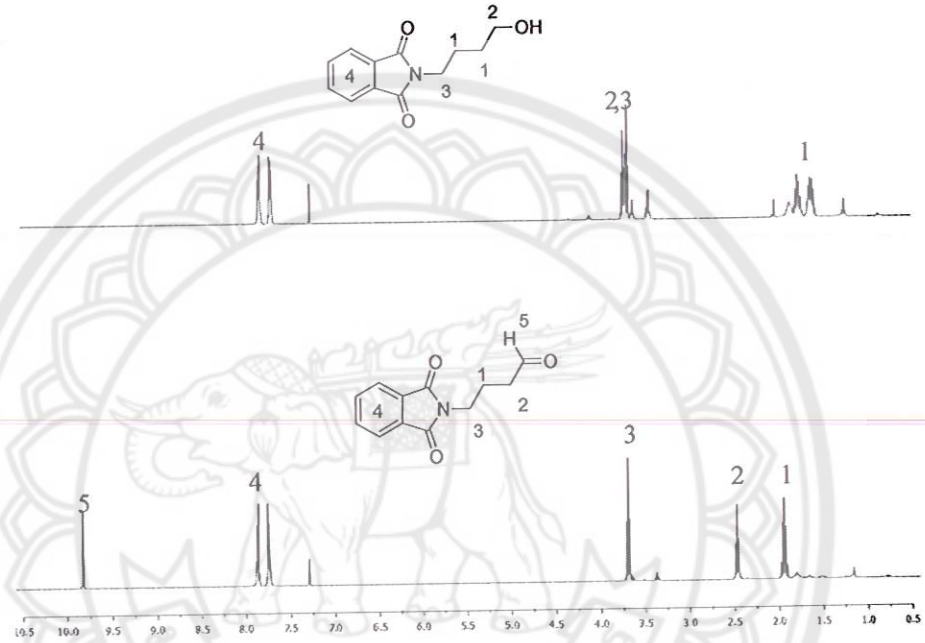

Figure 49 ^{1}H NMR spectrum of 4-phthalidino-butanol (10) and 4-phthalidino-butanal (11)

After all aldehyde modifier (**3, 6, 11**) were successfully synthesized, they were attached onto *acpc*PNA and the protecting groups were removed as following described

In this work, PNA sequences were designed and studied as homothymine with 1 position of aldehyde modifier [Ac-TTTT(T)TTTT-LysNH_2], mix-base with 1 position of modifier [Ac-GTAGA(T)CACT-LysNH_2] and mix-base with 3 position of modifier [Ac-GT(A)GA(T)CA(C)T-LysNH_2] for investigate the effect of sequence and amount of modifier. At middle or specific position of oligomers were replaced by APC spacer (parenthesis position). Each PNA sequence was connected with one out of 3 kinds of modifiers as C_4OH, C_4NH_2 and C_4Gua (total in 9 sequences). For

nucleobase monomer (A, T, C and G) and spacer (ACPC and APC) used in this research, there were supported from Professor Tirayut Vilaivan's laboratory research group. APC-modified *acpc*PNA oligomers (1.5 μmol) were synthesized by solid phase peptide synthesis technique[Ref] which composes of 3 steps of procedure as deprotection, coupling and capping and synthesized PNA will be monitored by MALDI-TOF mass spectroscopy as shown in **Table 9**.

Table 8 Mass of *apc/acpc*PNA oligomers before modification

PNA	Sequence (N→C)	m/z calcd	m/z found
T_4XT_4	Ac-TTTT(T)TTTT-LysNH_2	3180.4	3179.6
$M_{10}X1$	Ac-GTAGA(T)CACT-LysNH_2	3559.8	3559.7
$M_{10}X3$	Ac-GT(A)GA(T)CA(C)T-LysNH_2	3561.8	3563.2

*Parenthesis position was replaced apc spacer instead of *acpc* spacer.

Reductive alkylation of *apc/acpc*PNA on solid supports

After the PNA oligomers (15 μmol) were successfully synthesized after nucleobase protecting group (Benzoyl; Bz and Isobutyryl; Ibu) on the PNA oligomers were removed by treatment with NH_3/dioxane in 1:1 ratio at 60°C for overnight. The next step, aldehyde modifier (**3, 6, 11**) (15 μmol) was added into PNA oligomers by reductive alkylation according to the literature proceduce [14]. PNA oligomers were reacted with aldehyde modifier in the presence of acetic acid in methanol followed by addition of sodium cyanoborohydride ($NaBH_3CN$) for 4 hours. (**Figure 50**) The trityl and Boc protecting group on the modifier were deprotected by acid condition similar to the condition for cleavage of PNA from the solid support. For phthalimide protecting group, it must be deprotected by 40% methylamine solution after the reductive alkylation step. In the final step, PNA was cleavage from resin by trifluoroacetic acid (TFA). The success of addition of hydrophilic modifier to acpcPNA can be monitored by MALDI-TOF mass spectroscopy. For singly-modified PNA (T_4XT_4 and $M_{10}X1$) have increase mass for 72, 73 and 114 unit for 4-aminobutyl

($C4NH_2$), 4-hydroxybutyl (C4OH) and 4-guanidinobutyl (C4Gua) respectively. For triply-modified PNA ($M_{10}X3$) has increase mass for 216, 219 and 342 unit for 4-aminobutyl (C_4NH_2), 4-hydroxybutyl (C_4OH) and 4-guanidinobutyl (C_4Gua) respectively.

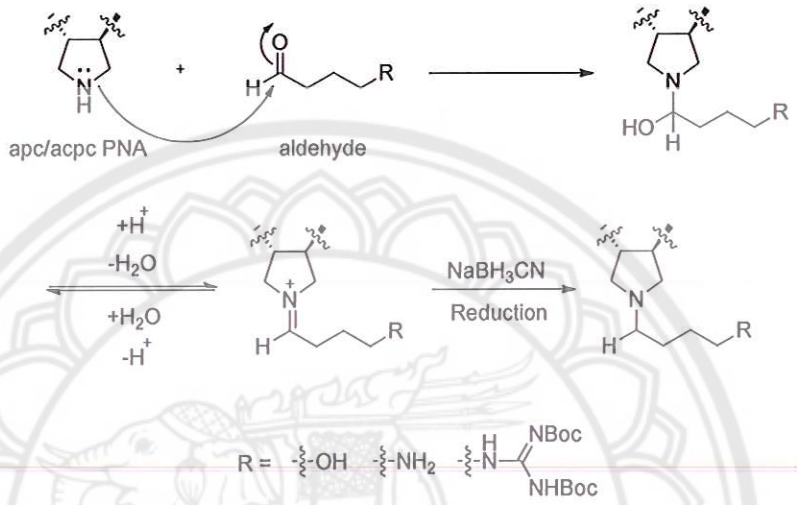

Figure 50 The mechanism of reductive alkylation of 4-hydroxybutyl (C_4OH), 4-aminobutyl (C_4NH_2) and 4-guanidinobutyl (C_4Gua)

Table 9 Mass, hplc retention time and yield of PNA sequence

PNA	sequence	m/z calcd	m/z found	T_R(min)	%yield
PNA1	Ac-TTTT(T_{C4OH})TTTT-LysNH_2	3252.4	3253.5	31.9	6.5
PNA2	Ac-TTTT(T_{C4NH2})TTTT-LysNH_2	3251.4	3250.3	31.8	2.7
PNA3	Ac-TTTT(T_{C4Gua})TTTT-LysNH_2	3293.4	3293.6	33.2	12.2
PNA4	Ac-GTAGA(T_{C4OH})CACT-LysNH_2	3631.8	3629.9	29.1	13.8
PNA5	Ac-GTAGA(T_{C4NH2})CACT-LysNH_2	3630.8	3628.1	25.2	6.6
PNA6	Ac-GTAGA(T_{C4Gua})CACT-LysNH_2	3672.4	3671.0	29.7	4.5
PNA7	Ac-GT(A_{C4OH})GA(T_{C4OH})CA(C_{C4OH})T-LysNH_2	3777.8	3779.2	27.4	6.3
PNA8	Ac-GT(A_{C4NH2})GA(T_{C4NH2})CA(C_{C4NH2})T-LysNH_2	3774.8	3776.9	29.9	1.7
PNA9	Ac-GT(A_{C4Gua})GA(T_{C4Gua})CA(C_{C4Gua})T-LysNH_2	3900.8	3898.6	26.9	0.4

Melting temperature (T_m) measurement

The determination of PNA·DNA hybridization by UV spectrophotometer was performed at wavelength 260 nm. The temperature range at 20-90°C was seted in this analysis. The hybridization between PNA and DNA can be regularly occurred via hygrogen bond between nucleobase of PNA strand and DNA strand including π-π interaction of stacking base. Upon temperature increasing, the PNA·DNA duplex were dissociated to single strand because the destruction of π-π interaction and H-bond were denatured. The molar extinction coefficient (ε), hyperchromism, has increased value at absorbance 260 nm. The melting curve of PNA·DNA duplex presents *S* curve by plot between temperature and A_{260} as shown in **Figure 51A**. The midpoint of *S* curve is melting temperature which 50% of duplex has been dissociated. This value is represented as the stability of the duplex structure. The stable duplexes melt at a higher melting temperature than less stable duplexes. The cooperative between base-base interactions required the melting process that rapidly occuring within only 10-20°C range. The first hydrogen bond between base pair was broken by input energy until double stand was completely separated to single stand. The melting tempereture (T_m) could be also determined from maxima of the first derivative graph plot between dA/dT and temperature by calculated KaleidaGraph 4.0 **(Figure 51B)** [31]

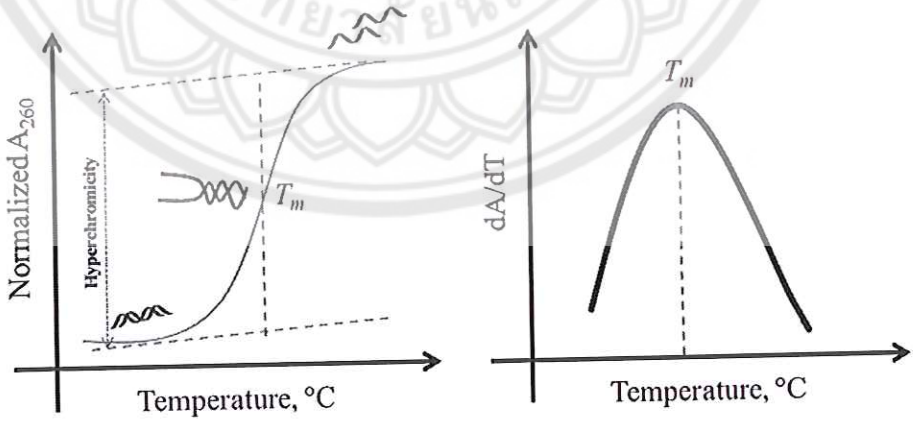

Figure 51 A. Thermal melting temperature (T_m) with change of UV absorbance of duplex and B. The first derivative of Thermal melting temperature (T_m)

In this experiment, hydrophilic-modified *acpc*PNAs were studied as following; homothymine PNA such as PNA1: Ac-TTTT(T_{C4OH})TTTT-LysNH_2, PNA2 Ac-TTTTT_{C4NH2}TTTT-LysNH_2 and PNA3: Ac-TTTT($_{TC4Gua}$)$_{TTTT}$-LysNH_2. The stability of PNA1-PNA3 were investigated by using hydrophilic-modified *acpc*PNAs with complementary DNA. The T_m value of PNA1-PNA3 in 1 μM of PNA, 1.2 μM of DNA in 100mM phosphate buffer pH 7 showed at 71.9, 79.7 and 80.6°C respectively when compared with *acpc*PNA (76.8°C) and *apc/acpc*PNA (71.1°C) [13]. PNA2 and PNA3 showed high binding affinity because of positively charged of quarternary ammonium and protonated guanidine group (pKa of amino and guanidine group are 10.51 and 13.6 respectively). [32] This can supplement charge-charge interaction with negative charge of phosphate group of DNA while the hydroxyl group of modifier in PNA1 can form only hydrogen bond.

At high salt concentration (same condition with 100 mM NaCl), the T_m value of PNA1-PNA3 showed at 67.1, 71.9 and 72.9°C respectively. The high ionic strength solution can interact with phosphate group of DNA and also the functional group of hydrophilic modifier to neutralize charge. Thus, the stability of DNA hybridization of PNA1-PNA3 have slightly decreased. However, the hydrophilic homothymine still showed high stability when compared with natural DNA duplex (20.7°C). [11]

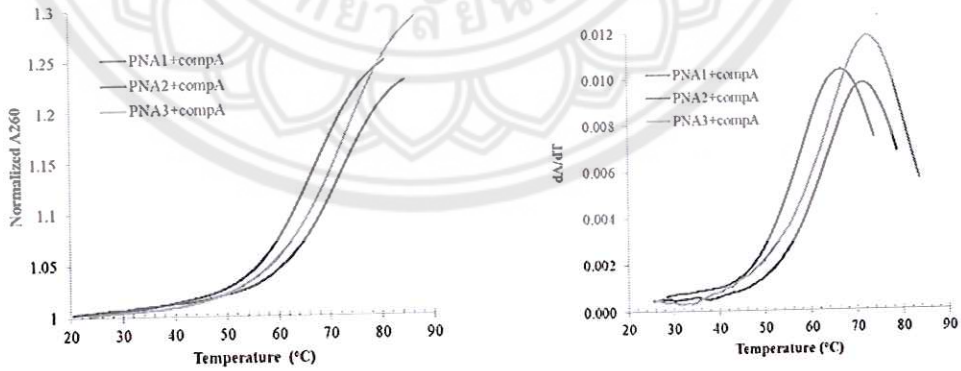

Figure 52 T_m curve and first derivative of PNA1-PNA3 hybrid with complementary DNA in 1 μM of PNA, 1.2 μM of DNA, 100 mM phosphate buffer pH 7.0 and 100 mM sodium chloride

Next, base specificity of homothymine PNA was verified by comparing the affinity of hydrophilic-modified *acpc*PNAs with complementary and single mismatch DNA (AAAAXAAAA; where X = C, G or T). T_m value with single mismatch DNA were represented in **Table 10**. It has remarkably decreased from complementary DNA (ΔT_m 25-40°C). This results indicated that hydrophilic-modified *acpc*PNAs still hybridized to target DNA with high base sequence specificity.

Table 10 T_m **data of homothymine (PNA1; Ac-TTTT(T_{C4OH})TTTT-LysNH$_2$, PNA2; Ac-TTTT(T_{C4NH2})TTTT-LysNH$_2$ and PNA3; Ac-TTTT(T_{C4Gua})TTTT-LysNH$_2$ hybrid with complementary and single mismatch DNA**

PNA	Sequence DNA	Note	T_m (°C)[a]	ΔT_m(°C)
PNA1	dA9 AAA AAA AAA	Perfect match	67.1	-5.4[b]
	dA9_smC AAA ACA AAA	Single mismatch	36.0	31.1[c]
	dA9_smG AAA AGA AAA	Single mismatch	26.3	40.8[c]
	dA9_smT AAA ATA AAA	Single mismatch	38.9	28.2[c]
PNA2	dA9 AAA AAA AAA	Perfect match	71.9	-0.6[b]
	dA9_smC AAA ACA AAA	Single mismatch	46.7	25.2[c]
	dA9_smG AAA AGA AAA	Single mismatch	39.0	32.9[c]
	dA9_smT AAA ATA AAA	Single mismatch	46.7	25.2[c]
PNA3	dA9 AAA AAAAAA	Perfect match	72.9	-0.4[b]
	dA9_smC AAA ACA AAA	Single mismatch	44.8	28.1[c]
	dA9_smG AAA AGA AAA	Single mismatch	35.1	37.8[c]
	dA9_smT AAA ATA AAA	Single mismatch	<20	nd

Note: [a]Condition: [PNA] = 1 μM, [DNA] = 1.2 μM, 100 mM phosphate buffer pH 7.0 and 100 mM sodium chloride. [b]$\Delta T_m = T_m$ value was compared with unmodified PNA (*acpc*PNA : Ac-TTTTTTTTT-Lys 72.2°C in high ionic strength condition)[8] [c]$\Delta T_m = T_{m(complementary)} - T_{m(single\ mismatch)}$ (same PNA, different DNA), nd = not determined

The base specificity of hydrophilic-modified *acpc*PNA in internal position of mix base decamer sequence (PNA4, PNA5 and PNA6) and hydrophilic-modified *acpc*PNA in three positions of mix base decamer sequence (PNA7, PNA8 and PNA9) were also investigated as shown in **Table 11**. The unmodified *acpc*PNA (Ac-GTAGATCACT-LysNH$_2$) has T_m value at 52.5°C, when APC spacer was inserted in middle position of *acpc*PNA turning to *apc/acpc*PNAs that destabilization of duplex (T_m = 50.8°C). In case of hydrophilic-modified *acpc*PNAs (PNA4-PNA6), it was found that hydrophilic-modified *acpc*PNAs can still improve stability of duplex as expected by T_m = 53.5, 58.3 and 58.3 for PNA4-6 respectively (ΔT_m 1-5.8°C). The modifiers C4NH$_2$ and C4Gua displayed higher stability than C4OH hydrophilic modifier as same as in homothymine sequence. For triply-modified M10X3 (PNA7-9), it represented that T_m value was higher than singly-modified M10X1 by T_m = 54.4, 65.1 and 66.8 for PNA7-9 respectively. This means that the presence of positively charged modifier can effectively enhance the stability of hybridization of duplex in C4NH$_2$ and C4Gua modifier and the effect is additive.

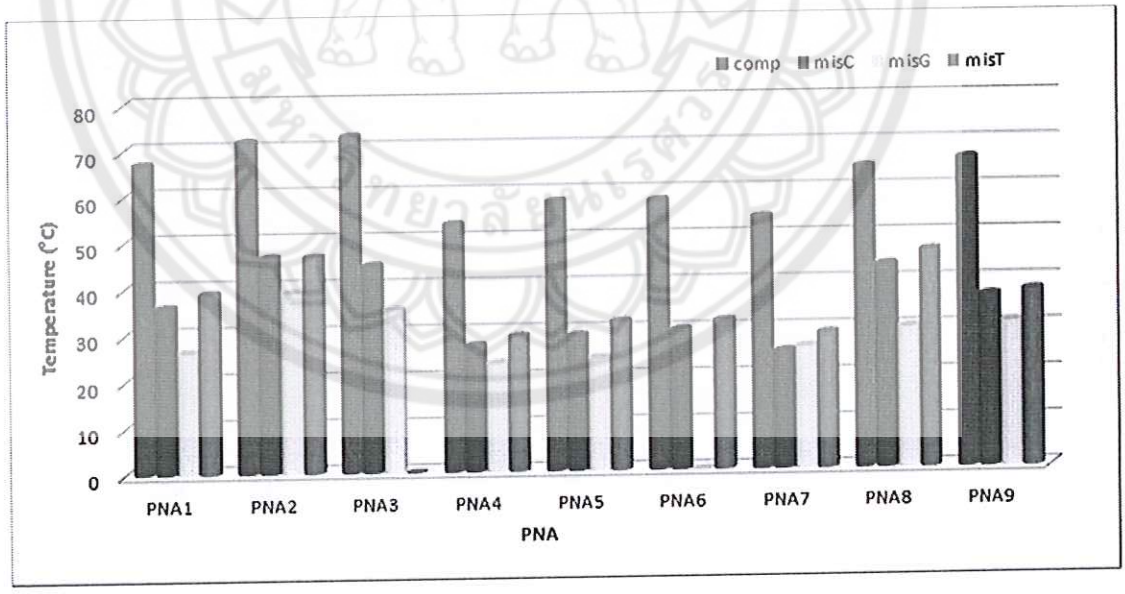

Figure 53 The comparesion between complemantary DNA and single mismatch DNA (C, G, T) of PNA1-PNA9

Table 11 T_m data of the singly-modified and triply-modified mix base sequence hybrid with complementary DNA and single mismatch DNA

PNA	Sequence DNA (5'→3')	Note	T_m (°C)[a]	ΔT_m(°C)[b,c]
PNA4	M10 CAT CTA GTG A	Perfect match	53.5	1.0
	M10_smC CAT CTC GTG A	Single mismatch	27.3	26.2
	M10_smG CAT CTG GTG A	Single mismatch	23.4	30.1
	M10_smT CAT CTT GTG A	Single mismatch	29.2	24.3
PNA5	M10 CAT CTA GTG A	Perfect match	58.3	5.8
	M10_smC CAT CTC GTG A	Single mismatch	29.2	29.1
	M10_smG CAT CTG GTG A	Single mismatch	24.4	33.9
	M10_smT CAT CTT GTG A	Single mismatch	32.1	26.2
PNA6	M10 CAT CTA GTG A	Perfect match	58.3	5.8
	M10_smC CAT CTC GTG A	Single mismatch	30.2	28.1
	M10_smG CAT CTG GTG A	Single mismatch	<25	<33.3
	M10_smT CAT CTT GTG A	Single mismatch	32.1	26.2
PNA7	M10 CAT CTA GTG A	Perfect match	54.4	-
	M10_smC CAT CTC GTG A	Single mismatch	25.4	29
	M10_smG CAT CTG GTG A	Single mismatch	26.3	28.1
	M10_smT CAT CTT GTG A	Single mismatch	29.2	25.2
PNA8	M10 CAT CTA GTG A	Perfect match	65.1	-
	M10_smC CAT CTC GTG A	Single mismatch	43.8	21.3
	M10_smG CAT CTG GTG A	Single mismatch	30.2	34.9
	M10_smT CAT CTT GTG A	Single mismatch	46.8	18.3
PNA9	M10 CAT CTA GTG A	Perfect match	66.8	-
	M10_smC CAT CTC GTG A	Single mismatch	37.0	29.8
	M10_smG CAT CTG GTG A	Single mismatch	31.2	35.6
	M10_smT CAT CTT GTG A	Single mismatch	38.0	28.8

Note: [a]Condition: 1 μM of PNA, 1.2 μM of DNA, 100 mM phosphate buffer pH 7.0 and 100 mM sodium chloride. [b]$\Delta T_m = T_m$ value was compared with unmodified PNA [c]$\Delta T_m = T_{m(complementary)} - T_{m(single\ mismatch)}$ (same PNA, different DNA)

Circular dichroism studies of hydrophilic-modified *acpc*PNAs hybrid with DNA

Circular Dichroism (CD) Spectroscopy was a technique which investigate the conformation of small molecule and macromolecule such as amino acid, protein and DNA. The chirality of molecule and conformation change is a crucial factor for characterization by responsiveness of the molecular chirality with polarized light of detector. The CD spectroscopy detected the wavelength dependence of this ellipticity and positive or negative signal is observed when either clockwise (right-handed) and counter-clockwise (left-handed). [33] CD spectroscopy is highly sensitive method to distinguish of conformation binding and can apply to analyse the conformation change of PNA and its hybrid with DNA.

For homothymine modified acpcPNAs can exhibited two electronic transition of amide chromophore as $n \rightarrow \pi^*$ transition around 210 nm and high amplitude $\pi \rightarrow \pi^*$ transition at negative band 220 nm. While the strong region of 250-280 nm is especially of base chromophore. [34] PNA1-9 was investigated by CD spectroscopy and all spectrums exhibited high amplitude peak at 210, 220 and 248 nm which give similar pattern of conformation of duplex. An example of CD spectrum of PNA1 was shown in **Figure 63** and others CD spectrums of PNA2-9 were shown in appendix.

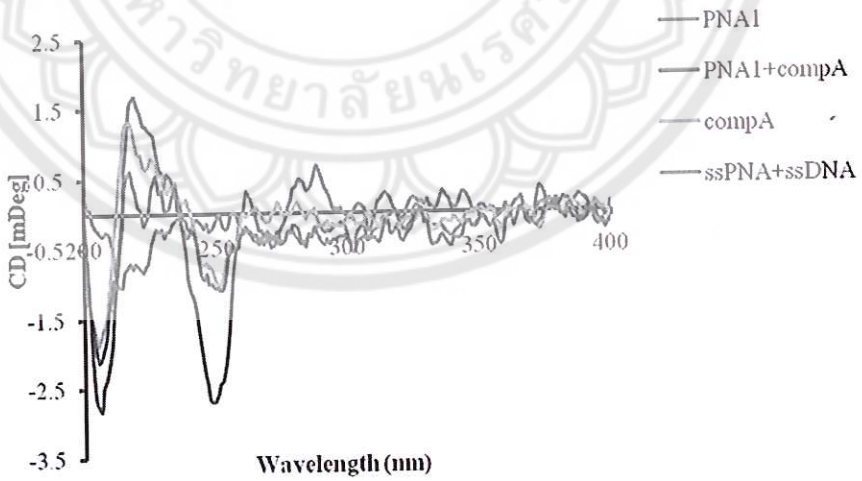

Figure 54 The CD spectra of PNA1 with complementary DNA (5'-AAA AAA AAA-3') condition : 2.5 μM PNA and 2.5 μM DNA in 100 mM phosphate buffer pH 7.0

The solubility experiment

The hydrophilic-modified *acpc*PNA was evaluated for the water solubility by determining the saturated concentration of aqueous solution of PNA (**Table 12**). The results showed that unmodified *acpc*PNA required at least 30 μL of water to reach the saturated concentration at 3.25 mM. While, complete dissolution of linker modified *acpc*PNA can be obtained in only 1 to 5 μL of water. The optical density of the solution was determined by measuring the UV absorption at 260 nm with Nanodrop 2000 instrument and the saturated concentration calculated using molar extinction coefficients of PNA. PNA1-PNA3 which bearing hydroxyl, amino and guanidine function group respectively showed higher saturated concentration than unmodified *acpc*PNA (31.8, >12.0 and >13.3 mM compared to 3.3 mM). However, it should be noted that the saturated concentration ummodified *apc/acpc*PNA also showed a very high value at 49.0 mM (it can be presumed that even each functional gorup at terminus of linker can occur hydrogen bonding with water molecule but the length of 4 carbon atom of the linker stand out in duplex may effect to hydrophobicity of molecule). This can be suggested that the nitrogen of *apc*PNA may protonated to positively charge at backbone which can efficiently interact with water molecule without interference of alkyl side chain.

Table 12 The saturated concentration of PNA

PNA	Volume of water (μL)	Absorbance	Obtical density (OD)[c]	Original OD	The saturated concentration (mM)
unmodified[a]	30	25.74	257.4	257.4	3.25
*apc/acpc*PNA[b]	10	7.76	77.6	3881.0	49.00
PNA1	5	5.04	50.4	2520.0	31.82
PNA2	1	1.91	19.1	953.5	>12.04
PNA3	3	2.11	21.1	1055.0	>13.321

[a]unmodified Ac-TTTTTTTTT-Lys, [b]*apc/acpc*PNA Ac-TTTTTTTTT-Lys, [c]1 μL of hydrophilic-modified *acpc*PNA was diluted with water 50 μL, no dilution for unmodified of PNA.

CHAPTER V

CONCLUSION

Novel hydrophilic side chain was successfully added to APC β-amino acid spacer of *apc/acpc*PNA as a water solubility enhancement linker. Hydroxybutanal (C4OH), aminobutanal ($C4NH_2$) and guanidinobutanal (C4Gua) were prepared in a form of protected aldehyde with trityl-protected for hydroxybutanal, phthalimide-protected for aminobutanal and Boc-protected for guanidinobutanal. acpcPNA sequences (homothymine and mixbase) with 1 position and 3 position APC-insertion were synthesized by solid phase peptide. Then, the hydrophilic side chain was linked to *apc/acpc*PNA by reductive alkylation at nitrogen atom of APC spacer. The identity of linker-modified *acpc*PNA was confirmed by MALDI-TOF mass spectrometry. The thermal melting temperature (T_m) of homothymines (Ac-TTTT(T)TTTT-LysNH_2) has value 67.1, 71.9 and 72.9 °C for C4OH, $C4NH_2$ and C4Gua, respectively (72.5 °C for unmodified *acpc*PNA). The T_m of internal modified mix bases (Ac-GTAGA(T)CACT-LysNH_2) has value 53.5, 58.3 and 58.3 °C for C4OH, $C4NH_2$ and C4Gua, respectively (52.2 °C for unmodified). The T_m of three positions modified mixbases has value 54.4, 65.1 and 66.8 °C for C4OH, $C4NH_2$ and C4Gua, respectively. Accordingly, the hydrophilic side chain indicates slightly affected to hybridization of duplex. The water solubility was studied and found that the linker-modified *acpc*PNAs used only 1 μL to reach saturation compared with unmodified (30 μL). The result can be concluded that novel linker-modified acpcPNA can improve water solubility and still remain high affinity binding.

REFERENCES

REFERENCES

[1] Nielsen, P.E.,Egholm, M., Berg, R.H., & Buchardt, O. (1991). Sequence-selective recognition of DNA by strand displacement with a thymine-substituted polyamide. *Science, 254*, 1497-1500.

[2] Nielsen, P.E. (2010). Peptide nucleic acids (PNA) in chemical biology and drug discovery. *Chemistry&Biodiversity, 7*, 786-804.

[3] Nicola, M. Howarth, & Laurence, P. G. Wakelin. (1997). α-PNA: A novel peptide nucleic acid analogue of DNA. *J. Org. Chem, 62*, 5441-5450.

[4] D'Costa,M., Kumar,V., & Ganesh,K. N. (2001). Aminoethylprolyl (aep) PNA: Mixed purine/pyrimidine oligomers and binding orientation preferences for PNA: DNA duplex formation. *Org. Lett, 3*, 1281-1284.

[5] Fader,L. D., &Tsantrizos, Y. S.(2002). Hybridization properties of aromatic peptide nucleic acids: A novel class of oligonucleotide analogues. *Org. Lett, 4*, 63-66.

[6] Püschl, A., BoeSen, T., & Zuccarello, G. (2001). Synthesis of pyrrolidinone PNA: A novel conformationally restricted PNA analogue. *J. Org. Chem, 66*, 707-712.

[7] Guler, M. O., Pokorski, J. K., Appella, D.H., & Stupp, S. I. (2005). Enhanced oligonucleotide binding to self-assembled nanofibers. *Bioconjugate Chem, 16*, 501-503.

[8] Kundu, L.M., Tsukada, H., Matsuoka, Y., Kanayama, N., Takarada, T., & Maeda, M. (2012). Estimation of binding constants of peptide nucleic acid and secondary-structured DNA by affinity capillary electrophoresis. *Anal.Chem, 84*, 5204-5209.

[9] Wancewicz, E. V., Maier, M. A., Siwkowski, A. M.,Albertshofer, K., Winger, T. M., Berdeja, A., … Kinberger, G. A. (2010). Peptide nucleic acids conjugated to short basic peptides show improved pharmacokinetics and antisense activity in adipose tissue. *J. Med. Chem, 53*, 3919-3926.

[10] Muse, O., Zengeya, T., Mwaura, J., Hnedzko, D., McGee, D. W., Grewer, C. T., & Rozners, E. (2013). Sequence selective recognition of double-stranded RNA at physiologically relevant conditions using PNA-peptide conjugates. *ACS Chem. Biol, 8*, 1683-1686.

[11] Suparpprom, C., Srisuwannaket, C., Sangvanich, P., & Vilaivan, T. (2005). Synthesis and oligodeoxynucleotide binding properties of pyrrolidinyl peptide nucleic acids bearing prolyl-2-aminocyclopentanecarboxylic acid (ACPC) backbones. *Tetrahedron Letters, 46*, 2833-2837.

[12] Ananthanawat, C., Vilaivan, T., Hoven, V. P., & Su, X. (2010). Comparison of DNA, aminoethylglycyl PNA and pyrrolidinyl PNA as probes for detection of DNA hybridization using surface Plasmon resonance technique. *Biosensors and Bioelectronics, 25*, 1064-1069.

[13] Reenabthue, N., Boonlua, C., Vilauvan, C., Vilaivan, T., & Suparpprom, C. (2011). 3-Aminopyrrolidine-4-carboxylic acid as versatile handle for internal labeling of pyrrolidinyl PNA. *Bioorganic and medical chemistry letters, 21*, 6465-6469.

[14] Ditmangklo, B., Boonlua, C., Suparpprom, C., & Vilaivan, T. (2013). Reductive alkylation and sequential reductive alkylation-click chemistry for on-solid-support modification of pyrrolidinyl peptide nucleic acid. *Bioconjugate Chem, 24*, 614-625.

[15] Kuwahara, M., Arimitsu, M., & Sisido, M. (1999). Novel peptide nucleic acid that shows high sequence specificity and all-or-none-type hybridization with the complementary DNA. *J. Am. Chem. Soc., 121*, 256-257.

[16] Kuwahara, M., Arimitsu, M., Shigeyasu, M., Saeki, N., & Sisido, M. (2001). Hybridization between oxy-peptide nucleic acid and DNAs: Dependence of hybrid stabilities on the chain-lengths, types of base pairs, and the chain directions. *J. Am. Chem. Soc., 123*, 4653-4658.

[17] Dragulescu-Andrasi, A., Rapireddy, S., Frezza, B. M., Gayathri, C., Gil, R. R., & Ly, D. H. (2006). A simple γ-backbone modification preorganizes peptide nucleic acid into a helical structure. *J. Am. Chem. Soc., 128*, 10258-10267.

[18] Englund, E., & Appella, D. H. (2005). Synthesis of γ-Subsituted peptide nucleic Acid: A new place to attach fluorphores without affecting DNA binding. *Org. Lett., 7*, 3465-3467.

[19] Zhou, P., Wang, M., Du, L., Fisher, G. W. ,Waggoner, A., & Ly, D. H. (2003) Novel binding and efficient cellular uptake of guanidine-based peptide nucleic acids (GPNA). *J. Am. Chem. Soc., 125*, 6878-6879.

[20] Sahu, B., Chenna, V., Lathrop. K. L., Thomas, S. M., Zon, G., Livak, K. J., & Ly, D.H. (2009). Synthesis of conformationally preorganized and cell-permeable guanidine-based γ-peptide nucleic acids (γGPNAs). *J. Org. Chem., 74*, 1509-1516.

[21] Sahu, B., Sacui, I., Rapireddy, S., Zanotti, K. J., Bahal, R., Armitage, B. A., & Ly, D. H. (2011). Synthesis and characterization of conformationally preorganized, (*R*)-diethylene glycol-containing γ-peptide nucleic acids with superior hybridization properties and water solubility. *J. Org. Chem., 76*, 5614-5627.

[22] Goldman, J. M., Zhang, L. A., Manna, A., Armitage, B. A., Ly, D. H., & Schneider, J. (2013). High affinity γPNA sandwich hybridization assay for rapid detection of short nucleic acid targets with single mismatch discrimination. *Biomacromolecules, 14*, 2253-2261.

[23] Jain, D.R., V, L. A., Lahiri, M., & Ganesh, K. N. (2014). Influence of pendant chiral C^{γ}-(Alkylideneamino/Guanidino) cationic side-chains of PNA backbone on hybridization with complementary DNA/RNA and cell permeability. *J. Org. Chem., 79*, 9567-9577.

[24] Kumar, V. A., & Ganesh, K. N. (2005). Conformationally constrained PNA analogues: Structural evolution toward DNA/RNA binding selectivity. *Accounts of chemical research, 2005*, 404-412.

[25] Vilaivan, T., & Srisuwannaket, C. (2006). Hybridization of pyrrolidinyl peptide nucleic acids and DNA: Selectivity, base-pairing specificity, and direction of binding. *Org. Lett., 8*, 1897-1900.

[26] Egholm, M., Buchardt, O., Christensen, L., Behrens, C., Freier, S. M., Driver, D. A., … Nielsen, P. E. (1993). PNA hybridizes to complementary oligonucleotides obeying the Watson–Crick hydrogen-bonding rules. *Nature, 365*, 566-568.

[27] Herth, M. M., Volk, B., Pallagi, K., & Kristensen, J. L. (2012). Synthesis and in vitro evaluation of oxindole derivatives as potential radioligands for 5-HT_7 receptor imaging with PET. *ACS Chem. Neurosci, 3*, 1002-1007.

[28] Liu, C., Guo, W., Shi, X., Kaium, M. A. Gu, X., & Zhu, Y. Z. (2011). Leonurine-cysteine analog conjugates as a new class of multifunctional anti-myocardial ischemia agent. *European Journal of Medicinal Chemistry, 46*, 3996-4009.

[29] Shymanska, N. V., An, I. H., & Pierce, J. G. (2014). A rapid synthesis of 4-oxazolidinones: Total synthesis of synoxazolidinones A and B. *Angew. Chem. Int. Ed., 53*, 5401-5404.

[30] Eriks, J. C., Goot, H., Sterk, G. J., & Tinmerman, H. (1992). Histamine H_2 receptor agonists. synthesis, in vitro pharmacology, and qualitative structure activity relationships of substituted 4- and 5 4 2-Aminoethyl) thiazoles. *J. Med. Chem, 35*, 3239-3246.

[31] Blackburn, G. M., & Gait, M. J. (1996). *Nucleic acid in chemistry and biology.* New York: Oxford University.

[32] Dissociation constants of organic acids and bases. (n.d.). CRC Handbook of Chemistry and Physics. N.P.: n.p.

[33] Hammes, G. G. (2005). *Spectroscopy for the biological sciences.* USA: John wiley.

[34] Sewald, N., & Jakubke, H. D. (2009). *Peptide: Chemistry and biology* (2nd ed.). USA: Wiley-vch Verlag GmbH&Co. KGaA.

APPENDIX

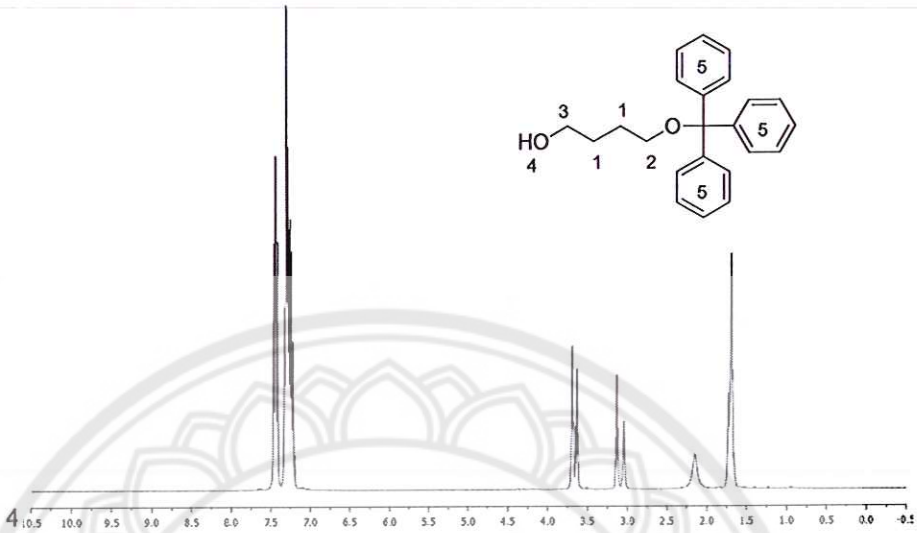

Figure 55 ^{1}H NMR spectrum of 4-trityloxy-1-butanol (Compound 2)

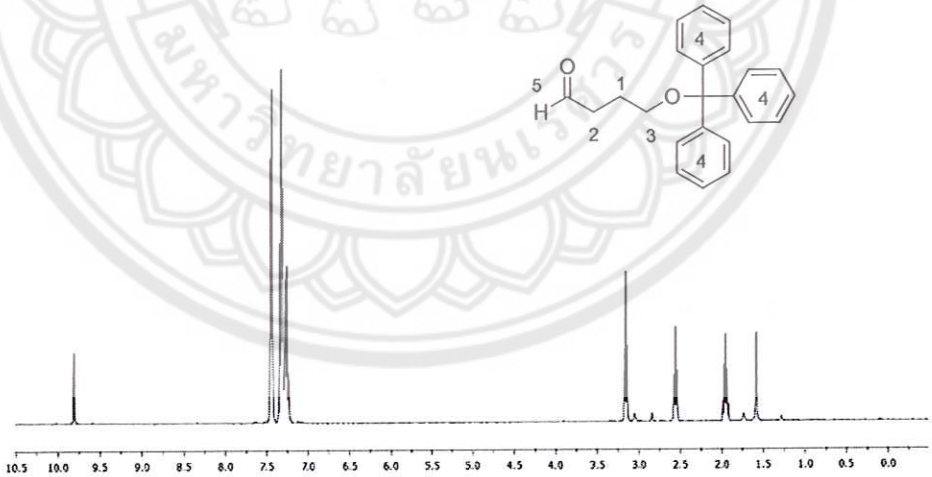

Figure 56 ^{1}H NMR spectrum of 4-trityloxy-1-butanal (Compound 3)

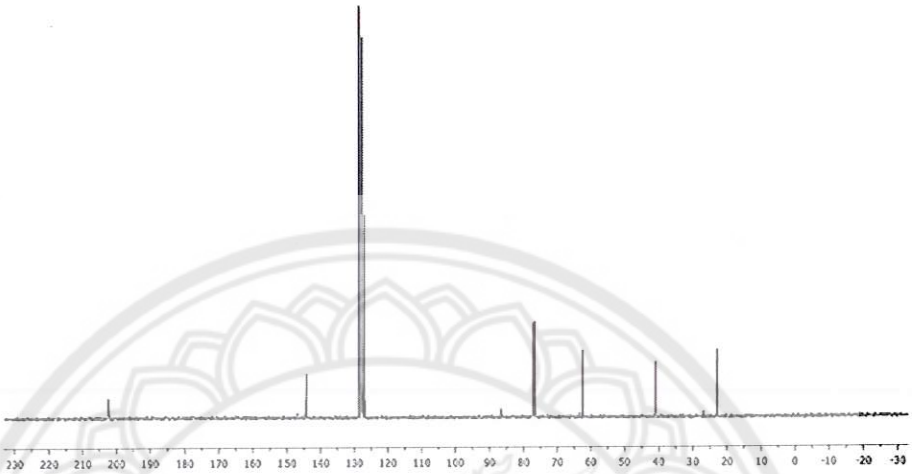

Figure 57 ^{13}C NMR spectrum of 4-trityloxy-1-butanal (Compound 3)

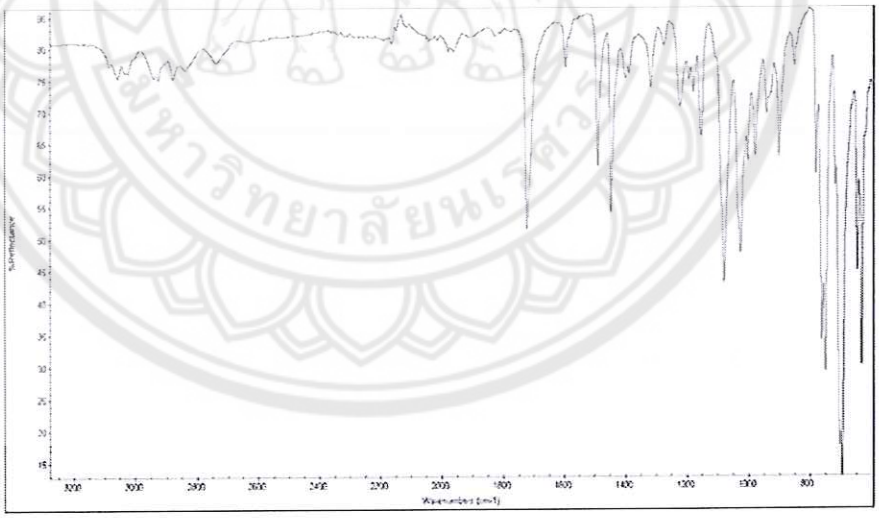

Figure 58 IR spectrum of 4-trityloxy-1-butanal (Compound 3)

Mass Spectrum List Report

Analysis Info

Analysis Name	OSCUT5803100021.d	Acquisition Date	3/19/2015 10:43:15 AM
Method	MKE_tune_low_positive_20130204.m	Operator	Administrator
Sample Name	C23H22O2	Instrument	micrOTOF 72
	C23H22O2		

Acquisition Parameter

Source Type	ESI	Ion Polarity	Positive	Set Corrector Fill	79 V
Scan Range	n/a	Capillary Exit	130.0 V	Set Pulsar Pull	406 V
Scan Begin	50 m/z	Hexapole RF	90.0 V	Set Pulsar Push	388 V
Scan End	3000 m/z	Skimmer 1	45.5 V	Set Reflector	1300 V
		Hexapole 1	25.0 V	Set Flight Tube	9000 V
				Set Detector TOF	1910 V

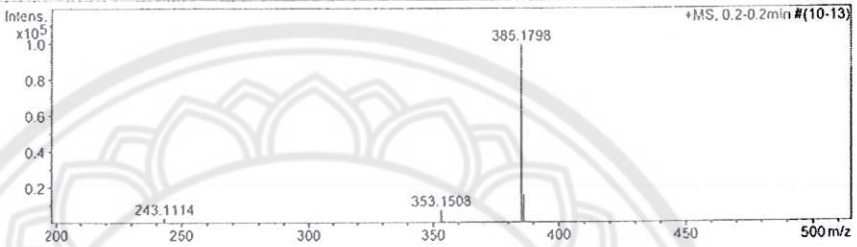

#	m/z	I	I %	S/N	FWHM	Res.
1	62.0927	125	0.1	44.8	0.0056	11094
2	165.0636	109	0.1	37.9	0.0276	5986
3	243.1114	3133	3.2	935.2	0.0373	6523
4	244.1163	530	0.5	157.6	0.0407	5997
5	274.2695	114	0.1	32.1	0.0415	6607
6	283.1062	199	0.2	55.1	0.0434	6524
7	290.2651	112	0.1	30.6	0.0455	6375
8	297.1218	115	0.1	31.0	0.0481	6182
9	301.1377	117	0.1	31.4	0.0424	7110
10	353.1508	7499	7.5	1855.3	0.0534	6609
11	354.1550	1304	1.3	322.0	0.0540	6562
12	355.1585	177	0.2	43.5	0.0552	6439
13	369.1762	112	0.1	28.5	0.0908	4067
14	371.1640	377	0.4	96.7	0.0694	5348
15	385.1798	99466	100.0	26648.7	0.0662	5814
16	386.1810	16288	16.4	4376.8	0.0632	6112
17	387.1849	1441	1.4	388.2	0.0616	6284
18	401.1545	137	0.1	38.3	0.0675	5944
19	413.2684	158	0.2	45.9	0.0849	4866
20	429.2048	437	0.4	134.5	0.0794	5405
21	430.2081	120	0.1	37.0	0.0785	5480

Bruker Daltonics DataAnalysis 3.3 printed: 3/20/2015 4:37:31 PM Page 1 of 1

Figure 59 HRMS of 4-trityloxy-1-butanal (Compound 3)

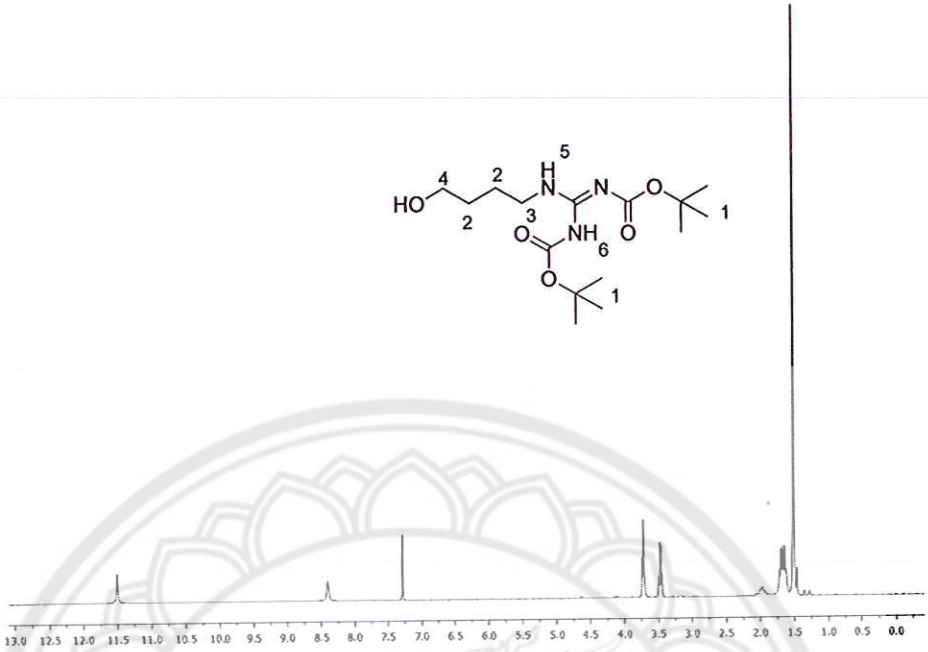

Figure 60 ^{1}H NMR spectrum of 4-guanidino-1-butanol (Compound 5)

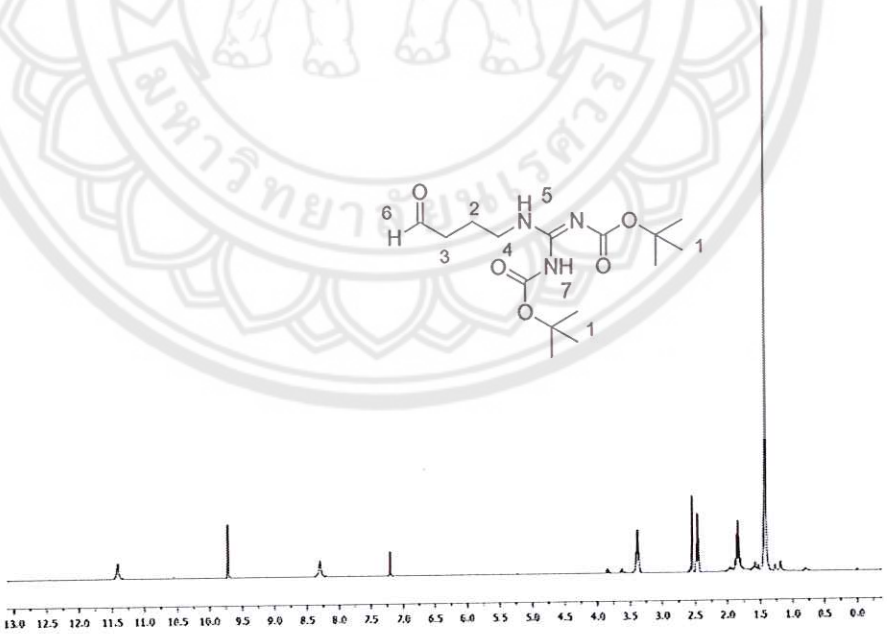

Figure 61 ^{1}H NMR spectrum of 4- guanidino-butanal (Compound 6)

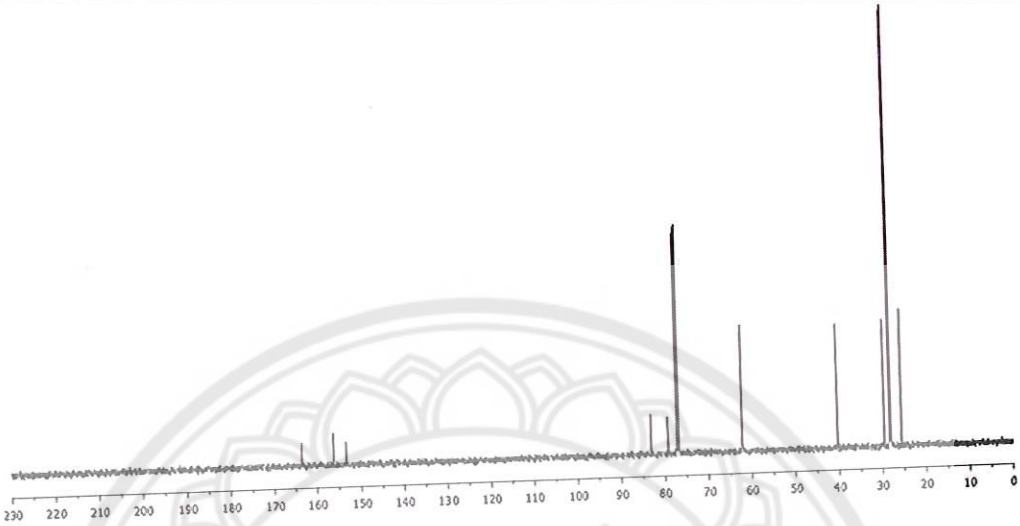

Figure 62 ^{13}C NMR spectrum of 4- guanidino -1-butanal (Compound 6)

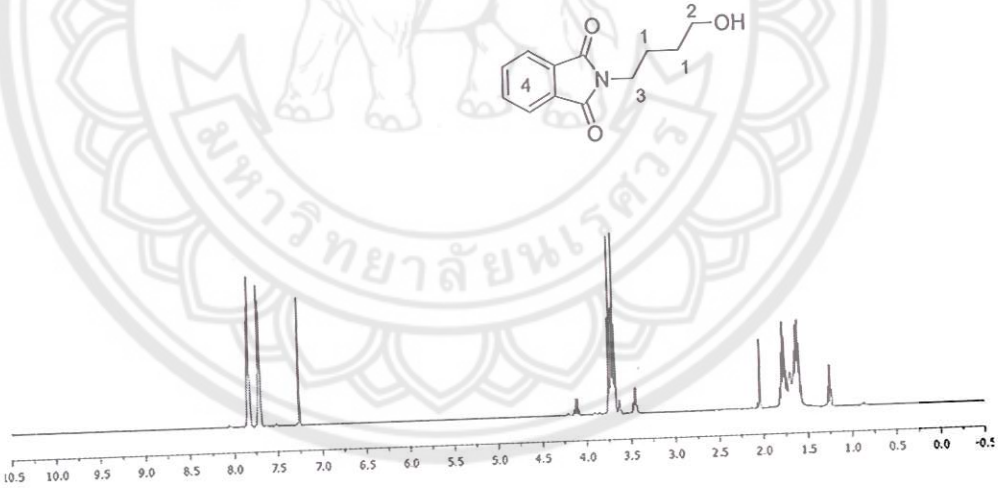

Figure 63 ^{1}H NMR spectrum of 4-phthalimide-butanol (Compound 8)

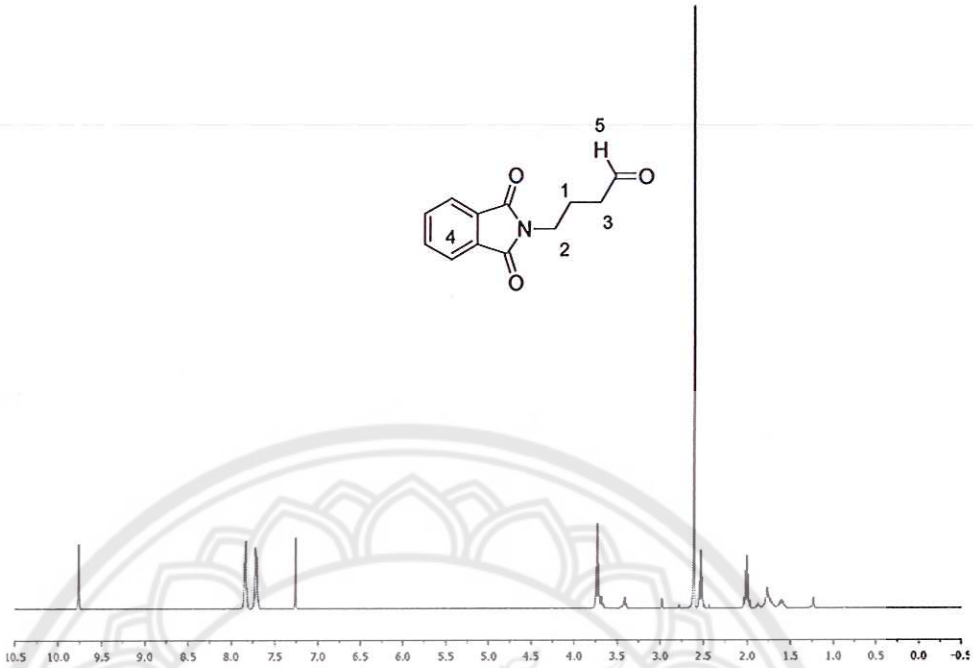

Figure 64 ^{1}H NMR spectrum of 4-phthalimide-butanal (Compound 9)

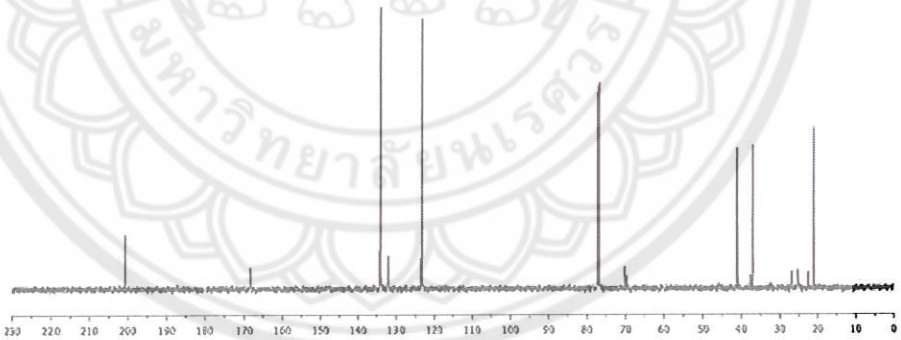

Figure 65 ^{13}C NMR spectrum of 4-phthalimide-butanal (Compound 9)

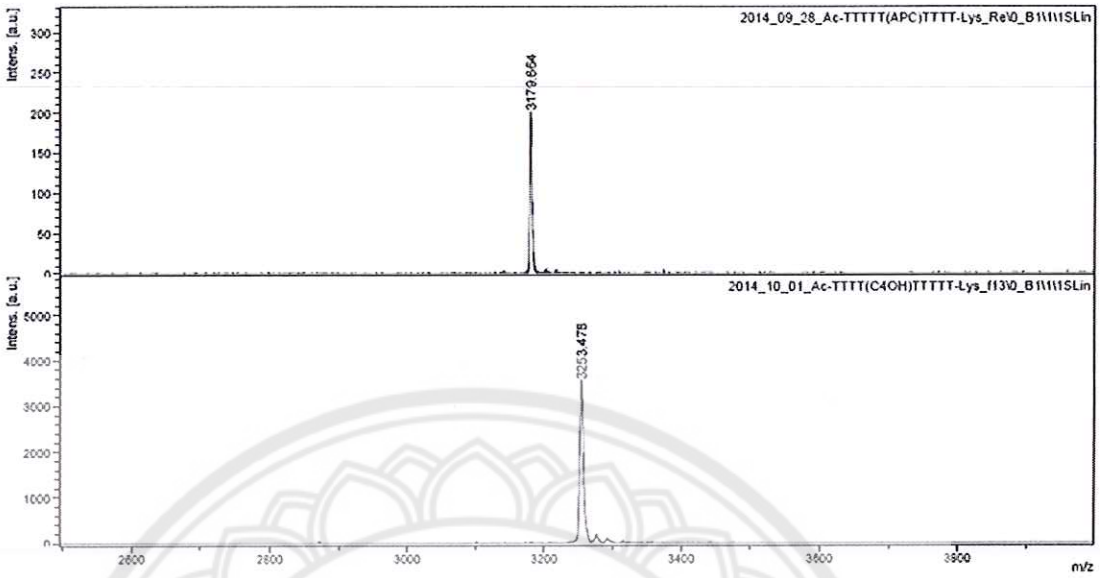

Figure 66 MALDI-TOF mass spectra of Ac-TTTT(T_{C4OH})TTTT-LysNH_2 (PNA1)

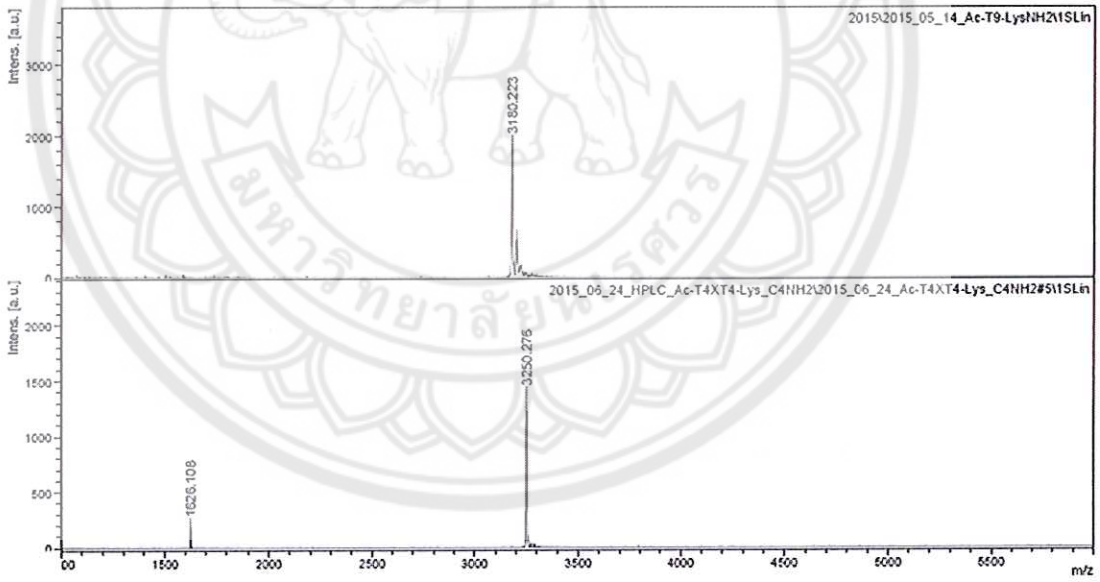

Figure 67 MALDI-TOF mass spectra of Ac-TTTT(T_{C4NH2})TTTT-Lys NH_2 (PNA2)

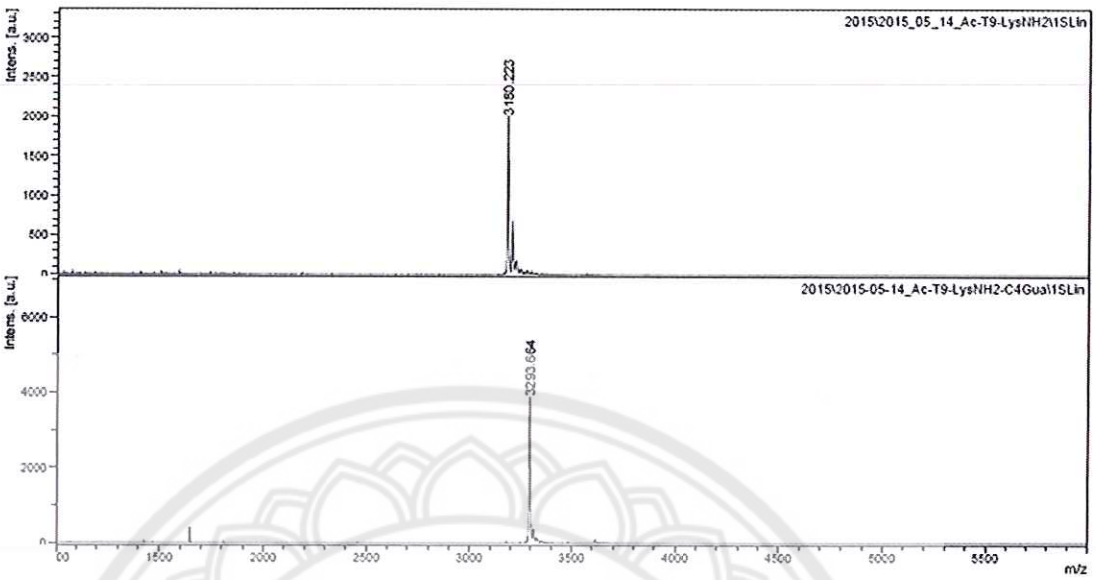

Figure 68 MALDI-TOF mass spectra of Ac-TTTTT($_{C4Gua}$)TTTT-Lys NH_2 (PNA3)

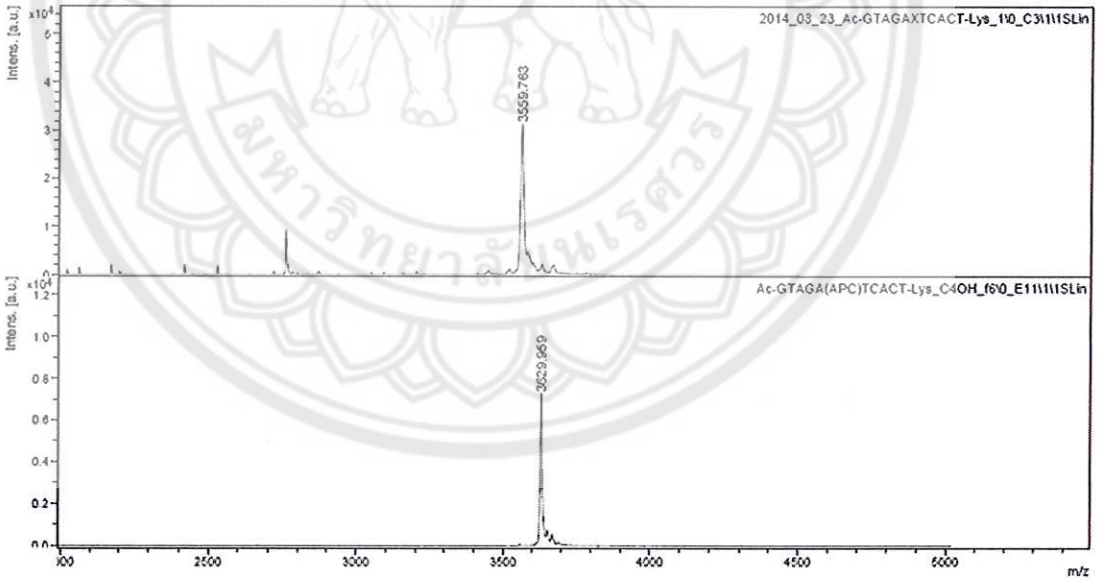

Figure 69 MALDI-TOF mass spectra of Ac-GTAGA(T_{C4OH})CACT-LysNH_2 (PNA4)

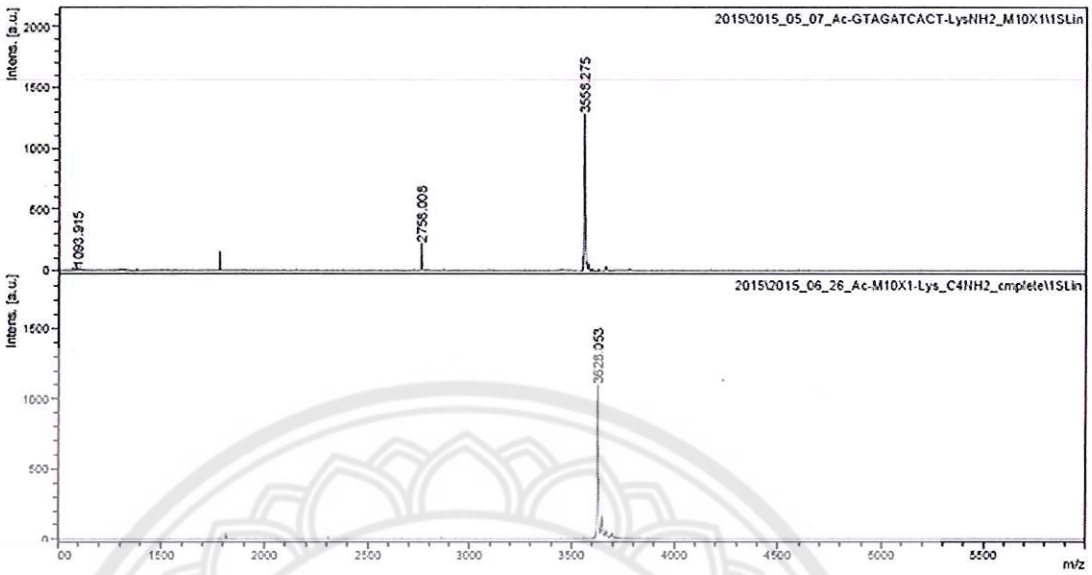

Figure 70 MALDI-TOF mass spectra of Ac-GTAGA(T_{C4NH2})CACT-LysNH$_2$ (PNA5)

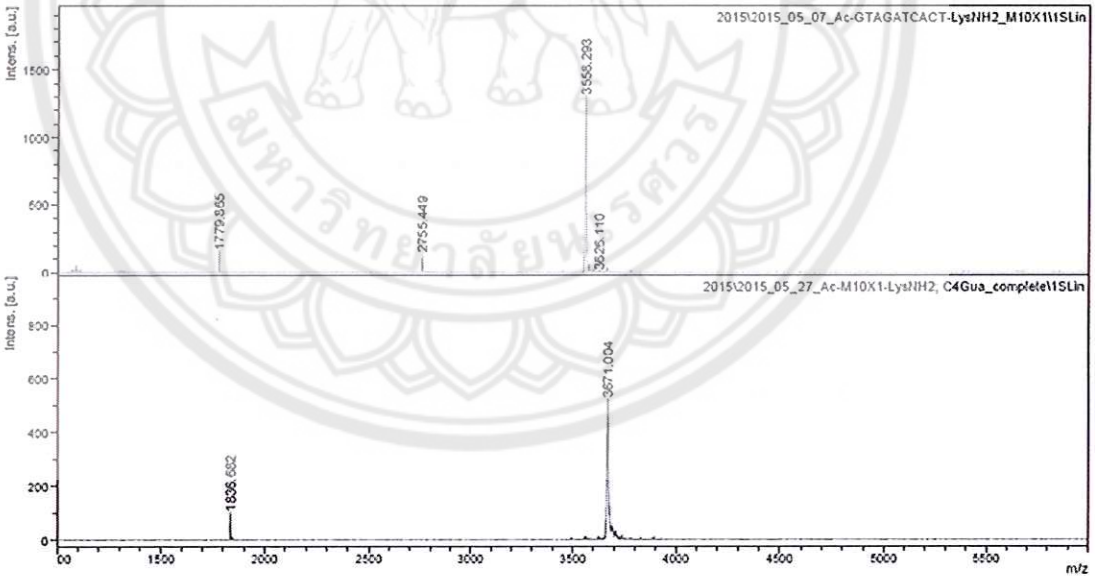

Figure 71 MALDI-TOF mass spectra of Ac-GTAGA(T_{C4Gua})CACT-LysNH$_2$ (PNA6)

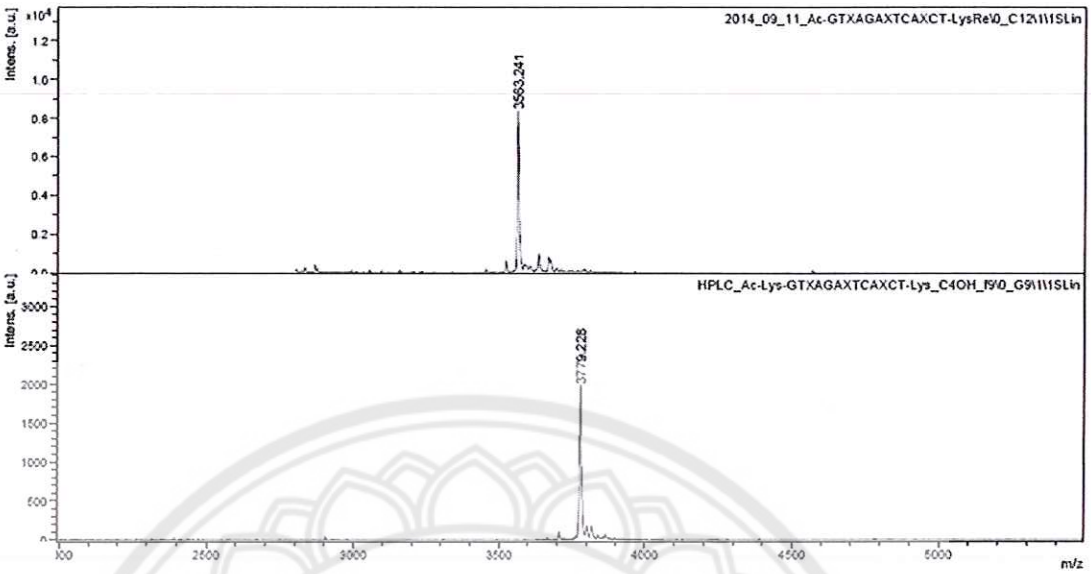

Figure 72 MALDI-TOF mass spectra of Ac-GT(A_{C4OH})GA(T_{C4OH}) CA(C_{C4OH}) T-LysNH_2 (PNA7)

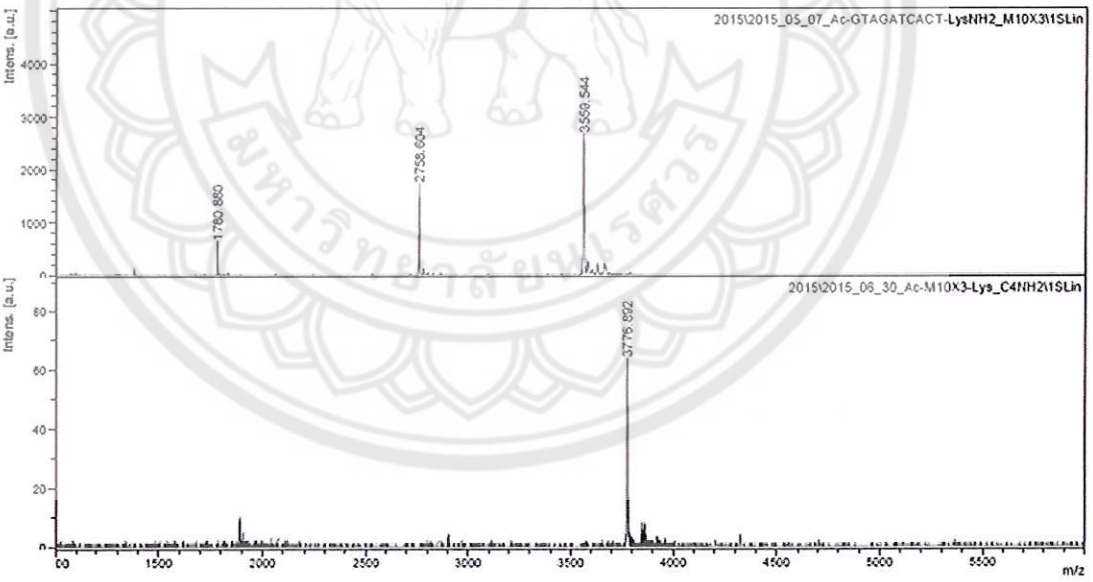

Figure 73 MALDI-TOF mass spectra of Ac-GT(A_{C4NH2})GA(T_{C4NH2})CA(C_{C4NH2}) T-LysNH_2 (PNA8)

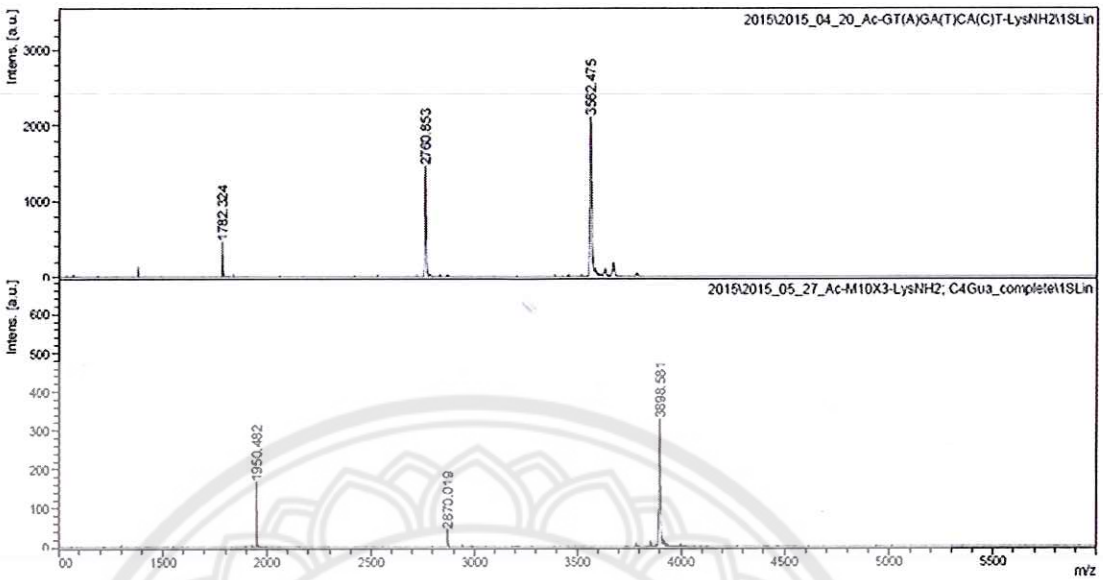

Figure 74 MALDI-TOF mass spectra of Ac-GT(A_{C4Gua})GA(T_{C4Gua})CA(C_{C4Gua}) T-LysNH_2 (PNA9)

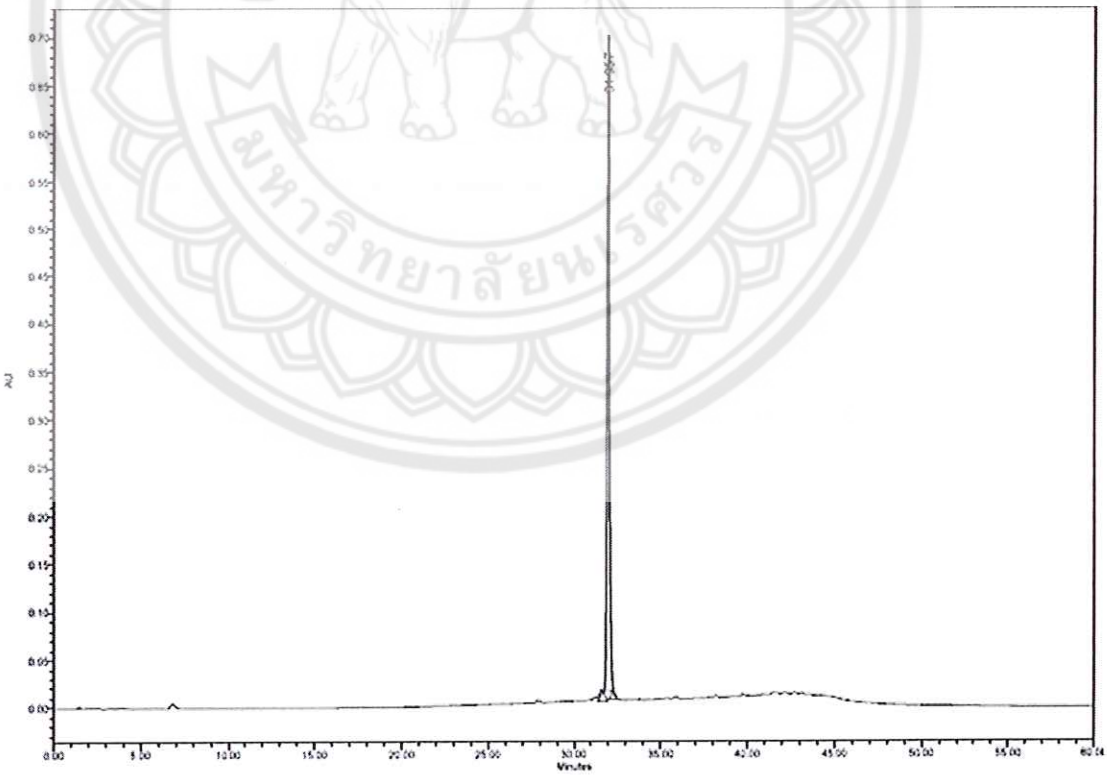

Figure 75 HPLC spectrum of Ac-TTTT(T_{C4OH})TTTT-LysNH_2 (PNA1)

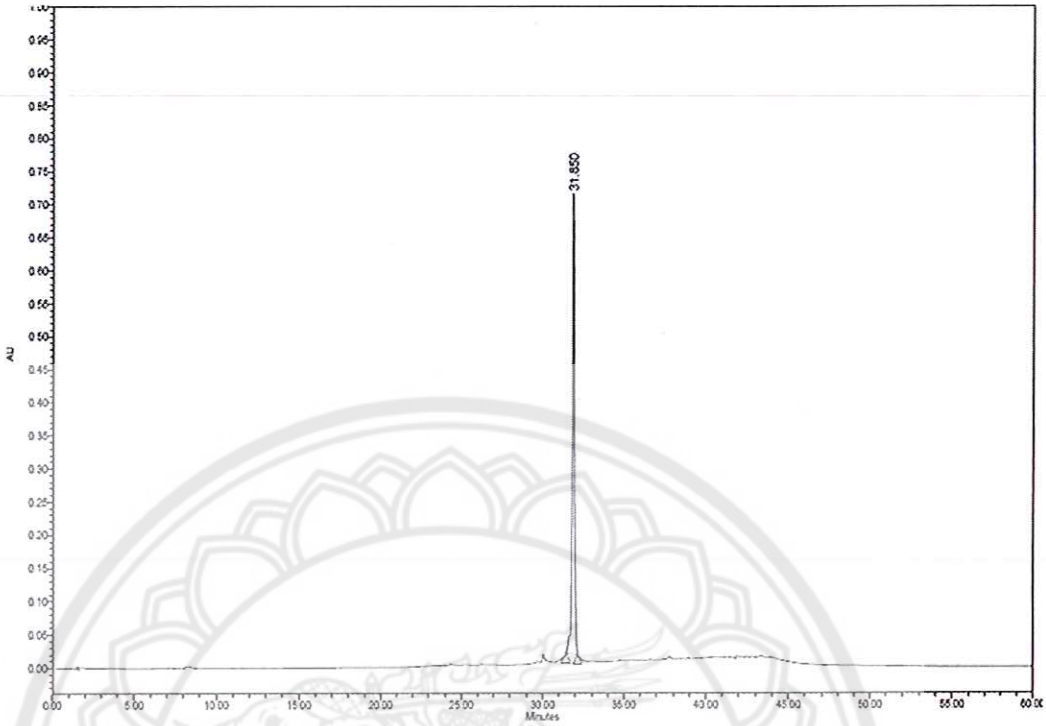

Figure 76 HPLC spectrum of Ac-TTTT(T_{C4NH2})TTTT-LysNH_2 (PNA2)

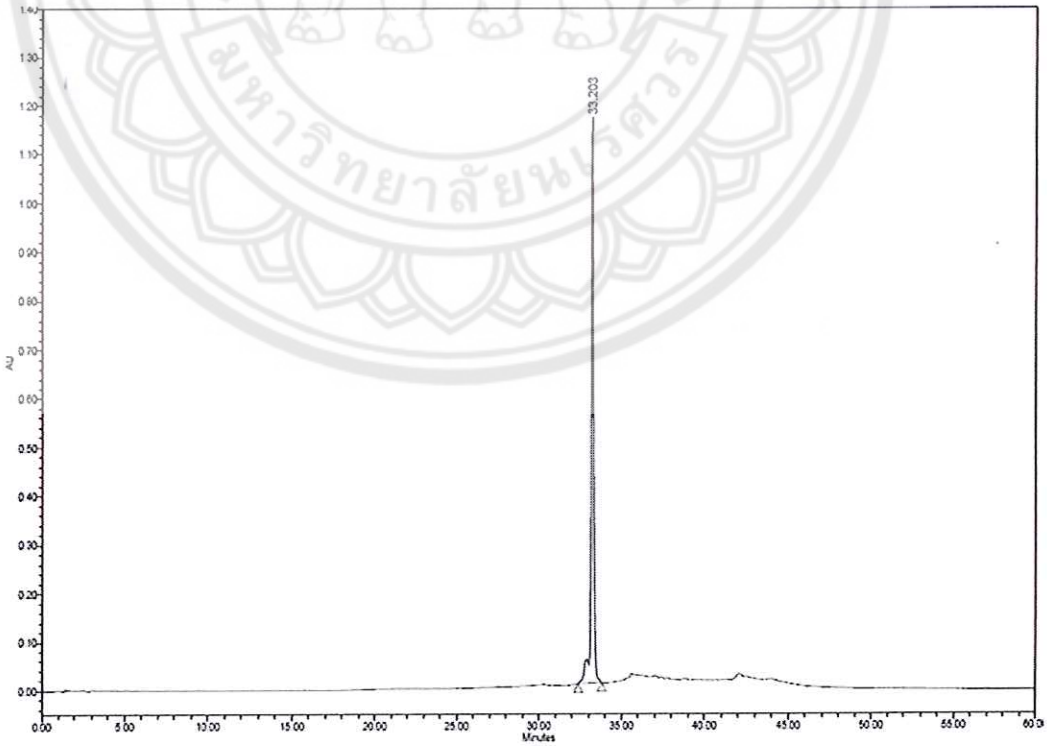

Figure 77 HPLC spectrum of Ac-TTTT(T_{C4Gua})TTTT-LysNH_2 (PNA3)

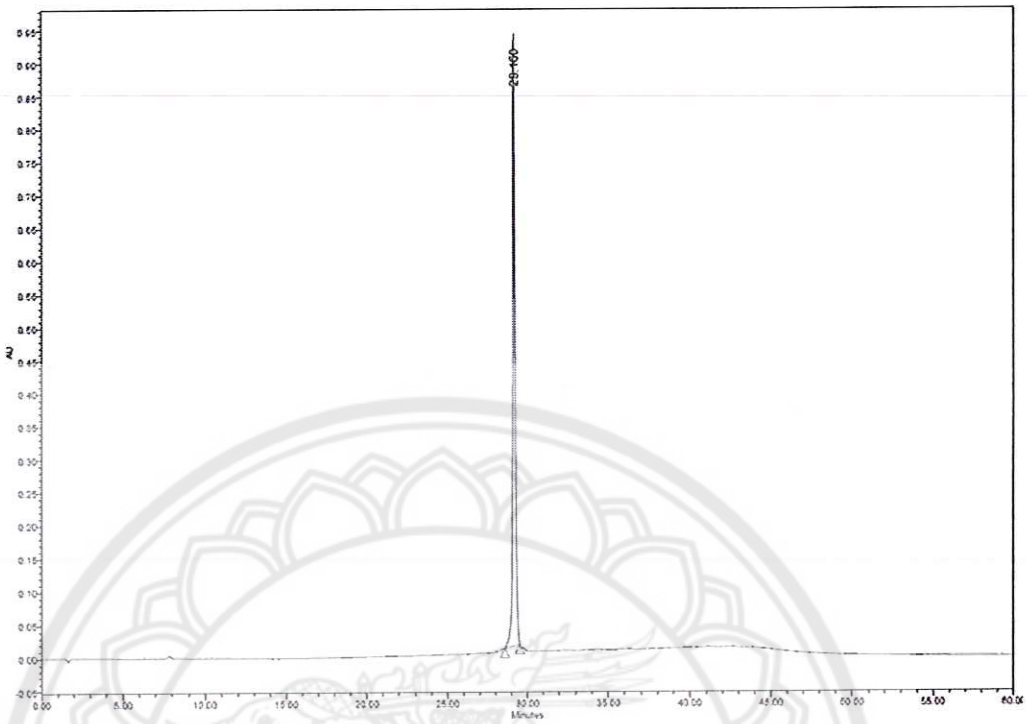

Figure 78 HPLC spectrum of Ac-GTAGA(T_{C4OH})CACT-LysNH_2 (PNA4)

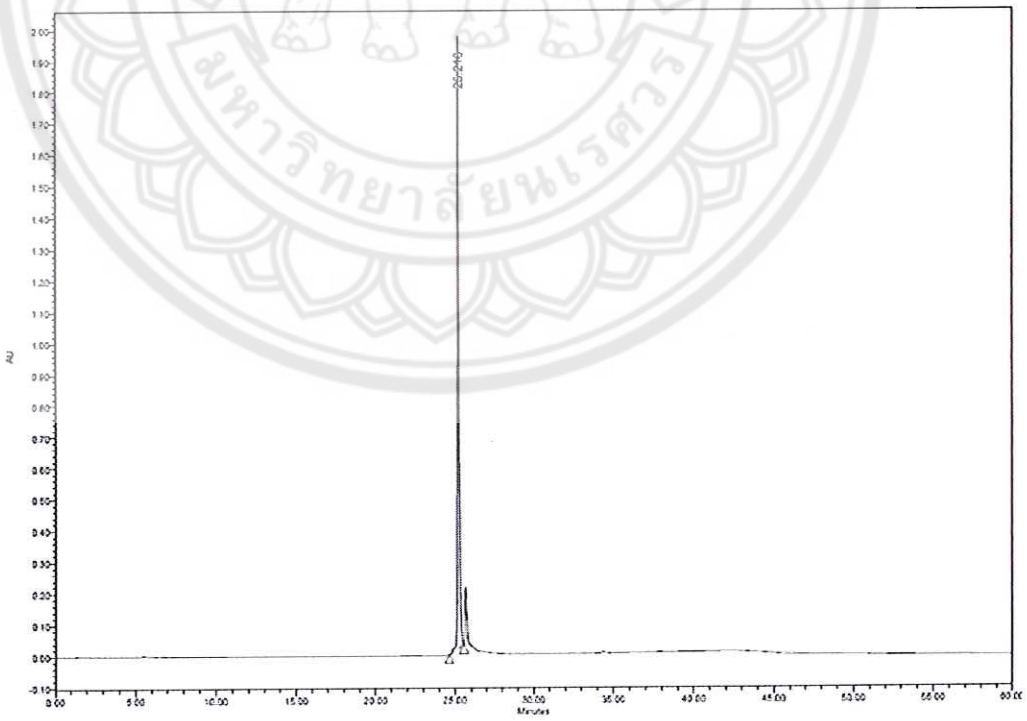

Figure 79 HPLC spectrum of Ac-GTAGA(T_{C4NH2})CACT-LysNH_2 (PNA5)

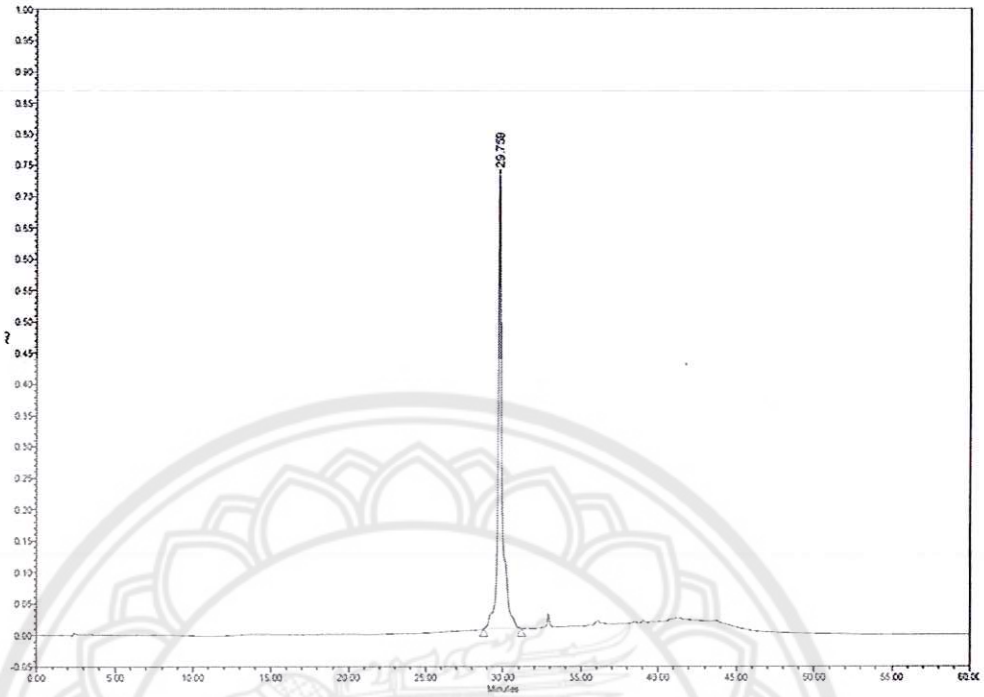

Figure 80 HPLC spectrum of Ac-GTAGA(T_{C4Gua})CACT-LysNH_2 (PNA6)

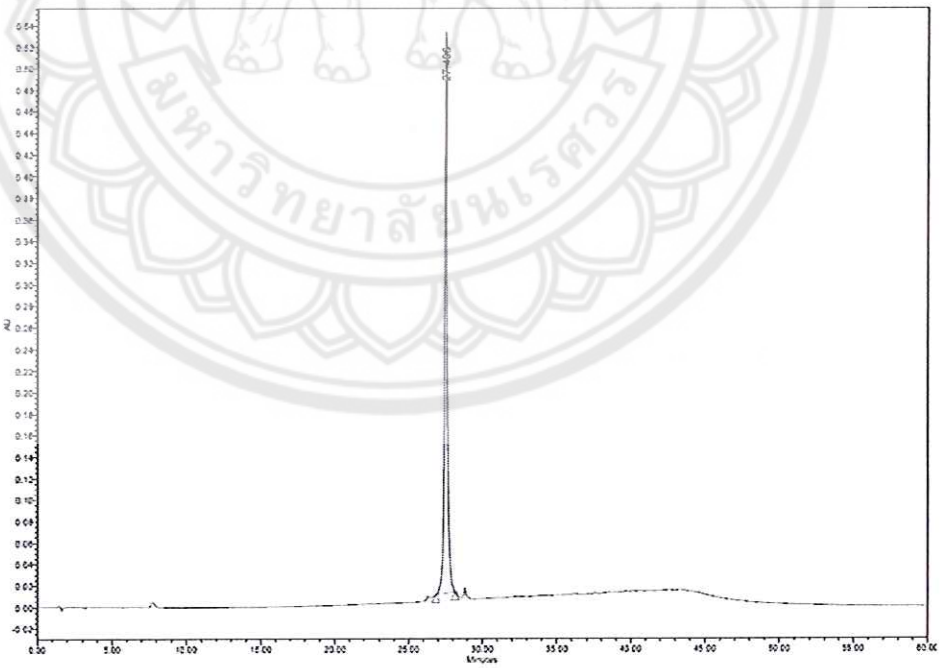

Figure 81 HPLC spectrum of Ac-GT(A_{C4OH})GA(T_{C4OH})CA(C_{C4OH})T-LysNH_2 (PNA7)

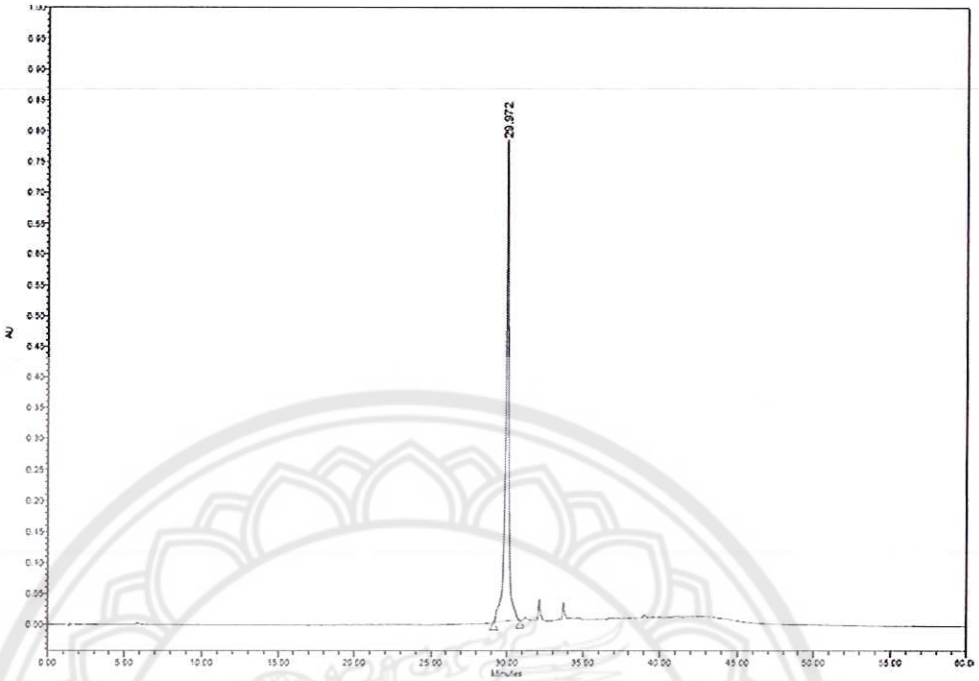

Figure 82 HPLC spectrum of Ac-GT(A_{C4NH2})GA(T_{C4NH2})CA(C_{C4NH2})T-LysNH$_2$ (PNA8)

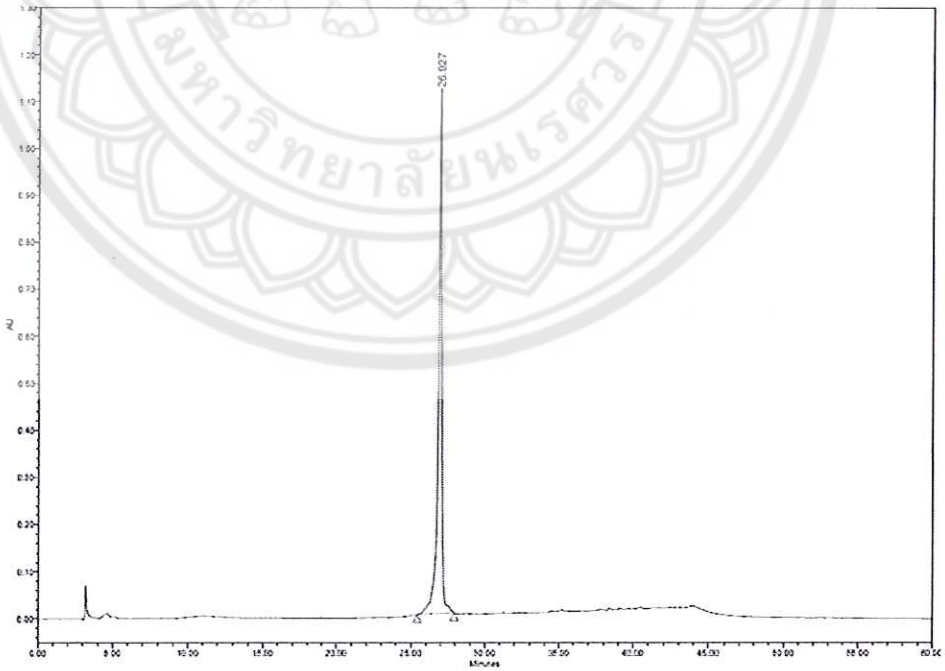

Figure 83 HPLC spectrum of Ac-GT(A_{C4Gua})GA(T_{C4Gua})CA(C_{C4Gua})T-LysNH$_2$ (PNA9)

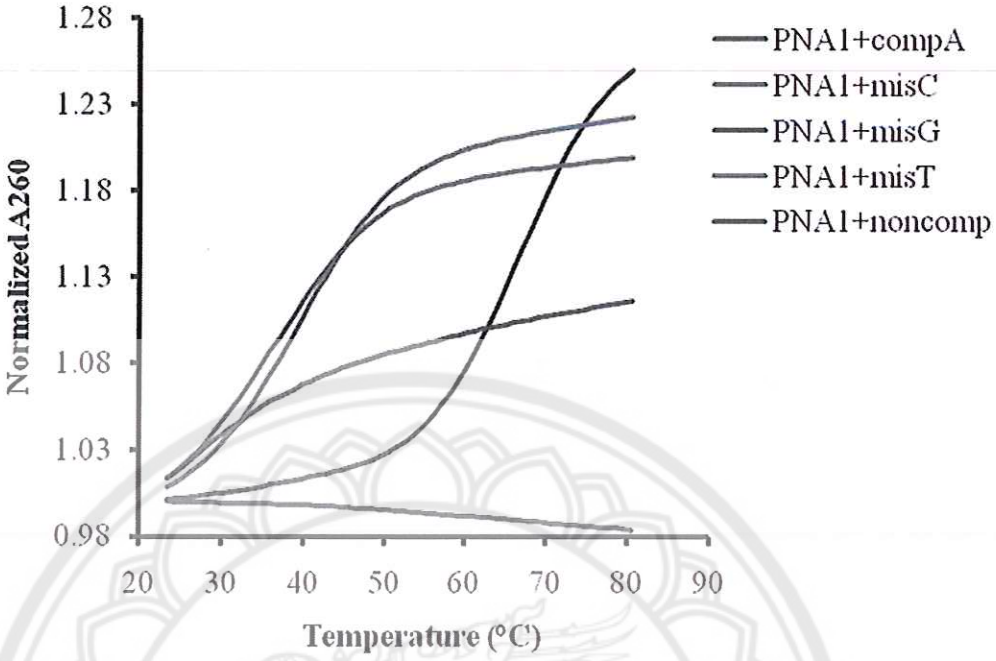

Figure 84 Thermal melting temperature of Ac-TTTT(T_{C4OH})TTTT-LysNH$_2$ (PNA1)

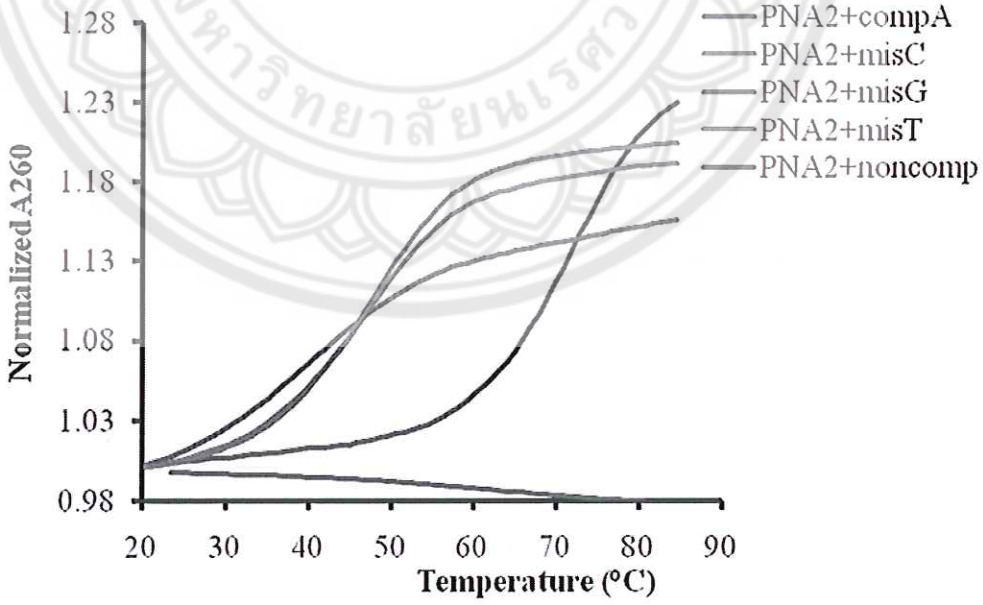

Figure 85 Thermal melting temperature of Ac-TTTT(T_{C4NH2})TTTT-LysNH$_2$ (PNA2)

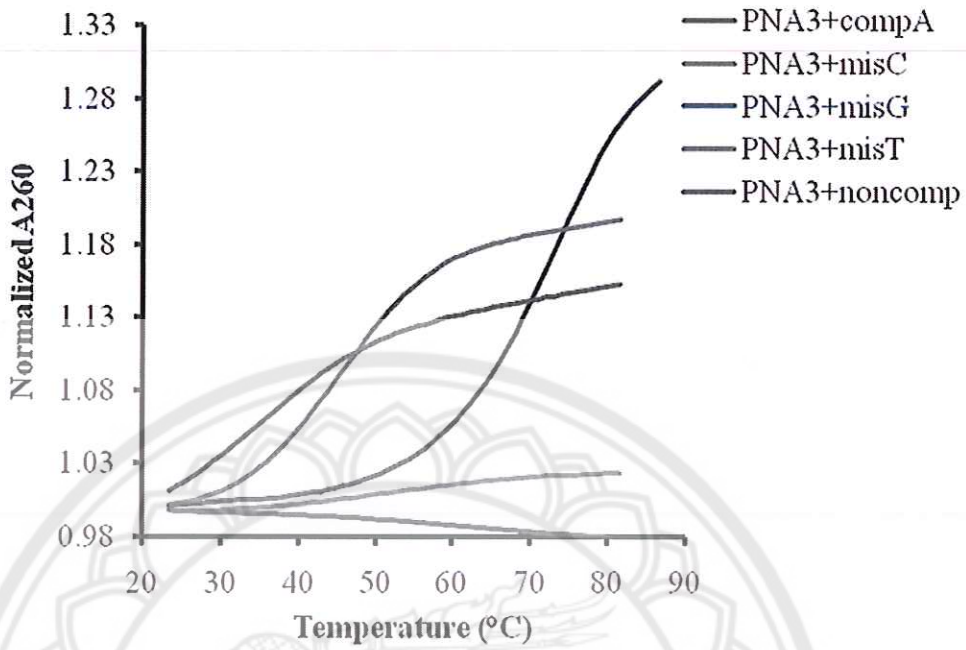

Figure 86 Thermal melting temperature of Ac-TTTT(T_{C4Gua})TTTT-LysNH$_2$ (PNA3)

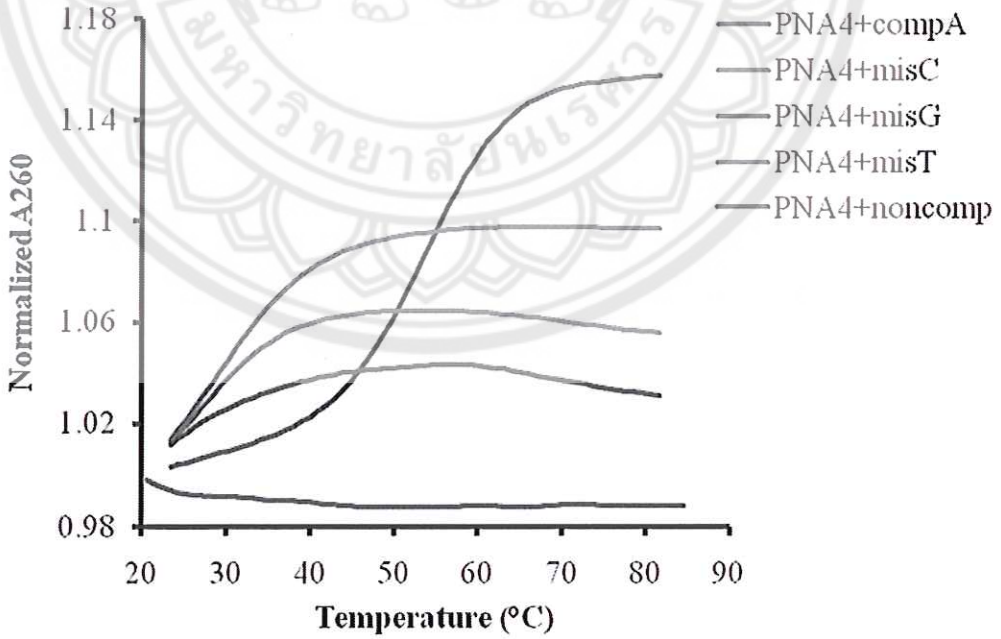

Figure 87 Thermal melting temperature of Ac-GTAGA(T_{C4OH})CACT-LysNH$_2$ (PNA4)

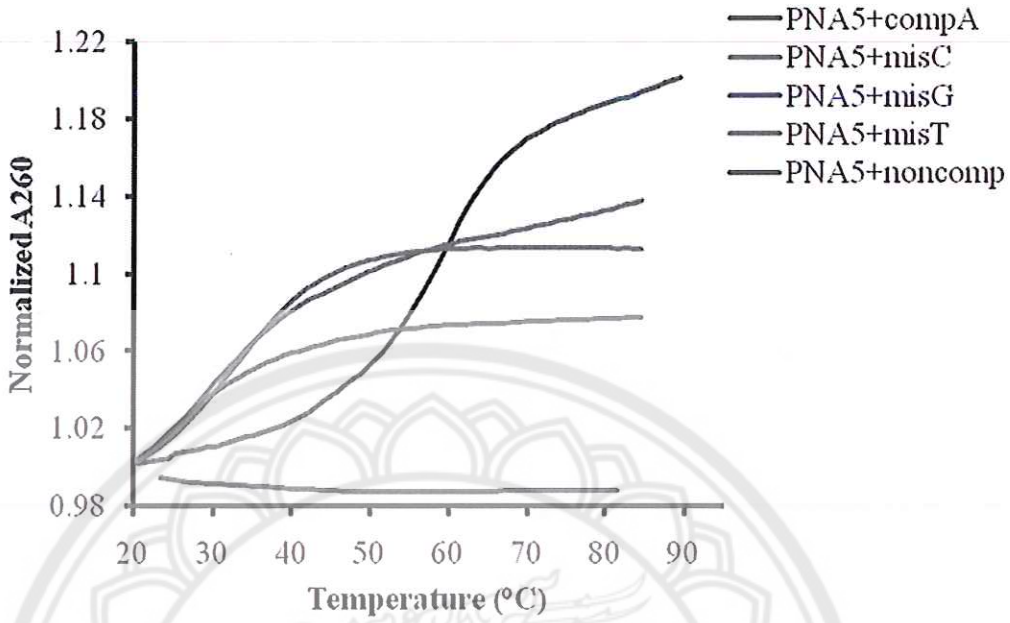

Figure 88 Thermal melting temperature of Ac-GTAGA(T_{C4NH2})CACT-LysNH$_2$ (PNA5)

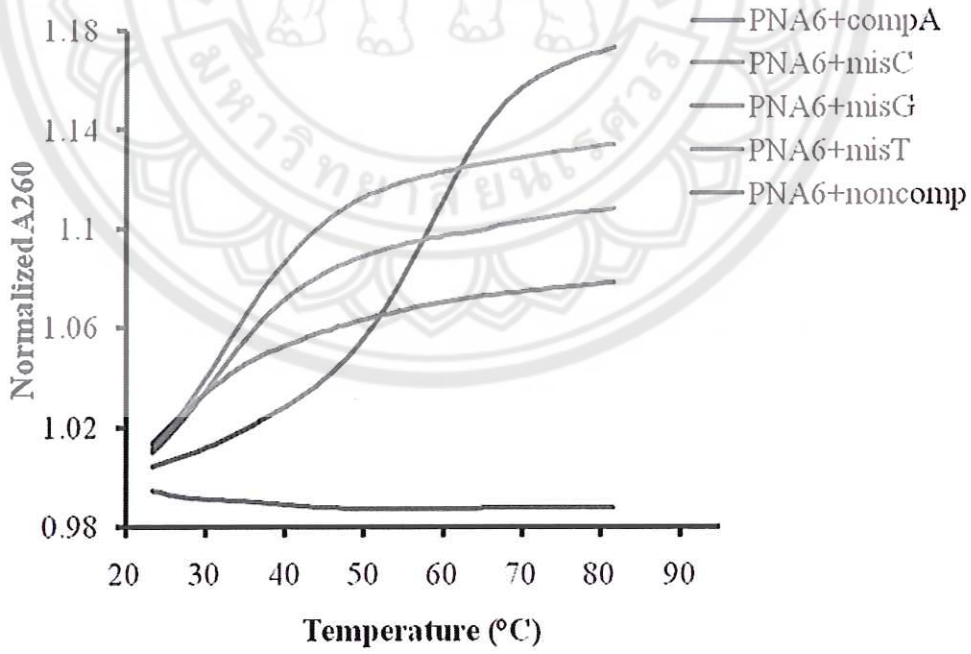

Figure 89 Thermal melting temperature of Ac-GTAGA(T_{C4Gua})CACT-LysNH$_2$ (PNA6)

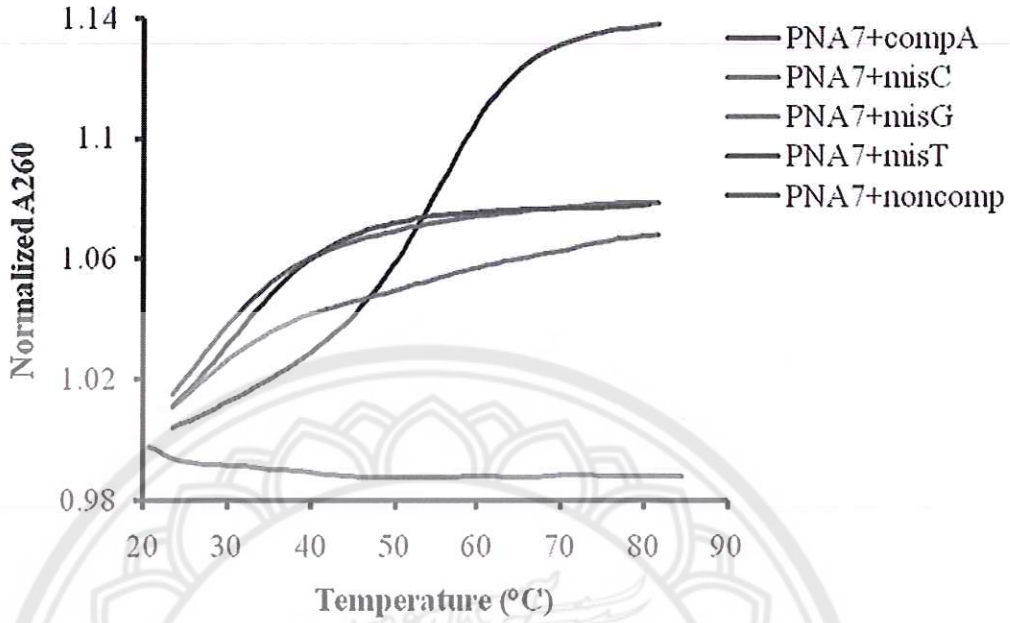

Figure 90 Thermal melting temperature of AcGT(A_{C4OH})GA(T_{C4OH})CA(C_{C4OH}) T-LysNH_2 (PNA7)

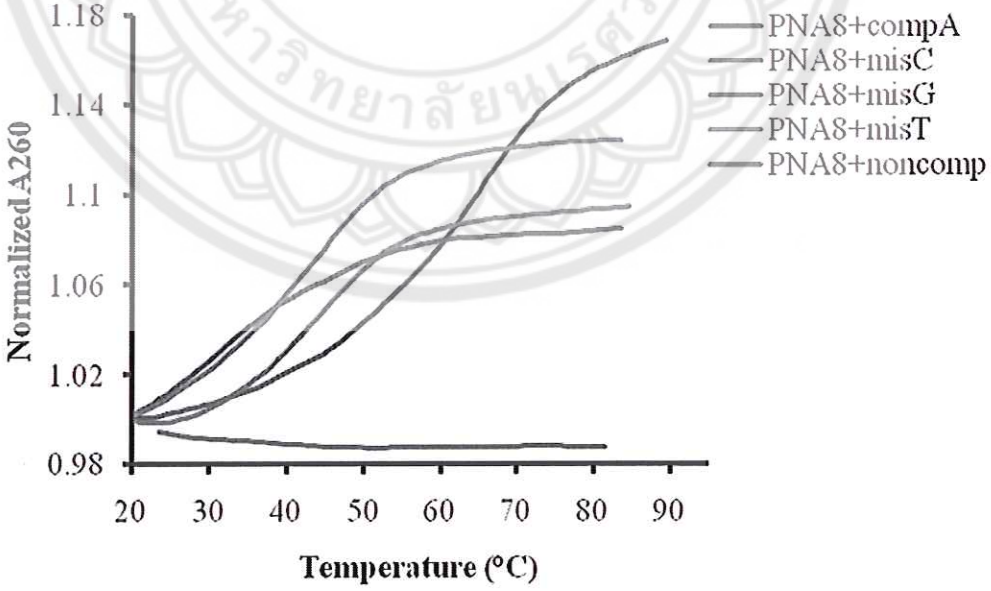

Figure 91 Thermal melting temperature of Ac-GT(A_{C4NH2})GA(T_{C4NH2})CA (C_{C4NH2})T-LysNH_2 (PNA8)

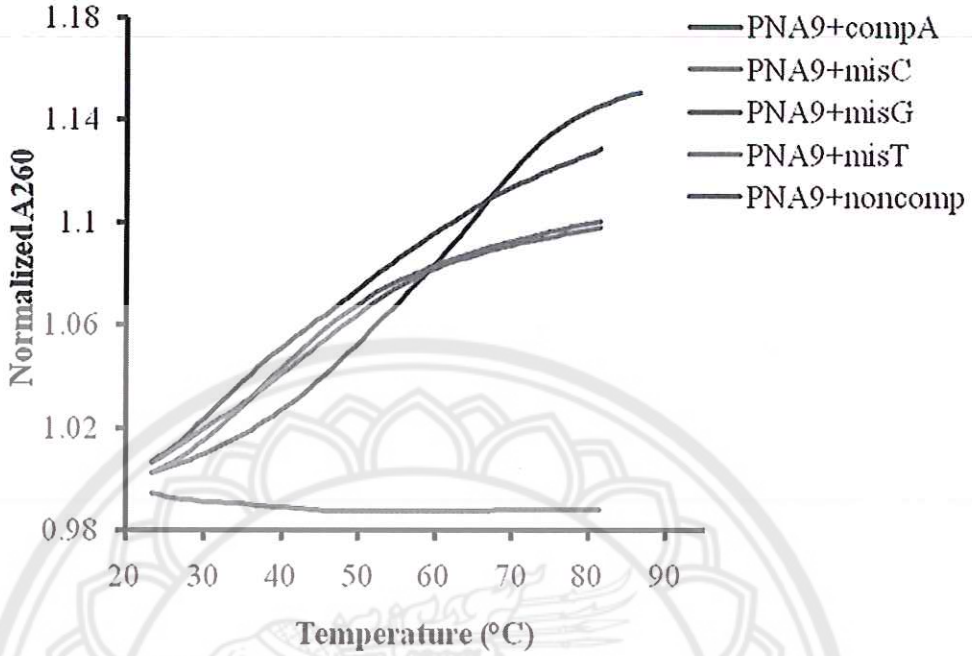

Figure 92 Thermal melting temperature of Ac-GT(A_{C4Gua})GA(T_{C4Gua})CA(C_{C4Gua}) T-LysNH_2 (PNA9)

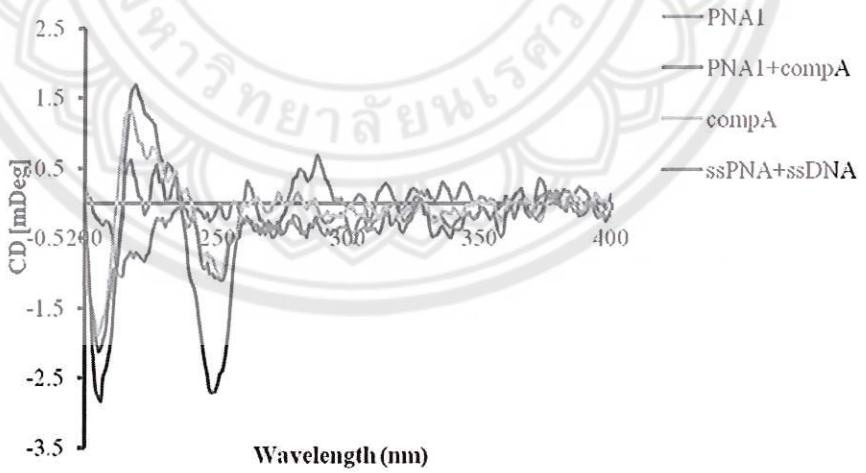

Figure 93 The CD spectra of PNA1 with complementary DNA (5'-AAA AAA AAA-3') condition : 2.5 μM PNA and 2.5 μM DNA in 100 mM phosphate buffer pH 7.0

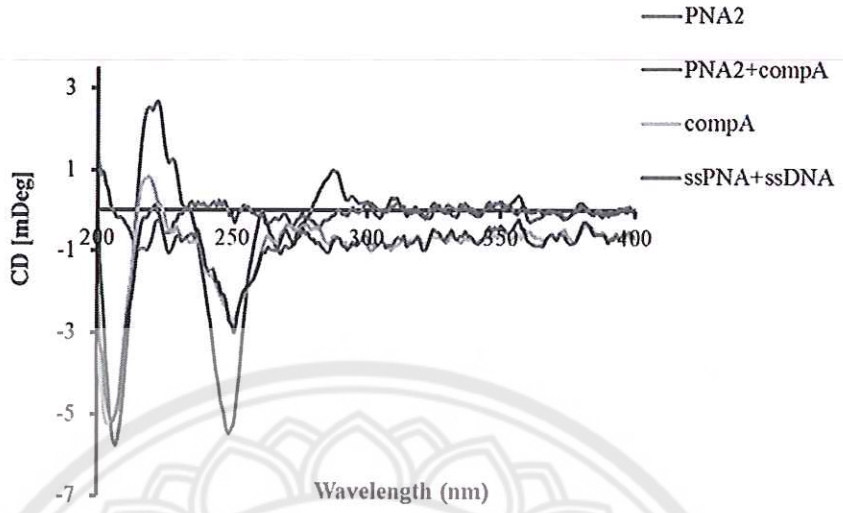

Figure 94 The CD spectra of PNA2 with complementary DNA (5'-AAA AAA AAA-3') condition :2.5 μM PNA and 2.5 μM DNA in 100 mM phosphate buffer pH 7.0

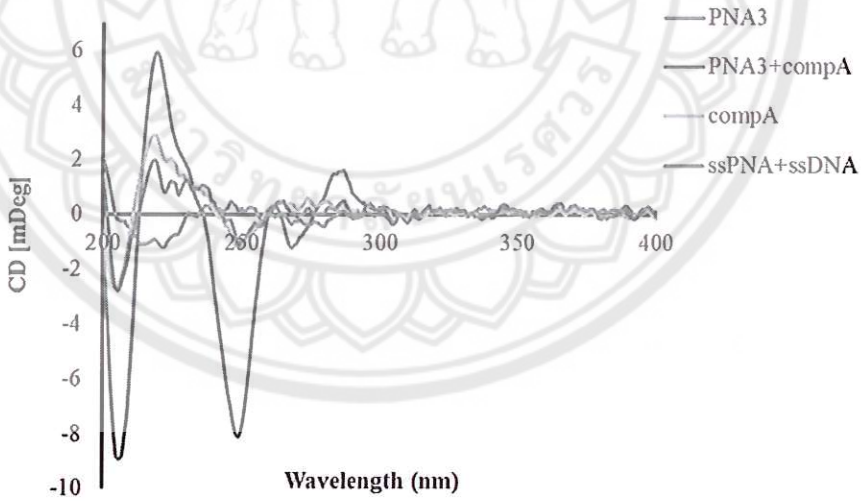

Figure 95 The CD spectra of PNA3 with complementary DNA (5'-AAA AAA AAA-3') condition : 2.5 μM PNA and 2.5 μM DNA in 100 mM phosphate buffer pH 7.0

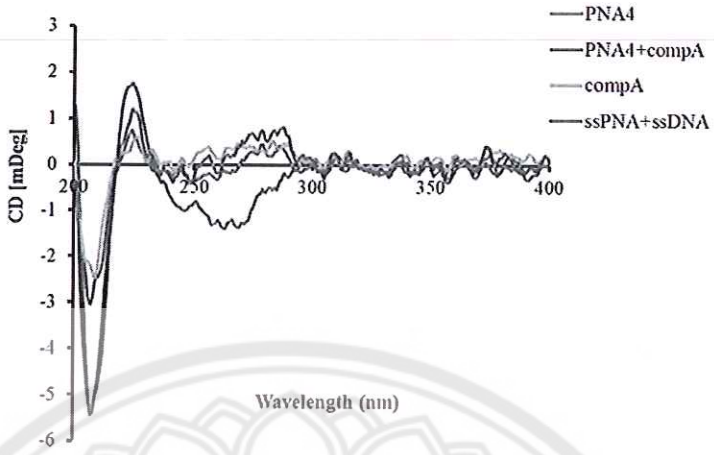

Figure 96 The CD spectra of PNA4 with complementary DNA (5'- CAT CTA GTG A -3') condition : 2 μM PNA and 2 μM DNA in 100 mM phosphate buffer pH 7.0

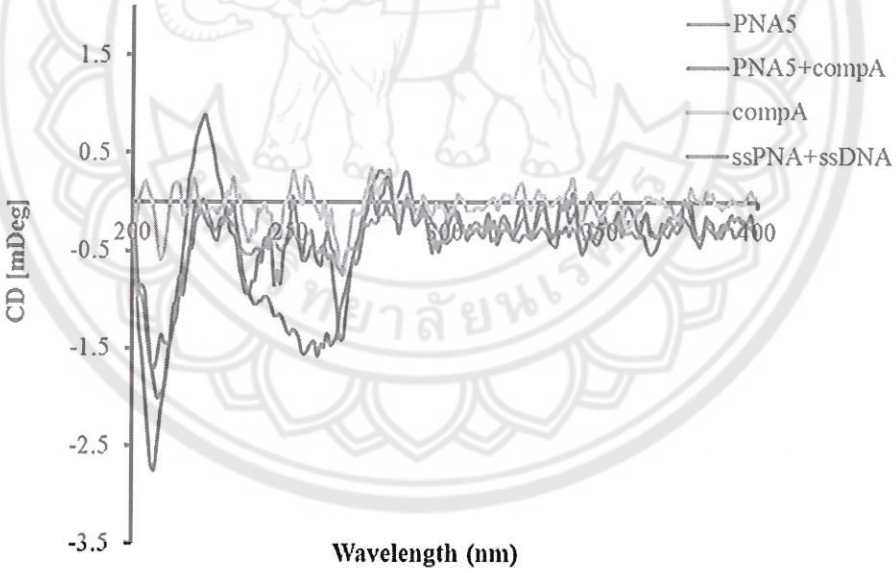

Figure 97 The CD spectra of PNA5 with complementary DNA (5'- CAT CTA GTG A -3') condition : 2 μM PNA and 2 μM DNA in 100 mM phosphate buffer pH 7.0

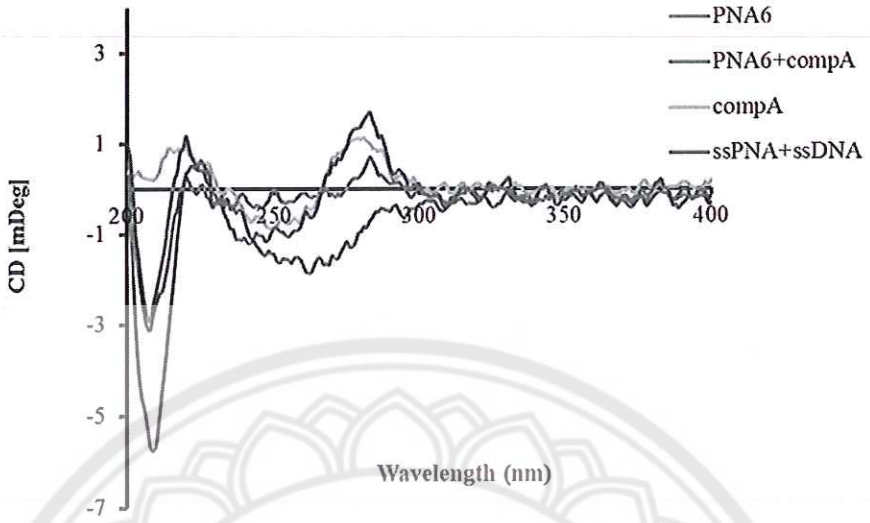

Figure 98 The CD spectra of PNA6 with complementary DNA (5'- CAT CTA GTG A -3') condition : 2 μM PNA and 2 μM DNA in 100 mM phosphate buffer pH 7.0

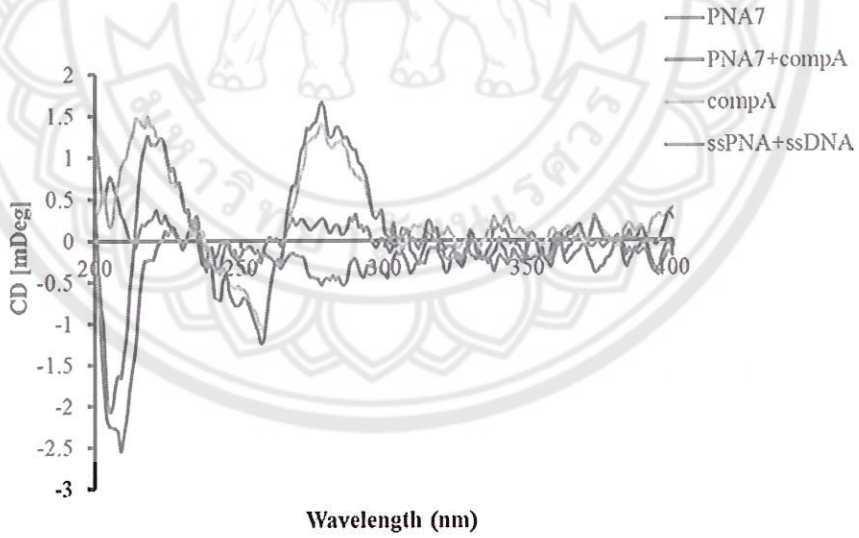

Figure 99 The CD spectra of PNA7 with complementary DNA (5'- CAT CTA GTG A -3') condition : 2 μM PNA and 2 μM DNA in 100 mM phosphate buffer pH 7.0

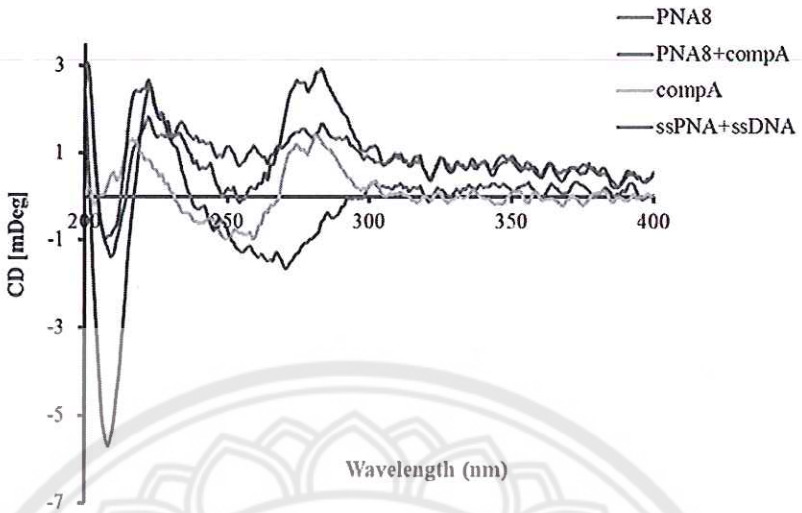

Figure 100 The CD spectra of PNA8 with complementary DNA (5'- CAT CTA GTG A -3') condition : 2 μM PNA and 2 μM DNA in 100 mM phosphate buffer pH 7.0

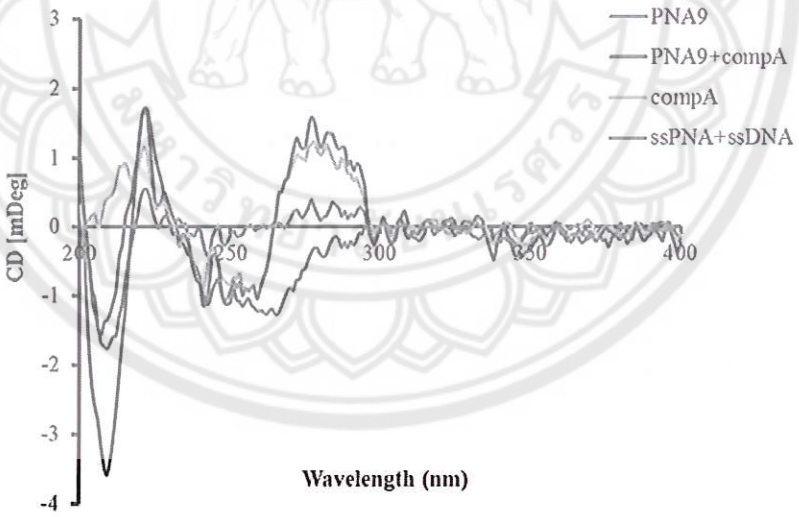

Figure 101 The CD spectra of PNA9 with complementary DNA (5'- CAT CTA GTG A -3') condition : 2 μM PNA and 2 μM DNA in 100 mM phosphate buffer pH 7.0

The example for calculation of saturated concentration For PNA1

1. PNA was adding 30 μL for saturated solubility and then centrifuged
2. The solution was monitored by nanodrop 2000 instrument as absorbance value of unmodified acpcPNA = 25.74

Absorbance at 260 nm = 25.74

3. Optical density (OD) was calculated by

OD = Abs x 10 (correction factor of instrument)

= 25.74 x 10

= 257.4

4. Epsilon (ε) of sequence (Ac-TTTTTTTTT-Lys) is 79.2 which was calculated by program from http://www.chemistry.sc.chula.ac.th/pna/pna.asp
5. The calculation of saturated concentration by equation

$$\text{Concentration (mM)} = \frac{\text{O.D}}{\varepsilon}$$

$$\text{Concentration (mM)} = \frac{257.4}{79.2}$$

$$\text{Concentration (mM)} = 3.25 \text{ mM}$$